

A revision of the early neotheropod genus *Sarcosaurus* from the Early Jurassic (Hettangian–Sinemurian) of central England

Ezcurra, Martin; Butler, Richard; Maidment, Susannah; Sansom, Ivan; Meade, Luke; Radley, Jonathan

DOI:

[10.1093/zoolinnean/zlaa054](https://doi.org/10.1093/zoolinnean/zlaa054)

License:

Other (please specify with Rights Statement)

Document Version

Peer reviewed version

Citation for published version (Harvard):

Ezcurra, M, Butler, R, Maidment, S, Sansom, I, Meade, L & Radley, J 2021, 'A revision of the early neotheropod genus *Sarcosaurus* from the Early Jurassic (Hettangian–Sinemurian) of central England', *Zoological Journal of the Linnean Society*, vol. 191, no. 1, pp. 113-149. <https://doi.org/10.1093/zoolinnean/zlaa054>

[Link to publication on Research at Birmingham portal](#)

Publisher Rights Statement:

This is a pre-copyedited, author-produced version of an article accepted for publication in *Zoological Journal of the Linnean Society* following peer review. The version of record Martín D Ezcurra, Richard J Butler, Susannah C R Maidment, Ivan J Sansom, Luke E Meade, Jonathan D Radley, A revision of the early neotheropod genus *Sarcosaurus* from the Early Jurassic (Hettangian–Sinemurian) of central England, *Zoological Journal of the Linnean Society*, zlaa054 is available online at:
<https://academic.oup.com/zoolinnean/article/doi/10.1093/zoolinnean/zlaa054/5861188> & <https://doi.org/10.1093/zoolinnean/zlaa054>

General rights

Unless a licence is specified above, all rights (including copyright and moral rights) in this document are retained by the authors and/or the copyright holders. The express permission of the copyright holder must be obtained for any use of this material other than for purposes permitted by law.

- Users may freely distribute the URL that is used to identify this publication.
- Users may download and/or print one copy of the publication from the University of Birmingham research portal for the purpose of private study or non-commercial research.
- User may use extracts from the document in line with the concept of 'fair dealing' under the Copyright, Designs and Patents Act 1988 (?)
- Users may not further distribute the material nor use it for the purposes of commercial gain.

Where a licence is displayed above, please note the terms and conditions of the licence govern your use of this document.

When citing, please reference the published version.

Take down policy

While the University of Birmingham exercises care and attention in making items available there are rare occasions when an item has been uploaded in error or has been deemed to be commercially or otherwise sensitive.

If you believe that this is the case for this document, please contact UBIRA@lists.bham.ac.uk providing details and we will remove access to the work immediately and investigate.

1
2
3 **A revision of the early neotheropod genus *Sarcosaurus* from the Early**
4
5
6 **Jurassic (Hettangian–Sinemurian) of central England**
7
8
9

10
11 Martín D. Ezcurra^{1,2*}, Richard J. Butler², Susannah C. R. Maidment^{2,3}, Ivan J. Sansom², Luke
12
13 E. Meade² and Jonathan D. Radley²
14
15

16
17
18 ¹ *Sección Paleontología de Vertebrados, CONICET-Museo Argentino de Ciencias Naturales,*
19
20 *Ángel Gallardo 470, C1405DJR, Buenos Aires, Argentina*
21

22
23 ² *School of Geography, Earth and Environmental Sciences, University of Birmingham,*
24
25 *Edgbaston, Birmingham B15 2TT, UK*
26

27
28 ³ *Department of Earth Sciences, Natural History Museum, Cromwell Road, London SW7*
29
30 *5BD, UK*
31

32
33 * *Corresponding author: martindezcurra@yahoo.com.ar*
34
35

36
37 Running title: Revision of the Jurassic theropod *Sarcosaurus*
38
39

40
41 **Abstract.** Neotheropoda represents the main evolutionary radiation of predatory dinosaurs
42
43 and its oldest records come from Upper Triassic rocks (ca. 219 Mya). The Early Jurassic
44
45 record of Neotheropoda is taxonomically richer and geographically more widespread than
46
47 that of the Late Triassic. The Lower Jurassic (upper Hettangian–lower Sinemurian) rocks of
48
49 central England have yielded three neotheropod specimens that have been assigned to two
50
51 species within the genus *Sarcosaurus*, *S. woodi* (type species) and *S. andrewsi*. These species
52
53 have received little attention in discussions of the early evolution of Neotheropoda, and
54
55 recently have been considered as *nomina dubia*. Here, we provide a detailed redescription of
56
57 one of these specimens (WARMS G667–690) and reassess the taxonomy and phylogenetic
58
59
60

1
2
3 relationships of the genus *Sarcosaurus*. We propose that the three neotheropod specimens
4
5 from the Early Jurassic of central England represent a single valid species, *S. woodi*, and
6
7 ~~The~~ The second species of the genus, '*S. andrewsi*', is a subjective junior synonym of the former.
8
9

10 A quantitative phylogenetic analysis of early theropods recovered *S. woodi* as one of the
11
12 closest sister taxa to *Averostra* and provides new information on the sequence of character-
13
14 state transformations in the lead up to the phylogenetic split between Ceratosauria and
15
16 Tetanurae.
17
18
19

20
21 Key words: Dinosauria, Theropoda, Coelophysoidea, *Averostra*, phylogeny, Europe
22
23
24
25
26
27
28
29
30
31
32
33
34
35
36
37
38
39
40
41
42
43
44
45
46
47
48
49
50
51
52
53
54
55
56
57
58
59
60

INTRODUCTION

The oldest known dinosaurs come from Upper Triassic continental rocks in South America, dated to approximately 233–231 Mya, and probably coeval strata in Africa and India (Rogers *et al.*, 1993; Furin *et al.*, 2006; Langer, Ramezani & Da Rosa, 2018). These first recorded dinosaurs include some predatory forms, such as the early theropod *Eodromaeus murphi* (Martinez *et al.*, 2011) and the herrerasaurids (alternatively interpreted as early theropods or non-eusaurischian saurischians; e.g. Langer & Benton, 2006; Nesbitt *et al.*, 2009; Martínez *et al.*, 2011). However, the main evolutionary radiation of predatory dinosaurs is represented by Neotheropoda, the oldest records of which (*Camposaurus arizonensis*: Hunt *et al.*, 1998; Ezcurra & Brusatte, 2011; *Lepidus praecisio*: Nesbitt & Ezcurra, 2015) come from rocks of the southwestern USA dated to 219.39 ± 0.16 Mya (Ramezani *et al.*, 2014; Marsh *et al.*, 2019a) or older (Nesbitt & Ezcurra, 2015). Younger Triassic neotheropods are unambiguously restricted to middle Norian to probably Rhaetian beds of Argentina (Arcucci & Coria, 2003; Ezcurra, 2017; Martínez & Apaldetti, 2017), USA (e.g. Cope, 1889; Padian, 1986; Colbert, 1989; Carpenter, 1997), Europe (Fraas, 1913; Jaekel, 1913; Huene, 1932, 1934; Rauhut & Hungerbühler, 2000; Dzik, Sulej & Niedźwiedzki, 2008) and India (Novas *et al.*, 2010). By contrast, the Early Jurassic record of Neotheropoda is taxonomically richer and geographically more widespread, with multiple known species and occurrences on all continents with the exception of Australia (e.g. Woodward, 1908; Talbot, 1911; Andrews, 1921; Huene, 1932; Camp, 1936; Young, 1948; Welles, 1954; Raath, 1969; Yadagiri, 1982; Rowe, 1989; Hu, 1993; Hammer & Hickerson, 1994; Benton, Martill & Taylor, 1995; Lucas & Heckert, 2001; Irmis, 2004; Yates, 2005; Munter & Clark, 2006; Allain *et al.*, 2007; Delsate & Ezcurra, 2014; Langer *et al.*, 2014; You *et al.*, 2014; Martill *et al.*, 2016; Wang *et al.*, 2017a; Dal Sasso, Maganuco & Cau, 2018).

1
2
3 The Lower Jurassic rocks of central England have yielded three neotheropod
4
5 specimens that, although rather incomplete, were the best records of the group from this time
6
7 interval in the UK (Huene, 1932; Carrano & Sampson, 2004), prior to the recent discovery of
8
9 *Dracoraptor hanigani* (Martill *et al.*, 2016). Andrews (1921) described a fragmentary
10
11 theropod specimen collected from the lower part of the Lias Group (*bucklandi* zone, lower
12
13 Sinemurian) of Barrow upon Soar in Leicestershire (Fig. 1). This specimen, NHMUK PV
14
15 R4840 includes a partial posterior dorsal vertebra, pelvis, and left femur. Andrews (1921)
16
17 made this specimen the type species of a new genus and species, *Sarcosaurus woodi*
18
19 [Andrews, 1921](#). The taxon has received little subsequent attention, but was reviewed and
20
21 redescended by Carrano & Sampson (2004), who referred it to Coelophysoidea. They argued
22
23 that *Sarcosaurus woodi* was likely to be distinct from all other known taxa based on its
24
25 provenance, but considered it as a *nomen dubium* because they were unable to diagnose the
26
27 species based on either autapomorphies or a distinct combination of character states.
28
29
30
31
32

33 Two additional Lias Group theropod specimens were described from Wilmcote in
34
35 Warwickshire (Fig. 1). Woodward (1908) described NHMUK PV R3542, a right tibia, from
36
37 the late Hettangian *angulata* zone. Huene (1932) subsequently made this specimen the type
38
39 of the new species, *Sarcosaurus andrewsi* [Huene, 1932](#), which was also considered a *nomen*
40
41 *dubium* by Carrano & Sampson (2004). Huene (1932) also described a fragmentary partial
42
43 skeleton, WARMS G667–690 (Fig. 2), which he referred to *Sarcosaurus woodi*. This
44
45 material was briefly discussed by Carrano & Sampson (2004), who identified it as cf.
46
47 *Sarcosaurus woodi*, but without providing a full redescription or figuring any of the material.
48
49
50

51 Here, we provide a detailed redescription of WARMS G667–690, which, although
52
53 fragmentary, represents one of the most complete theropod specimens known from the Lower
54
55 Jurassic of the UK. We review the taxonomy of all three specimens that have been referred to
56
57
58
59
60

1
2
3 the genus *Sarcosaurus*; and assess their phylogenetic positions in an analysis of early
4
5 theropod dinosaurs.
6
7
8
9

10 INSTITUTIONAL ABBREVIATIONS

11
12 AMNH, American Museum of Natural History, New York, USA; CM, Carnegie Museum of
13
14 Natural History, Pittsburg, Pennsylvania, USA; IVIC, Colección Paleontológica del Centro
15
16 de Ecología, Instituto Venezolano de Investigaciones Científicas, Caracas, Venezuela;
17
18 LPRP/USP, Laboratório de Paleontologia de Ribeirão Preto, Universidade de São Paulo,
19
20 Ribeirão Preto, Brazil; MACN-Pv CH, Museo Argentino de Ciencias Naturales ‘Bernardino
21
22 Rivadavia’, Paleovertebrados, Colección Chubut, Buenos Aires, Argentina; HMN, Museum
23
24 für Naturkunde der Humboldt Universität, Berlin, Germany; MCZ, Museum of Comparative
25
26 Zoology, Cambridge, USA; MNA, Museum of Northern Arizona, Flagstaff, USA; MPEF,
27
28 Museo Paleontológico Egidio Feruglio, Trelew, Argentina; NHMUK PV, The Natural
29
30 History Museum, Palaeontology Vertebrates, London, UK; NMW, National Museum of
31
32 Wales, Cardiff, UK; PULR, Paleontología, Universidad Nacional de La Rioja, La Rioja,
33
34 Argentina; PVL, Paleontología de Vertebrados, Instituto ‘Miguel Lillo’, San Miguel de
35
36 Tucumán, Argentina; PVSJ, División de Paleontología de Vertebrados del Museo de Ciencias
37
38 Naturales y Universidad Nacional de San Juan, San Juan, Argentina; QG, Zimbabwe Natural
39
40 History Museum, Bulawayo, Zimbabwe; SMNS, Staatliches Museum für Naturkunde
41
42 Stuttgart, Stuttgart, Germany; UCM, University of Colorado Museum, Boulder, Colorado,
43
44 USA; UCMP, University of California Museum of Paleontology, Berkeley, CA, USA;
45
46 USNM, National Museum of Natural History (formerly United States National Museum),
47
48 Smithsonian Institution, Washington, D.C., USA; WARMS, Warwickshire Museum,
49
50 Warwick, UK.
51
52
53
54
55
56
57
58
59
60

MATERIALS AND METHODS

PHYLOGENETIC ANALYSIS

The phylogenetic relationships of the three Early Jurassic neotheropod specimens from central England were tested using the phylogenetic dataset originally published by Nesbitt *et al.* (2009) and iteratively modified by Ezcurra & Brusatte (2011), You *et al.* (2014), Nesbitt & Ezcurra (2015), Martill *et al.* (2016), Ezcurra (2017), Martínez & Apaldetti (2017), Marsola *et al.* (2019), Marsh *et al.* (2019b), and Griffin (2019) (Supporting Information I).

Here, WARMS G667–690 and the holotypes and only known specimens of *Sarcosaurus andrewsi* and *Sarcosaurus woodi* were added to the data-set. In addition, *Tachiraptor admirabilis* [Langer *et al.*, 2014](#) and the early ceratosaurian *Eoabelisaurus mefi* [Pol & Rauhut, 2012](#) were added to improve the sampling of early members of the lineage leading to Averostra and early averostrans, respectively (~~Pol & Rauhut, 2012; Langer *et al.*, 2014~~).

These specimens/species were scored based on first-hand observations of specimens (casts in the case of *Tachiraptor admirabilis*: LPRP/USP 0747, cast of IVIC-P-2867₃₅ and *Gojirasaurus quayi* [Carpenter, 1997](#): HMN MB.R. 4232.1, cast of UCM 47221). Five characters were added to this data matrix, character 252 was deactivated, and some character formulations, scorings and orderings were modified (rationale for these changes is given in Supporting Information I). ‘*Powellvenator podocitus* holotype’ and ‘*Lepidus praecisio* combined’ were deactivated before the analyses, whereas *Powellvenator podocitus* [Ezcurra, 2017](#) and ‘*Lepidus praecisio* holotype’ remained active following Ezcurra (2017).

Velociraptor mongoliensis [Osborn, 1924](#) was also deactivated following Ezcurra (2017). The resulting matrix consists of 379 characters and 57 active terminals (Supporting Information II and III). *Sarcosaurus woodi*, WARMS G667–690 and *Sarcosaurus andrewsi* were analysed in separate analyses as ~~separate-independent~~ terminals or alternatively merged into a single

1
2
3 terminal following the hypothesis that they belong to the same species (see below).
4

5 The outgroup choice follows Nesbitt *et al.* (2009) and the following multistate
6 characters were ordered: 17, 30, 67, 128, 129, 174, 184, 197, 213, 219, 231, 236, 248, 253,
7 254, 273, 329, 343, 345, 347, 349, 354, 366, 371, 374, and 377–379. The data matrix was
8 analysed under equally weighted parsimony using TNT 1.5 (Goloboff, Farris & Nixon, 2008;
9 Goloboff & Catalano, 2016). A heuristic search of 100 replications of Wagner trees (with
10 random addition sequence) followed by TBR branch swapping (holding ~~10~~ ten trees per
11 replicate) was performed. Branches with a maximum possible length of zero among any of
12 the recovered most parsimonious trees (MPTs) were collapsed (rule 3 of Swofford & Begle,
13 1993; Coddington & Scharff, 1994).
14
15
16
17
18
19
20
21
22
23
24
25

26 As a measure of branch support, decay indices (= Bremer support) were calculated
27 (Bremer, 1988, 1994), and as a measure of branch stability, a bootstrap resampling analysis
28 (Felsenstein, 1985) was conducted, performing 10,000 pseudoreplications. Both absolute and
29 GC (*i.e.*, difference between the frequency whereby the original group and the most frequent
30 contradictory group are recovered in the pseudoreplications; Goloboff *et al.*, 2003) bootstrap
31 frequencies are reported. In order to analyse the effect that a few topologically unstable
32 terminals may have on Bremer supports, this index was recalculated after the *a posteriori*
33 pruning of such terminals, which were previously detected in the subsample of suboptimal
34 trees with the iterPCR protocol (Pol & Escapa, 2009). Finally, analyses forcing topological
35 constraints were conducted to find the minimum number of steps necessary to force
36 alternative suboptimal positions for the three neotheropod specimens from the Early Jurassic
37 of central England.
38
39
40
41
42
43
44
45
46
47
48
49
50
51
52
53

54 THIN SECTION PROCEDURE

55
56
57
58 Doubly polished thin sections through the dorsal rib shaft were prepared, initially stabilized
59
60

1
2
3 using a surface impregnation of Epothin epoxy resin, before slicing using a Buehler IsoMet
4
5 Low Speed Saw (model 11-1180-160). The sections were then ground and polished (with
6
7 water suspended 0.3 micron alumina oxide) to a usable thickness (approximately 50 microns)
8
9
10 by hand on a Buehler MetaServ. Imaging was undertaken on a Zeiss Axioskop Pol
11
12 polarisation microscope using plane polarized and polarized light, the latter augmented by
13
14 the insertion of an accessory gypsum plate.
15
16
17
18

19 3D MODELS OF SPECIMENS

20
21 High-resolution 3D models were created of selected elements of WARMS G667–690 using
22
23 photogrammetry. These comprised a partial dorsal vertebra (G678), the femora (G681, G682)
24
25 and tibiae (G668, G680), and the partial left metatarsal II (G672). A tripod mounted Nikon
26
27 D5100 digital SLR camera with a Nikon 18–55mm VR lens was used to photograph the
28
29 specimens under artificial lighting against a uniformly coloured and contrasting background.
30
31 A minimal aperture ensured the whole specimen was in focus and the ISO setting was kept
32
33 below 400. Around 20–40 photographs were taken in a circular path around each specimen
34
35 for three different orientations to ensure even and complete coverage and a sufficient total
36
37 number of photographs (60–100). The software package Agisoft PhotoScan Professional
38
39 edition version 1.2.7 was used to mask the backgrounds of the photographs and create 3D
40
41 meshes using automated point picking and triangulation of point clouds. These surfaces were
42
43 then textured in PhotoScan and exported. The final models have been published in Zenodo
44
45 and can be downloaded from here: <https://zenodo.org/record/3663095>.
46
47
48
49

50
51 The holotypes of *Sarcosaurus woodi* (NHMUK PV R4840) and *Sarcosaurus*
52
53 *andrewsi* (NHMUK PV R3542) were scanned using a Faro Edge laser scanner with an arm
54
55 accuracy ± 0.041 mm. The line module samples 560,000 points/sec with repeatability 25 μ m.
56
57 Scans were processed in Geomagic Wrap 2017.0.2.18 64bit. Raw point data was aligned,
58
59
60

1
2
3 filtered for outliers, and a mesh generated with no noise reduction. The meshes were exported
4
5 at full size and also downsampled to 20% of the vertex count. The final models are freely
6
7 available and can be downloaded from the [Natural History Museum's](https://data.nhm.ac.uk/object/91a032f1-fd74-4464-9c37-bab839a83761/1580342400000) data portal [of the](https://data.nhm.ac.uk/object/91a032f1-fd74-4464-9c37-bab839a83761/1580342400000)
8
9 [Natural History Museum](https://data.nhm.ac.uk/object/91a032f1-fd74-4464-9c37-bab839a83761/1580342400000) here: [https://data.nhm.ac.uk/object/91a032f1-fd74-4464-9c37-](https://data.nhm.ac.uk/object/91a032f1-fd74-4464-9c37-bab839a83761/1580342400000)
10
11 [bab839a83761/1580342400000](https://data.nhm.ac.uk/object/91a032f1-fd74-4464-9c37-bab839a83761/1580342400000).
12
13
14

15 16 17 STRATIGRAPHIC AND PALAEOENVIRONMENTAL CONTEXT OF WARMS

18
19 G667–690

20
21 This specimen was collected from strata (*bucklandi* Zone) that were deposited in
22
23 epicontinental shallow marine settings affected by sealevel fluctuations and a warm,
24
25 predominantly humid climate (Simms *et al.*, 2004; Hesselbo, 2008). The *bucklandi* zone
26
27 (lower Sinemurian) in south-western Warwickshire, central England (Wilmcote area; source
28
29 of WARMS G667–690) is represented by the upper part of the Rugby Limestone Member
30
31 (*liasicus* up to *semicosatum* zones) of the Blue Lias Formation (Ambrose, 2001).
32
33

34
35 Representing typical Blue Lias lithofacies of alternating mudrocks and generally fine-grained
36
37 and frequently highly fossiliferous limestones (e.g. see Old, Sumbler & Ambrose, 1987;
38
39 Ambrose, 2001), the Rugby Limestone Member was deposited at a palaeolatitude of
40
41 approximately 35° N in a storm-influenced offshore setting (Weedon, Jenkyns & Page,
42
43 2017). Palaeodepths in the order of at least a few tens of metres seem likely (e.g. see Hallam,
44
45 1997), below normal storm wave base (Weedon, Jenkyns & Page, 2017).
46
47
48

49
50 Wilmcote was situated close to the eastern margin of the Worcester Graben during the
51
52 Early Jurassic, adjacent to the East Midlands Shelf (Radley, 2003). The western margin of the
53
54 emergent London Platform laid approximately 60–80 km to the south-east (Donovan, Horton
55
56 & Ivimey-Cook, 1979; Cox, Sumbler & Ivimey-Cook, 1999), and must have been the
57
58 principle source of terrestrial biodebris (plants and sporadic vertebrate remains), found
59
60

1
2
3 occasionally within the Blue Lias Formation of central England (e.g. see Old, Hamblin &
4
5 Ambrose, 1991).
6

7
8 Growing evidence for strong climatic influence on Blue Lias deposition in central
9
10 England illustrates the likely mechanism for emplacement of the terrestrial WARMS
11
12 G667–690 remains into an offshore shelf setting, likely from the western margin of the
13
14 London Platform. Weedon, Jenkyns & Page (2017) have suggested that the more calcareous
15
16 horizons (limestones and ‘marls’) within the Rugby Limestone Member were deposited
17
18 during relatively dry, stormier conditions, involving intermittent deposition of calcareous
19
20 mud as precursors of limestone beds. By contrast, the intercalated shales are equated to wetter
21
22 climatic phases, involving relative stability of the water column and high clay influx from
23
24 adjacent land.
25
26
27

28
29 Remnants of matrix on the bone surface of WARMS G667–690 are a light grey
30
31 mudstone and there is no evidence of limestone matrix. The specimen was collected probably
32
33 from an uncemented bed; either a calcareous mudstone or shale horizon. Either way, storm
34
35 flow and/or enhanced runoff provide effective mechanisms for derivation of terrestrial reptile
36
37 remains, and their introduction into a hemipelagic marine environment.
38
39

40
41 Bioerosion traces and the presence of invertebrate bioencrusters on some of the bones
42
43 of WARMS G667–690 (Fig. 3) suggests that the sea floor on which the bones were
44
45 ultimately buried was oxygenated, and that the remains remained free of sediment for some
46
47 time prior to burial. Comparison can be made with other occurrences of bioencrusted skeletal
48
49 substrates (‘benthic islands’ – commonly molluscan shells) present within the Rugby
50
51 Limestone Member (JDR, personal observations 1999–present). Emplacement during a dryer,
52
53 stormier interval seems more likely than a wetter phase, with its potential for high clay flux
54
55 and benthic anoxia (Weedon, Jenkyns & Page, 2017).
56
57
58
59
60

SYSTEMATIC PALAEOLOGY

ARCHOSAURIA Cope, 1869–1870 sensu Gauthier & Padian (1985)

DINOSAURIA Owen, 1842 sensu Padian & May (1993)

THEROPODA Marsh, 1881 sensu Gauthier (1986)

NEOTHEROPODA Bakker, 1986 sensu Sereno (1998)

Sarcosaurus Andrews, 1921*Type species:**Sarcosaurus woodi* Andrews, 1921.*Diagnosis:*

As for type and only valid species.

Sarcosaurus woodi Andrews, 1921*Megalosaurus* sp.: Huene, 1908 (NHMUK PV R3542)*Sarcosaurus* sp.: Andrews, 1921 (NHMUK PV R3542)*Megalosaurus* (subgenus a) sp.: Huene, 1926 (NHMUK PV R3542)*Sarcosaurus andrewsi*: Huene, 1932: page 51 (NHMUK PV R3542)*Magnosaurus woodwardi*: Huene, 1932: page 219 (NHMUK PV R3542)*Megalosaurus andrewsi*: Waldman, 1974 (NHMUK PV R3542)cf. *Sarcosaurus woodi*: Carrano and Sampson, 2004 (WARMS G667–690)*Holotype:*

NHMUK PV R4840, a posterior dorsal vertebra, partial left and right ilia each fused to the

1
2
3 proximal portion of their respective pubis, and left femur missing most of the femoral head
4
5 and with a severely damaged distal end.
6
7
8
9

10 *Ontogenetic stage of holotype:*

11
12 This specimen shows some indicators of skeletal maturity and is not an early juvenile, but its
13
14 ontogenetic stage cannot be constrained further based on the available evidence (see
15
16 Discussion).
17
18
19
20

21 *Type locality and horizon:*

22
23 Barrow upon Soar, Leicestershire, England, UK. *Bucklandi* Zone of the Scunthorpe
24
25 Mudstone Formation, Lias Group, Early Jurassic (lowermost Sinemurian) (Fig. 1).
26
27
28
29

30 *Referred specimens:*

31
32 NHMUK PV R3542, a complete right tibia (holotype of '*Sarcosaurus andrewsi*'). WARMS
33
34 G667–690, partial skeleton of a single individual (Fig. 2) including a partial middle–posterior
35
36 dorsal vertebra (G678), a partial anterior–middle caudal vertebra (G679), dorsal rib fragments
37
38 (G670, G675, G676, G685, G686), fragment of the pubic peduncle of the left ilium (G690),
39
40 partial right and left pubes (G683/684, G688), femora (G681, G682) and tibiae (G668,
41
42 G680), proximal end of left fibula (G669), probable distal half of fibula (G674), distal
43
44 portions of left metatarsal II (G672), metatarsal III (G673) and metatarsal IV (G677),
45
46 proximal end of a metatarsal II or III (G671), proximal half of left pedal phalanx II-1 (G687),
47
48 and three indeterminate bone fragments (G680, G681, G689) (collected by J. W. Kirshaw).
49
50
51
52
53
54
55

56 *Ontogenetic stage of referred specimens:*

57
58 NHMUK PV R3542 is considerably larger than the other referred specimen but its
59
60

1
2
3 ontogenetic stage is unknown. WARMS G667–690 was not a juvenile, but had not reached
4 skeletal maturity at the time of its death (see Discussion).
5
6
7
8
9

10 *Locality and horizons of referred specimens:*

11
12 Wilmcote, Warwickshire, England, UK. NHMUK PV R3542 is from the *angulata* *Z*zone of
13 the Blue Lias Formation, Lias Group, Early Jurassic (upper Hettangian); and WARMS
14 G667–690 comes from the *bucklandi* *Z*zone of the upper part of the Rugby Limestone
15 Member of the Blue Lias Formation, Early Jurassic (lowermost Sinemurian) (Fig. 1).
16
17
18
19
20
21
22
23

24 *Diagnosis:*

25
26 *Sarcosaurus woodi* is a medium-sized (estimated femoral length c. 48 cm in NHMUK PV
27 R3542) non-averostran neotheropod that differs from other dinosaurs in the following unique
28 combination of character states present in the holotype (autapomorphies indicated with an
29 asterisk): ilium with main axis of the preacetabular process strongly anteroventrally oriented
30 in lateral view (also present in the ceratosaurian *Eoabelisaurus mefi*); ilium with an only ~~very~~
31 slightly posteriorly projecting ischiadic peduncle*; ilium without a laterally exposed
32 ventromedial margin of the brevis fossa (only a ~~very~~-short portion of its base is exposed, also
33 present in *Cryolophosaurus ellioti* [Hammer & Hickerson, 1994](#)); ilium with a poorly
34 transversely expanded brevis fossa (also present in non-coelophysid neotheropods); femur
35 with a dorsolateral trochanter on the proximal end (also present in WARMS G667–690 and
36 non-averostran neotheropods); and femoral fourth trochanter ~~very~~-poorly posteriorly
37 expanded (also present in WARMS G667–690, coelophysids, and early ceratosaurians).
38
39
40
41
42
43
44
45
46
47
48
49
50
51
52
53

54 The diagnosis of the species can be expanded with the following unique combination
55 of character states present in the referred specimens, but unknown in the holotype
56 (autapomorphies indicated with an asterisk): femur without an anterior extensor groove on
57
58
59
60

1
2
3 the distal end (only known in WARMS G667–690); tibia with a fibular crest that reaches the
4
5 posterior lateral hemicondyle of the proximal end; tibia with an anteroposterior depth versus
6
7 mediolateral width ratio ≥ 0.6 ; tibia with an anteroposteriorly narrow facet for the reception
8
9 of the ascending process of the astragalus (indicating a non-blocky, but rather laminar
10
11 ascending process of the astragalus); tibia with an angle between the main axis of the lateral
12
13 half of the facet for reception of the ascending process of the astragalus and the longitudinal
14
15 axis of the bone $\geq 25^\circ$ in anterior view; tibia with a well proximally extended posteromedial
16
17 notch on the distal end; tibia with a poorly projected medial malleolus; and fibula with a
18
19 poorly projected and tab-like posterior margin of the proximal end in lateral view* (only
20
21 known in WARMS G667–690).
22
23
24
25

26 See Discussion for a differential diagnosis of the species among early neotheropods.
27
28
29

30 31 DESCRIPTION OF WARMS G667–690 32

33 The holotypes of *Sarcosaurus woodi* and ‘*Sarcosaurus andrewsi*’ have been recently
34
35 redescribed in detail ~~recently~~ by Carrano & Sampson (2004). Thus, we do not provide new
36
37 redescrptions here, although comments on their anatomy are provided in the discussion of
38
39 the taxonomy of the genus *Sarcosaurus* and we do refigure both specimens. By contrast,
40
41 WARMS G667–690 was described and figured with line drawings by Huene (1932), but no
42
43 detailed redescription has been provided to date.
44
45
46
47
48

49 **Dorsal vertebra.** A dorsal vertebra (WARMS G678) is partially preserved, including the
50
51 centrum and the left lateral wall of the neural canal (Fig. 4; Table 1). The left lateral surface
52
53 of the centrum is well preserved, but the anterior and posterior ends of the right lateral
54
55 surface of the centrum are eroded and the lateral surface has collapsed inwards. The
56
57 neurocentral suture is open (Huene, 1932) and strongly interdigitated (Fig. 4: ncs). The neural
58
59
60

1
2
3 arch preserves the distal ends of well-developed anterior and posterior centrodiapophyseal
4
5 laminae, with the former lamina extending further ventrally than the latter (Fig. 4: acdl, pcdl).
6
7 This element is interpreted as a middle or posterior (although not one of the most posterior)
8
9 dorsal vertebra because of the degree of ventral development and primarily anteroposterior
10
11 (rather than dorsoventral) orientation of the centrodiapophyseal laminae when compared to
12
13 the presacral vertebral series of *Liliensternus liliensterni* (Huene, 1934) (HMN MB.R. 2175)
14
15 and *Dilophosaurus wetherilli* (Welles, 1954) (UCMP 37302). The centrum is proportionally
16
17 long anteroposteriorly, being c. 1.9 times longer than its anterior height, resembling the
18
19 condition of the posterior dorsal vertebrae of *Eodromaeus murphi* (PVSJ 562: ratio =
20
21 2.0–2.18). This ratio is higher than in the middle–posterior dorsal vertebrae of *Liliensternus*
22
23 *liliensterni* (HMN MB.R. 2175: highest ratio = 1.67, middle dorsal vertebra), *Dracoraptor*
24
25 *hanigani* (NMW 2015.5G.1–2015.5G.11: ratio = 1.63–1.75, middle–posterior dorsal
26
27 vertebrae), *Dilophosaurus wetherilli* (UCMP 37302: highest ratio = 1.66, dorsal 10; UCMP
28
29 77270: highest ratio = 1.73, dorsal 10), *Eoabelisaurus mefi* (MPEF PV 3990: highest ratio =
30
31 1.19, dorsal 12) and *Piatnitzkysaurus floresi* Bonaparte, 1979 (PVL 4073: ratio = 1.11,
32
33 middle dorsal vertebra), but distinctly lower than in the coelophysids *Procompsognathus*
34
35 *triassicus* (SMNS 12591: 2.70–2.91, dorsals 7 and 8), *Coelophysis bauri* Cope, 1887
36
37 (Melbourne specimen: ca. 2.6, middle dorsal) and *Megapnosaurus rhodesiensis* (Raath, 1969)
38
39 (Raath, 1977: 2.33–2.64, dorsals 6 and 7 of QG1), *Procompsognathus triassicus* Fraas, 1913
40
41 (SMNS 12591: 2.70–2.91, dorsals 7 and 8). The preserved posterior dorsal vertebra of the
42
43 holotype of *Sarcosaurus woodi* lacks its posterior portion, but its length:anterior height ratio
44
45 as preserved is 1.00 and, thus, this ratio would have been considerably lower than 2
46
47 (NHMUK PV R4840). WARMS G678 is moderately transversely compressed around mid-
48
49 length, giving it an hourglass-shape in ventral view. The ventral surface of the centrum is
50
51 continuously transversely convex, without a median keel or groove. The presence of a
52
53
54
55
56
57
58
59
60

1
2
3 median ventral keel is variable along the dorsal series in early neotheropods, being, for
4 example, present up to the sixth dorsal vertebra in the holotype of *Dilophosaurus wetherilli*
5 (UCMP 37302). Among European early neotheropods, the available dorsal vertebrae of
6 *Liliensternus liliensterni* (HMN MB.R. 2175) and *Dracoraptor hanigani* (NMW 2015.5G.1–
7 2015.5G.11) and the posterior dorsal vertebra of the holotype of *Sarcosaurus woodi*
8 (NHMUK PV R4840) also lack a ventral keel or groove. The ventral margin of the centrum
9 of WARMS G678 is symmetrically dorsally arched in lateral view. The anterior and posterior
10 articular surfaces of the centrum are taller than broad and slightly concave, although their
11 original proportions are distorted by the inward collapse and erosion of the right lateral
12 surface. The lateral surface of the centrum possesses a shallow and weakly defined fossa
13 restricted to its dorsal half, located immediately ventral to the neurocentral suture (Huene,
14 1932; Fig. 4: fos). A similar fossa in the same location is present in other early neotheropods,
15 such as *Liliensternus liliensterni* (HMN MB.R. 2175), *Dilophosaurus wetherilli* (UCMP
16 37302) and the holotype of *Sarcosaurus woodi* (NHMUK PV R4840).

17
18
19
20
21
22
23
24
25
26
27
28
29
30
31
32
33
34
35
36
37 **Caudal vertebra.** A second vertebra, only represented by a centrum (WARMS G679; Fig. 5;
38 Table 1), is identified as belonging to the anterior or middle caudal series because it is
39 proportionately lower and narrower than the middle–posterior dorsal vertebra, which is a
40 condition that occurs in the vertebral series of the holotype of *Dilophosaurus wetherilli*
41 (UCMP 37302). The caudal centrum lacks the dorsal half of one of its sides and the anterior
42 and posterior articular surfaces are damaged and partially covered with sediment. The
43 presence of a facet for articulation with the haemal arch cannot be determined because of
44 damage to the ventral surfaces of the ends of the centrum. The centrum is similar in
45 morphology to the centrum of the dorsal vertebra, but the anterior and posterior articular
46 surfaces are subcircular and the lateral fossa is deeper (Fig. 5: fos). The surface for
47
48
49
50
51
52
53
54
55
56
57
58
59
60

1
2
3 articulation with the neural arch is complete on one side of the bone and is strongly
4
5 interdigitated (Fig. 5: f.na).
6
7
8
9

10 **Dorsal ribs.** Several rib shaft fragments are preserved (WARMS G670, G675, G676, G685,
11 G686; Fig. 6), and probably represent dorsal ribs. They possess a shallow groove along the
12 shaft on what is probably the posterior surface (Fig. 6: gr). The shafts are anteroposteriorly
13 compressed. The bone microstructure of one of these ribs (WARMS G676) is described
14 below.
15
16
17
18
19
20
21
22
23

24 **Ilium.** A bone (WARMS G690) that was not described or figured by Huene (1932) is
25 identified here as part of the pubic peduncle of the left ilium (Fig. 7A–C; Table 2). The bone
26 is somewhat transversely compressed taphonomically, and its lateral and medial surfaces are
27 slightly collapsed. The most anterior portion of a well-developed supra-acetabular crest is
28 preserved and terminates 10 mm before the distal end of the peduncle (Fig. 7A–C: sac), as
29 occurs in other early neotheropods [(e.g. *Dilophosaurus wetherilli*: UCMP 37302;
30 *Liliensternus liliensterni*: HMN MB.R. 2175; *Lophostropheus airelensis* (Cuny & Galton,
31 1993); *Notatesseraeraptor frickensis*: Zahner & Brinkmann, 2019, fig. 1j; *Dilophosaurus*
32 *wetherilli*: UCMP 37302)]. The preserved portion of the supra-acetabular crest faces mainly
33 ventrally, resembling the condition of several early neotheropods in which the supra-
34 acetabular crest is ventrolaterally oriented and partially obscures the acetabulum in lateral
35 view (e.g. *Coelophysis bauri*: CM 81768; *Dilophosaurus wetherilli*: UCMP 77270;
36 *Liliensternus liliensterni*: HMN MB.R. 2175; *Procompsognathus triassicus*: SMNS 12591;
37 *Coelophysis bauri*: CM 81768; *Lophostropheus airelensis*: Cuny & Galton, 1993;
38 *Procompsognathus triassicus*: SMNS 12591; *Liliensternus liliensterni*: HMN MB.R. 2175;
39 *Dilophosaurus wetherilli*: UCMP 77270; holotype of *Sarcosaurus woodi*: NHMUK PV
40
41
42
43
44
45
46
47
48
49
50
51
52
53
54
55
56
57
58
59
60

1
2
3 R4840). The preserved portion of the acetabular roof is transversely concave and the dorsal
4 surface of the peduncle is strongly transversely convex. The distal articular surface of the
5 peduncle is incomplete.
6
7
8
9

10
11
12 **Pubis.** The proximal thirds of both pubes are preserved (WARMS G683/684, G688), lacking
13 the articular surfaces for the ilium and ischium and the puboischiadic plate. The right pubis
14 (WARMS G683/684) is slightly more proximally and distally complete (Fig. 7G–I) than the
15 left element (WARMS G688; Fig. 7D–F; Table 2). The preserved portion of the proximal end
16 is dorsoventrally tall in lateral view and narrows gradually towards the shaft. The anterior
17 margin of the bone is slightly concave along the transition between the proximal end and
18 shaft in lateral view, as occurs in *Eodromaeus murphi* (PVSJ 560, 562) and several other
19 early neotheropods (e.g. *Coelophysis bauri*: CM 81768; *Liliensernus lilienserni*: HMN
20 MB.R. 2175; *Notatesseraeraptor frickensis*: Zahner & Brinkmann, 2019, fig. 1i; holotype of
21 *Sarcosaurus woodi*: NHMUK PV R4840). An oval scar, but not a tuberosity, indicates the
22 insertion area of the M. ambiens (Carrano & Hutchinson, 2002). The lateral surface of the
23 proximal end is gently dorsoventrally concave. The pubic apron (Fig. 7: pub.ap) arises from
24 the posteroventral corner of the proximal end of the bone as preserved. The pubic apron
25 twists to project increasingly more medially distally, until it is entirely medially directed. The
26 pubic apron is restricted at the anteromedial corner of the shaft and gives this part of the bone
27 a comma-shaped outline in cross-section. The medial edge of the pubic apron is broken in
28 both pubes and, as a result, its transverse width cannot be determined. The lateral surface of
29 the pubis possesses a shallow, longitudinal depression on both sides (Fig. 7: dp), resembling
30 the condition in *Liliensernus lilienserni* (HMN MB.R. 2175) and *Megapnosaurus*
31 *rhodesiensis* (cast of QG1). The pubic shafts are too incomplete to assess whether they were
32 bowed or straight in lateral view.
33
34
35
36
37
38
39
40
41
42
43
44
45
46
47
48
49
50
51
52
53
54
55
56
57
58
59
60

1
2
3
4
5
6 **Femur.** Both femora are preserved (WARMS G681, G682), but are badly damaged (Figs. 8,
7
8 9; Table 2). In both cases most of the femoral head is missing, the anterior and fourth
9
10 trochanters are damaged, and the distal end of the left femur only preserves part of the fibular
11
12 condyle. The distal end of the left femur is strongly anteroposteriorly compressed as a result
13
14 of taphonomic deformation.

15
16
17 The preserved portion of the head of the left femur shows that it was inturned and
18
19 anteromedially oriented, as occurs in other basal dinosaurs. The anterolateral corner of the
20
21 proximal end of the bone possesses a proximodistally elongated dorsolateral trochanter (=
22
23 greater trochanter) (Figs: 8, 9: dltr), as occurs in most early theropods (e.g. *Eodromaeus*
24
25 *murphi*: PVSJ 562; *Segisaurus halli*: UCMP 32101; ‘*Syntarsus*’ *kayentakatae*: MCZ 9175,
26
27 cast of MNA V2623; *Megapnosaurus rhodesiensis*: NHMUK PV R9584, cast of QG1;
28
29 *Liliensternus liliensterni*: HMN MB.R. 2175; *Dilophosaurus wehtherilli*: UCMP 37302;
30
31 holotype of *Sarcosaurus woodi*: NHMUK PV R4840). By contrast, a distinct,
32
33 proximodistally elongated dorsolateral trochanter is absent in averostrans, such as
34
35 *Eoabelisaurus mefi* (MPEF PV 3990), *Ceratosaurus nasicornis* (USNM 4735) and
36
37 *Piatnitzkysaurus floresi* (PVL 4073). The base of this trochanter is moderately broad in
38
39 WARMS G681 and G682, but its surface is not preserved in either femur and it cannot be
40
41 determined if it was sharp or mound-like. The most proximal portion of the dorsolateral
42
43 trochanter is rugose and likely represents the insertion of the M. puboischiofemoralis
44
45 externus (Hutchinson, 2001). The distal development of this muscle scar cannot be
46
47 determined because of damage to the bone. The anterior surface of the proximal end of the
48
49 femur, medial to the dorsolateral trochanter, is concave.

50
51
52 The base of the anterior trochanter is preserved in both femora (Figs: 8, 9: atr). The
53
54 anterior trochanter has a subtriangular outline where it is broken off in the left femur,
55
56
57
58
59
60

1
2
3 possessing a broad base and tapering proximal end. This condition resembles that of other
4
5 early theropods (e.g. *Eodromaeus murphi*: PVSJ 562; *Megapnosaurus rhodesiensis*:
6
7 NHMUK PV R9584, cast of QG1; *Coelophysis bauri*: Melbourne specimen; *Liliensternus*
8
9 *liliensterni*: HMN MB.R. 2175; *Cryolophosaurus ellioti*: Smith *et al.*, 2007; *Dilophosaurus*
10
11 *wehtherilli*: UCMP 37302; *Ceratosaurus nasicornis*: USNM 4735; holotype of *Sarcosaurus*
12
13 *woodi*: NHMUK PV R4840), but contrasts with the aliform anterior trochanter of tetanuran
14
15 theropods (e.g. *Piatnitzkysaurus floresi*: PVL 4073; *Megalosaurus bucklandii*: NHMUK PV
16
17 R31806). The anterior trochanter is located adjacent to the medial margin of the shaft in
18
19 anterior view. It cannot be determined whether the proximal portion of the anterior trochanter
20
21 was separated from the rest of the bone by a cleft, which is the condition that occurs in the
22
23 holotype of *Sarcosaurus woodi* (NHMUK PV R4840). The preserved surfaces of the anterior
24
25 trochanter are finely striated and may indicate the insertion area of the M. iliotrochantericus
26
27 caudalis (Hutchinson & Gatesy, 2000). Lateral to the base of the anterior trochanter there is a
28
29 low, rounded, inflated area that is covered by a series of very low ridges (Figs. 8, 9: ife). This
30
31 area may represent the insertion scar of the M. iliofemoralis externus and, as a result, is
32
33 interpreted as homologous to the trochanteric shelf of robust morphotypes of basal
34
35 neotheropods (Hutchinson, 2001), such as the holotype of *Sarcosaurus woodi* (NHMUK PV
36
37 R4840). The areas of attachment of the Mm. iliotrochantericus caudalis and iliofemoralis
38
39 externus are separated by a smooth and gently concave surface. There is no sharp anterior
40
41 intermuscular line (which separates the origins of the Mm. femorotibialis externus and
42
43 femorotibialis internus in extant crocodiles; Hutchinson, 2001) extending along the
44
45 anteromedial surface of the shaft distal to the base of the anterior trochanter, contrasting with
46
47 the holotype of *Sarcosaurus woodi* (NHMUK PV R4840). The absence of a trochanteric shelf
48
49 and anterior intermuscular line in WARMS G681 and G682 could be a result of skeletal
50
51 immaturity (Raath, Carpenter & Currie, 1990; Griffin, 2018).
52
53
54
55
56
57
58
59
60

1
2
3 The fourth trochanter is restricted to the proximal half of the bone (Figs. 8, 9: ft) and
4
5 proximally extends to the level of the distal end of the anterior trochanter. The fourth
6
7 trochanter is very low and blade-like, as occurs in the holotype of *Sarcosaurus woodi*
8
9 (NHMUK PV R4840), coelophysids (e.g. *Megapnosaurus rhodesiensis*: NHMUK PV R9584,
10
11 cast of QG1); *Segisaurus halli* Camp, 1936: UCMP 32101; ‘*Syntarsus*’ *kayentakatae* Rowe,
12
13 1989: MCZ 9175, cast of MNA V2623; *Megapnosaurus rhodesiensis*: NHMUK PV R9584,
14
15 east of QG1), and early ceratosaurians (e.g. *Berberosaurus liassicus* Allain et al., 2007:
16
17 *Ceratosaurus nasicornis*: USNM 4735; *Eoabelisaurus mefi*: MPEF PV 3990; *Berberosaurus*
18
19 *liassicus*: Allain et al., 2007). The preserved margins of the fourth trochanter on the left
20
21 femur suggest that it may have been symmetric, as occurs in other neotheropods (Nesbitt,
22
23 2011). The fourth trochanter is mainly longitudinally orientated, but it slants slightly from
24
25 proximomedially to distolaterally in posterior view. Immediately medial to the base of the
26
27 fourth trochanter there is an oval depression that was probably associated with the insertion
28
29 of the M. caudofemoralis longus (Carrano & Hutchinson, 2002) (Figs. 8, 9: cfl). A low ridge
30
31 runs along the posterolateral surface of the femoral shaft from the distal end of the fourth
32
33 trochanter, but does not reach the distal end of the bone. The shaft has an oval cross-section
34
35 at mid-length, being slightly wider transversely than anteroposteriorly.
36
37
38
39
40
41

42 The distal end of the femur possesses a proximodistally well-developed mediodistal
43
44 crest (Fig. 9: mdc), as occurs in other basal neotheropods (Rowe & Gauthier, 1990; Rauhut,
45
46 2003). The degree of medial development cannot be determined because the margins of the
47
48 structure are broken in both femora. The preserved anterior surface of the mediodistal crest
49
50 possesses a series of thin longitudinal striations that may indicate the attachment of the distal
51
52 portion of the Mm. femorotibialis externus (Hutchinson, 2001) (Fig. 9: fte). The mediodistal
53
54 crest does not extend as far as the distal margin of the bone and delimits a semilunate,
55
56 concave depression on the medial surface of the bone. The lateral surface of the distal end of
57
58
59
60

1
2
3 the femur is gently anteroposteriorly convex and smooth. The cortical bone of the anterior
4 surface of the distal end of the right femur has collapsed inwards, but the anterior margin is
5 continuously transversely convex in distal view (Fig. 9E). As a result, an extensor fossa was
6 absent, resembling the condition in the *Coelophysis* sp. specimen from the Chinle Formation
7 (UCMP 129618, ‘Padian’s *Coelophysis*’), *Cryolophosaurus ellioti* (Smith *et al.*, 2007),
8 *Eodromaeus murphi* (PVSJ 562), *Liliensternus liliensterni* (HMN MB.R. 2175), *Zupaysaurus*
9 *rougieri* Arcucci & Coria, 2003 (PULR 076), *Liliensternus liliensterni* (HMN MB.R. 2175),
10 *Coelophysis* sp. specimen from the Chinle Formation (UCMP 129618, ‘Padian’s
11 *Coelophysis*’ and *Cryolophosaurus ellioti* (Smith *et al.*, 2007). By contrast, an extensor fossa
12 is present on the distal end of the femur of *Coelophysis bauri* (USNM 529376),
13 *Dilophosaurus wetherilli* (UCMP 37302, 77270), *Megapnosaurus rhodensis* (NHMUK
14 PV R9585, cast of QG CT6/G), ‘*Syntarsus*’ *kayentakatae* (MCZ 9175, cast of MNA V2623),
15 *Powellvenator podocitus* (PVL 4414-5, 8), *Segisaurus halli* (UCMP 32101), ‘*Syntarsus*’
16 *kayentakatae* (MCZ 9175, cast of MNA V2623), *Coelophysis bauri* (USNM 529376),
17 *Dilophosaurus wehtherilli* (UCMP 37302, 77270), an indeterminate Hettangian–Sinemurian
18 theropod from Dorset (NHMUK PV OR39496), and averostrans (e.g. *Ceratosaurus*
19 *nasicornis*: USNM 4735; *Eoabelisaurus mefi*: MPEF PV 3990; *Ceratosaurus nasicornis*:
20 USNM 4735; *Piatnitzkysaurus floresi*: PVL 4073). The presence of an extensor fossa cannot
21 be determined in the holotype of *Sarcosaurus woodi* because of the substantial damage to and
22 taphonomic deformation of the distal end of the bone (NHMUK PV R4840; contra Carrano &
23 Sampson, 2004). The popliteal fossa on the posterior surface of the distal end of WARMS
24 G682 is moderately broad and poorly extended proximally (Fig. 9: pf). Just proximal to the
25 popliteal fossa there is a shallowly depressed and gently striated surface that probably
26 represents the insertion of the M. adductor femoris 1 (Carrano & Hutchinson, 2002) (Fig. 9A:
27
28
29
30
31
32
33
34
35
36
37
38
39
40
41
42
43
44
45
46
47
48
49
50
51
52
53
54
55
56
57
58
59
60

1
2
3 af1). The infrapopliteal ridge was absent, contrasting with ‘*Syntarsus*’ *kayentakatae* (Rowe,
4
5 1989).
6

7
8 The tibial condyle (= medial condyle) (Fig. 9: tc) lacks its posterior end in the right
9
10 femur and is completely absent in the left one. The preserved portion of this condyle is
11
12 mainly posteriorly directed in distal view and its distal surface is continuously convex. The
13
14 fibular condyle (= lateral condyle) and the tibiofibular crest (Fig. 9: fc, tfc) are separated from
15
16 each other by a narrow and deep groove (Fig. 9E: gr), a condition widespread among early
17
18 theropods (e.g. *Dilophosaurus wetherilli*: UCMP 37302; *Eodromaeus murphi*: PVSJ 562;
19
20 *Liliensternus liliensterni*: HMN MB.R. 2175; *Zupaysaurus rougieri*: PULR 076;
21
22 *Dilophosaurus wetherilli*: UCMP 37302). Both structures form a ~~very~~ slight obtuse angle
23
24 between each other on the posterolateral corner of the bone in distal view. The medial margin
25
26 of the tibial condyle and the lateral margin of the fibular condyle are slightly convex in distal
27
28 view. Most of the tibiofibular crest is missing and, as a consequence, it cannot be determined
29
30 if it extended posteriorly beyond the level of the tibial condyle. The tibiofibular crest is
31
32 placed at the level of the proximal half of the fibular condyle and extends proximally beyond
33
34 this structure. Immediately proximally to the broken surface of the tibiofibular crest there is a
35
36 striated surface that should represent the scar for the origin of the *M. gastrocnemius* pars
37
38 *lateralis*/*M. flexor hallucis longus* (Carrano & Hutchinson, 2002) (Fig. 9A: gpl). The fibular
39
40 condyle is more convex than the tibial one and both are separated from each other by a broad
41
42 and deep intercondylar cleft in posterior view (Fig. 9A: icc). Both tibial and fibular condyles
43
44 are subequally distally projected in posterior view.
45
46
47
48
49
50
51
52
53

54 **Tibia.** Both tibiae are preserved (WARMS G668, G680), but the cnemial crests, posterior
55
56 hemicondyles of the proximal ends, and posterolateral process of the distal ends are damaged
57
58 (Figs. 10, 11; Table 2). In addition, only the base of the fibular crest is preserved, the shaft of
59
60

1
2
3 the left element is strongly transversely crushed, and the medial end of the distal end of the
4
5 right element is missing. The tibia is slightly shorter than the femur and possesses a gently
6
7 anteriorly bowed shaft in lateral or medial view, as is common among early neotheropods
8
9 (e.g. *Liliensternus liliensterni*: HMN MB.R. 2175; *Megapnosaurus rhodensiensis*: cast of QG
10
11 1). The proximal end possesses a well anteriorly developed and slightly laterally curved
12
13 cnemial crest (Figs 10, 11: cn), as occurs in other dinosaurs (Irmis *et al.*, 2007). The profile
14
15 of the cnemial crest in medial view cannot be determined because of breakage. The very base
16
17 of a diagonal, anteroproximally to posterodistally oriented elevation is present on the lateral
18
19 surface of the right cnemial crest, resembling the position of the paramarginal ridges of other
20
21 early neotheropods (e.g. *Dilophosaurus wetherilli*: UCMP 77270; *Liliensternus liliensternis*:
22
23 HMN MB.R. 2175; *Megapnosaurus rhodensiensis*: cast of QG1; *Powellvenator podocitus*:
24
25 PVL 4414-4; *Dilophosaurus wetherilli*: UCMP 77270; ‘*Sarcosaurus andrewsi*’: NHMUK PV
26
27 R3542). However, although the presence of a paramarginal ridge seems likely, it should be
28
29 considered tentative in this specimen because of the substantial damage present in this area.
30
31
32
33
34

35 The medial margin of the proximal end is more proximally extended than the lateral
36
37 one and, as a result, the proximal surface of the bone faces proximolaterally. The posterior
38
39 margins of the posterior hemicondyles are missing (Figs 10, 11: pc) and, as a result, it cannot
40
41 be determined if they were separated from each other by a groove, as in ‘*Sarcosaurus*
42
43 *andrewsi*’ (NHMUK PV R3542), nor can their complete posterior development be assessed.
44
45 The cortical bone of the medial surface of the proximal end has collapsed in both tibiae. The
46
47 medial surface of the proximal end of the right tibia is distinctly ornamented by longitudinal
48
49 striations located close to the posterior margin that may represent the scar of origin of the M.
50
51 gastocnemius pars medialis (Carrano & Hutchinson, 2002) (Fig. 11C: gms). The proximal
52
53 half of the medial surface of the cnemial crest also possesses a similarly ornamented surface
54
55 on both tibiae. Most of the lateral surface of the cnemial crest is missing in both bones.
56
57
58
59
60

1
2
3 A proximodistally well extended fibular crest is present on the centre of the lateral
4 surface of the proximal end of the tibia (Figs. 10, 11: fc). The fibular crest reaches the
5 posterior lateral hemicondyle of the proximal end, as occurs in other non-tetanuran
6 neotheropods (Rauhut, 2003), including '*Sarcosaurus andrewsi*' (NHMUK PV R3542) and
7 the indeterminate Hettangian–Sinemurian theropod from Dorset (Benson, 2010). The
8 posterolateral surface of the proximal half of the fibular crest possesses a series of thin,
9 parallel and longitudinally oriented striations on both tibiae (Figs. 10, 11: str). This surface
10 may be correlated with the attachment of the interosseum tibiofibular ligament that
11 participated in the linkage between the proximal ends of the tibia and fibula (Baumel &
12 Witmer, 1993). The fibular crest is distally extended up to approximately the same level as
13 the distal margin of the cnemial crest. The shaft of the tibia possesses a subtriangular cross-
14 section, with anteromedially and laterally facing, moderately rounded apices. The anterior
15 surface of the shaft is gently transversely convex, whereas the posterior surface is distinctly
16 more convex.

17
18
19
20
21
22
23
24
25
26
27
28
29
30
31
32
33
34
35 The distal end of the bone is transversely and ~~very~~ gently posteriorly expanded with
36 respect to the shaft. The posterior expansion is a result of the presence of a thick, longitudinal
37 posteromedial ridge (Figs. 10, 11: pmr), a plesiomorphic condition among neotheropods
38 (Nesbitt, 2011). This ridge separates a transversely convex posteromedial surface from a
39 concave posterolateral surface in the distal end of the bone (Fig. 10: plc). The posterolateral
40 surface, immediately proximal to the distal margin, possesses a series of mainly
41 longitudinally oriented, parallel, and thin striations (Fig. 10D: str). The posteromedial surface
42 also possesses a series of thin, parallel longitudinal striations on an anteroposteriorly narrow,
43 but proximodistally extended area (Fig. 10D: str). This striated surface is placed proximally
44 to the level of the posterolateral surface in both tibiae. The medial diagonal tuberosity (sensu
45 Ezcurra & Brusatte, 2011) that is present in *Camposaurus arizonensis*, *Megapnosaurus*

1
2
3 *rhodensis* and *Powellvenator podocitus* and *Megapnosaurus rhodensis* (Ezcurra &
4
5 Brusatte, 2011; Ezcurra, 2017) is absent in WARMS G668, G680 and ‘*Sarcosaurus*
6
7 *andrewsi*’ (NHMUK PV R3542).
8
9

10 The anterior surface of the tibia possesses a facet for reception of the ascending
11
12 process of the astragalus (Figs: 10, 11: fap) that is proximolaterally to mediodistally oriented
13
14 at an angle of 25° with respect to the horizontal plane, resembling the condition in
15
16 *Cryolophosaurus ellioti* (Smith *et al.*, 2007: fig. 19b: 24°), *Dilophosaurus wetherilli* (UCMP
17
18 77270: 23°), *Eoabelisaurus mefi* (MPEF PV 3990: 24°) and *Tachiraptor admirabilis*
19
20 (LPRP/USP 0747, cast of IVIC-P-2867: 23°) and *Eoabelisaurus mefi* (MPEF PV 3990: 24°).
21
22 By contrast, this angle is lower in *Zupaysaurus rougieri* (PULR 076: 19°), *Liliensternus*
23
24 *liliensterni* (HMN MB.R. 2175: ~17°), *Powellvenator podocitus* (PVL 4414-1: 18°),
25
26 *Procompsognathus triassicus* (SMNS 12591: 17°), *Zupaysaurus rougieri* (PULR 076: 19°)
27
28 and coelophysines (e.g. *Camposaurus arizonensis*: UCMP 34498, 10°; *Coelophysis bauri*:
29
30 AMNH unnumbered, 18°; *Lepidus praecisio*: Nesbitt & Ezcurra, 2015, 15°; *Megapnosaurus*
31
32 *rhodesiensis*: cast of QG 1, 17°). Notably, the angle between the facet for reception of the
33
34 ascending process of the astragalus and the shaft is ~38° in ‘*Sarcosaurus andrewsi*’, but this
35
36 angle could be greater as preserved than was originally the case in life because of the
37
38 transverse taphonomic compression that the bone has suffered. The facet for reception of the
39
40 ascending process of the astragalus of WARMS G 668 and G 680 is proximodistally more
41
42 developed and anteroposteriorly narrower, thus indicating the presence of a higher and more
43
44 laminar ascending process of the astragalus, than in coelophysids [(e.g. *Coelophysis bauri*:
45
46 AMNH unnumbered; *Dilophosaurus wetherilli* (UCMP 77270), *Gojirasaurus quayi* (HMN
47
48 MB.R. 4232.1, cast of UCM 47221), *Liliensternus liliensterni* (HMN MB.R. 2175),
49
50 *Megapnosaurus rhodesiensis*: Raath, 1977), and *Liliensternus liliensterni* (HMN MB.R.
51
52 2175), *Gojirasaurus quayi* (HMN MB.R. 4232.1, cast of UCM 47221), *Zupaysaurus rougieri*
53
54
55
56
57
58
59
60

1
2
3 (PULR 076)] and *Dilophosaurus wetherilli* (UCMP 77270). The degree of anteroposterior
4
5 development of this facet resembles that of ‘*Sarcosaurus andrewsi*’ (NHMUK PV R3542)
6
7 and *Tachiraptor admirabilis* (LPRP/USP 0747, cast of IVIC-P-2867), but is anteroposteriorly
8
9 thicker than in averostran neotheropods (e.g. *Berberosaurus liassicus*: Allain *et al.*, 2007;
10
11 *Ceratosaurus nasicornis*: USNM 4735; *Berberosaurus liassicus*: Allain *et al.*, 2007;
12
13 *Piatnitzkysaurus floresii*: MACN-Pv CH 895). Woodward (1908) recognized that the shape of
14
15 the facet for the reception of the ascending process suggests closer affinities of ‘*Sarcosaurus*
16
17 *andrewsi*’ with Jurassic rather than Triassic theropods. This facet extends mediodistally to the
18
19 preserved corner of the bone in WARMS G668, G680.
20
21
22
23

24 The anterior surface of the tibia immediately proximal to the facet for reception of the
25
26 astragalar ascending process lacks the thick anterior diagonal tuberosity present in several
27
28 coelophysoids (i.e. *Camposaurus arizonensis*, *Coelophysis bauri*, *Lepidus praecisio*,
29
30 *Megapnosaurus rhodensiensis*, *Procompsognathus triassicus*, ~~*Camposaurus arizonensis*,~~
31
32 ~~*Megapnosaurus rhodensiensis*, *Coelophysis bauri*, *Lepidus praecisio*~~; Ezcurra & Brusatte,
33
34 2011; Nesbitt & Ezcurra, 2015; Ezcurra 2017) and ‘*Sarcosaurus andrewsi*’ (NHMUK PV
35
36 R3542). By contrast, WARMS G 668 and G 680 possess in this area a series of longitudinally
37
38 oriented striations, which are better preserved on the right tibia (Figs: 10A, 11A: str). The
39
40 anterior diagonal tuberosity also possesses a rough, striated surface in other neotherpods
41
42 (e.g. *Coelophysis bauri*: AMNH FARB 30615; *Procompsognathus triassicus*: SMNS 12591)
43
44 and may have been involved in the attachment of homologous soft tissues. The longitudinal
45
46 ridge present along the lateral surface of the distal third of the tibia of *Camposaurus*
47
48 *arizonensis* (Ezcurra & Brusatte, 2011) is absent in WARMS G 668 and G 680 and
49
50 ‘*Sarcosaurus andrewsi*’ (NHMUK PV R3542).
51
52
53
54
55

56 The posterolateral process of the distal end is directly laterally oriented (Figs, 10, 11:
57
58 plp), but because its edge is missing in both tibiae its degree of development and complete
59
60

1
2
3 outline cannot be determined. There is an inflexion that separates the more distally extended
4 posterolateral process from the medial portion of the bone, as occurs in other early
5
6 neotheropods (Nesbitt & Ezcurra, 2015; Ezcurra, 2017). The medial portion of the distal end
7
8 gradually expands medially with respect to the shaft in anterior or posterior view, resembling
9
10 the condition in non-averostran theropods (e.g. ‘*Sarcosaurus andrewsi*’: NHMUK PV
11
12 R3542), but contrasting with the more distinct medial development present in *Tachiraptor*
13
14 *admirabilis* (LPRP/USP 0747, cast of IVIC-P-2867) and averostrans (e.g. *Ceratosaurus*
15
16 *nasicornis*: USNM 4735; *Eoabelisaurus mefi*: MPEF PV 3990; *Piatnitzkysaurus floresi*:
17
18 MACN-Pv CH 895). The distal surface of the tibia possesses a subtriangular outline in distal
19
20 view that closely resembles that present in non-averostran neotheropods (e.g. *Coelophysis*
21
22 *bauri*: AMNH unnumbered; *Dilophosaurus wetherilli*: UCMP 77270; *Zupaysaurus rougieri*:
23
24 ~~PULR-076~~; *Liliensternus liliensterni*: HMN MB.R. 2175; *Dilophosaurus wetherilli*: UCMP
25
26 ~~77270~~; ‘*Sarcosaurus andrewsi*’: NHMUK PV R3542; *Zupaysaurus rougieri*: PULR 076;
27
28 *Coelophysis bauri*: AMNH unnumbered). By contrast, *Tachiraptor admirabilis* and
29
30 averostrans possess a proportionally anteroposteriorly wider distal end (Rauhut, 2003; Langer
31
32 *et al.*, 2014). The distal surface of the bone has a distinct posteromedial notch located
33
34 immediately distal to the posteromedial ridge (Figs: 10, 11: pmn). This notch would have
35
36 received a pyramidal posteromedial process of the astragalus and is widely distributed among
37
38 basal neotheropods (Ezcurra & Novas, 2007). The development of this notch is similar to that
39
40 in ‘*Sarcosaurus andrewsi*’ (NHMUK PV R3542) and some other early neotheropods (e.g.
41
42 *Dilophosaurus wetherilli*: UCMP 77270; *Liliensternus liliensterni*: HMN MB.R. 2175;
43
44 *Zupaysaurus rougieri*: PULR 076; *Liliensternus liliensterni*: HMN MB.R. 2175;
45
46 *Dilophosaurus wetherilli*: UCMP 77270).

1
2
3 **Fibula.** The proximal end of the left fibula (WARMS G669) is preserved (Fig. 12A–C; Table
4
5 2). This element was originally interpreted by Huene (1932) as the distal end of the left pubis,
6
7 but it is too large and its morphology is not consistent with this interpretation.
8
9

10 The fibula is comma-shaped in proximal view, with a transversely broader anterior
11 portion (Fig. 12C), as occurs in other early neotheropods (e.g. *Dilophosaurus wetherilli*:
12 UCMP 37302; *Liliensternus liliensterni*: HMN MB.R. 2175; *Megapnosaurus rhodesiensis*:
13 cast of QG1; *Liliensternus liliensterni*: HMN MB.R. 2175; *Dilophosaurus wetherilli*: UCMP
14 37302; *Piatnitzkysaurus floresi*: PVL 4073). By contrast, the anterior portion of the bone
15 tapers in proximal view in *Eodromaeus murphi* (PVSJ 562). The proximal surface of the
16 bone is slightly transversely convex and distinctly concave anteroposteriorly in side view,
17 resembling the condition in several other early theropods (e.g. *Berberosaurus liassicus*:
18 Allain et al., 2007; *Dilophosaurus wetherilli*: UCMP 37302; *Dracoraptor hanigani*: NMW
19 2015.5G.3; *Eodromaeus murphi*: PVSJ 562; *Liliensternus liliensterni*: HMN MB.R. 2175;
20 *Dilophosaurus wetherilli*: UCMP 37302; *Piatnitzkysaurus floresi*: PVL 4073; *Dracoraptor*
21 *hanigani*: NMW 2015.5G.3; *Liliensternus liliensterni*: HMN MB.R. 2175; *Berberosaurus*
22 *liassicus*: Allain et al., 2007). The posterior margin is apparently more projected than the
23 anterior margin in lateral view, but it is difficult to determine this confidently based only on
24 the proximal end of the bone. The posterior expansion is less conspicuous and developed than
25 in *Coelophysis bauri* (MCZ 4331), *Dilophosaurus wetherilli* (UCMP 37302), *Dracoraptor*
26 *hanigani* (NMW 2015.5G.3); and *Megapnosaurus rhodesiensis* (cast of QG1); *Coelophysis*
27 *bauri* (MCZ 4331) and *Dilophosaurus wetherilli* (UCMP 37302), but resembles more closely
28 the condition in *Eodromaeus murphi* (PVSJ 562) and *Liliensternus liliensterni* (HMN MB.R.
29 2175). The anterior margin of the bone is slightly weathered, but it seems to have been
30 mostly straight. The posterior edge is straight proximally and slightly concave more distally
31 in lateral view. The lateral surface is anteroposteriorly convex and the portion of bone
32
33
34
35
36
37
38
39
40
41
42
43
44
45
46
47
48
49
50
51
52
53
54
55
56
57
58
59
60

1
2
3 adjacent to the proximal edge is laterally inflated. This inflated surface is rounded and
4
5 decreases in height posteriorly. The anterolateral surface of the bone approximately 2 cm
6
7 distal to the proximal margin possesses a rugose scar, but this appears to be too proximal for
8
9 the insertion of the M. iliofibularis. The medial surface of the bone is anteroposteriorly
10
11 concave and lacks a ridge or well-rimmed fossa, as occurs in *Dilophosaurus wetherilli*
12
13 (UCMP 37302), *Dracoraptor hanigani* (NMW 2015.5G.3) and *Liliensternus liliensterni*
14
15 (UCMP 37302), *Dracoraptor hanigani* (NMW 2015.5G.3) and *Dilophosaurus wetherilli*
16
17 (HMN MB.R. 2175), *Dracoraptor hanigani* (NMW 2015.5G.3) and *Dilophosaurus wetherilli*
18
19 (UCMP 37302), but contrasting with the presence of these features in several other early
20
21 theropods (e.g. *Berberosaurus liassicus*: Allain *et al.*, 2007; *Eodromaeus murphi*: PVSJ 562;
22
23 *Megapnosaurus rhodesiensis*: cast of QG1; *Powellvenator podocitus*: PVL 4414-4;
24
25 *Segisaurus halli*: UCMP 32101; ‘*Syntarsus*’ *kayentakatae*: Tykoski, 2005: fig. 93; *Segisaurus*
26
27 *halli*: UCMP 32101; *Powellvenator podocitus*: PVL 4414-4; *Megapnosaurus rhodesiensis*:
28
29 cast of QG1; *Berberosaurus liassicus*: Allain *et al.*, 2007). The most distal preserved portion
30
31 of the medial surface of the bone has a depression that appears to be the result of the collapse
32
33 of cortical bone.
34
35
36

37
38 Huene (1932) originally identified a distal end of a fibula. This bone (WARMS G674,
39
40 Fig. 12D, E; Table 2) does not possess distinct characters to allow an unambiguous
41
42 identification, but it is larger than would be expected and its morphology is not consistent
43
44 with those of the distal half of an ulna, radius, pubis, ischium, or metatarsal. This bone
45
46 apparently lacks the anteroposterior and somewhat transverse expansion that is observed in
47
48 the distal end of the fibula of other basal neotheropods (e.g. *Zupaysaurus rougieri*: PULR
49
50 076). As a result, this bone might belong to the distal portion of a fibula with a damaged
51
52 distal end.
53
54

55
56 The bone possesses a straight shaft with a suboval cross-section, in which one of the
57
58 shorter margins is sharper than the other. The most proximally preserved portion of the shaft
59
60

1
2
3 is heavily taphonomically distorted and crushed. The distal end of the bone is more
4
5 compressed than the shaft and slightly anteroposteriorly expanded if interpreted as a fibula.
6
7 The lateral surface of the distal end is rugose (Fig. 12E: rug), indicating a soft tissue
8
9 attachment area. The medial surface of this end has a shallow, rather well-defined
10
11 longitudinal groove, adjacent to which there is a rounded inflated surface (Fig. 12D: gr).
12
13 There is a sharp, longitudinal ridge running along the anterior or posterior surface of the
14
15 bone, which does not reach the distal margin. The distal surface is partially eroded, but its
16
17 better-preserved region is ~~very~~ slightly concave.
18
19
20
21
22
23

24 **Metatarsus.** The metatarsus is represented by the distal halves of metatarsals II and IV₅ and
25
26 the distal portion of metatarsal III from the left side. In addition, the proximal end of a
27
28 metatarsal II or III is also preserved, although it is unclear whether this element is from the
29
30 left or right side (Fig. 13A–H, L; Table 2).
31
32

33 The preserved portion of the shaft of metatarsal II (WARMS G672) is straight and
34
35 possesses a suboval cross-section, with a less convex posterolateral surface (Fig. 13A–C).
36
37 The distal end of the bone is anteroposteriorly and ~~very~~ gently transversely expanded. The
38
39 collateral fossae have a similar development and shape on both sides (Fig. 13A–C: clf),
40
41 resembling the condition in *Liliensternus liliensterni* (HMN MB.R. 2175). By contrast, the
42
43 lateral collateral fossa is distinctly bigger than the medial one in the metatarsal II of
44
45 *Dilophosaurus wetherilli* (UCMP 37302) and *Megapnosaurus rhodesiensis* (cast of QG1)
46
47 ~~and *Dilophosaurus wetherilli* (UCMP 37302)~~. There is no extensor fossa on the anterior
48
49 surface of the bone, immediately proximal to the distal articular surface, as occurs in
50
51 *Dracoraptor hanigani* (NMW 2015.10G.1a/b), *Liliensternus lilienstenri* (HMN MB.R. 2175)
52
53 and *Dilophosaurus wetherilli* (UCMP 37302). There is a subtle extensor depression in the
54
55 metatarsal II of *Megapnosaurus rhodesiensis* (cast of QG1). Nevertheless, there is a
56
57
58
59
60

1
2
3 subtriangular roughened area in WARMS G672 that probably is the scar of the attachment
4 area of extensor ligaments. The distal articular surface is approximately as tall as broad (Fig.
5 13C). However, this surface is asymmetric in anterior and posterior views, with the lateral
6 portion more distally developed than the medial one. As a result, the entire surface slants
7 medially. This should have resulted in an intumed proximal phalanx, as usually occurs in the
8 foot of other theropods (e.g. *Dilophosaurus wetherilli*: UCMP 37302). The medial and lateral
9 halves of the distal articular surface are separated from each other by a deep median posterior
10 groove, as it is typical of metatarsal II of neotheropods (e.g. *Dilophosaurus wetherilli*: UCMP
11 37302; *Liliensternus lilienstenri*: HMN MB.R. 2175; ~~*Dilophosaurus wetherilli*: UCMP~~
12 ~~37302~~). The medial portion of the bone is complete and the lateral one lacks its posterior end,
13 but as far as it is preserved it extends posteriorly up to the same level as the medial one.
14 Therefore, the latter facet was probably more extended posteriorly than the medial one, as
15 occurs in other neotheropods (e.g. *Dilophosaurus wetherilli*: UCMP 37302; *Liliensternus*
16 *lilienstenri*: HMN MB.R. 2175); ~~*Dilophosaurus wetherilli*: UCMP 37302~~).

17
18
19
20
21
22
23
24
25
26
27
28
29
30
31
32
33
34
35
36 The distal portion of metatarsal III (WARMS G673) possesses a subtriangular shaft in
37 cross-section where it is broken off (Fig. 13D–F). This is as a consequence of a gently
38 transversely convex anterior surface and a posteriorly facing apex that forms a strongly
39 transversely convex posterior surface. The distal end is anteroposteriorly and slightly
40 transversely expanded with respect to the shaft. The collateral fossae are present on both
41 sides and possess a teardrop-shaped outline, with a proximally oriented apex (Fig. 13F: clf).
42 The medial fossa is longer and higher than the lateral one, but both possess a similar depth, as
43 occurs in *Megapnosaurus rhodesiensis* (cast of QG1). The distal articular surface is strongly
44 anteroposteriorly convex and rather symmetric, being slightly deeper than broad with the
45 medial portion slightly higher than the lateral one (Fig. 13D). There is no intercondylar
46 groove on the articular surface and only a broad and shallow notch separates both surfaces on
47
48
49
50
51
52
53
54
55
56
57
58
59
60

1
2
3 the posterior surface of the bone, as occurs in the metatarsal III of other neotheropods (e.g.

4
5 *Dilophosaurus wetherilli*: UCMP 37302; *Liliensternus liliensterni*: HMN MB.R. 2175;

6
7 *Dilophosaurus wetherilli*: UCMP 37302). The anterior and posterior surfaces of the distal end
8
9 are damaged, but apparently there was no extensor fossa on the former surface.

10
11
12 The preserved portion of shaft of metatarsal IV (WARMS G677) is straight (Fig. 13G,
13
14 H), although it may have bowed laterally more proximally as is common among theropods

15
16 (e.g. *Dilophosaurus wetherilli*: UCMP 37302; *Megapnosaurus rhodesiensis*: cast of QG1;

17
18 *Liliensternus liliensterni*: HMN MB.R. 2175; *Megapnosaurus rhodesiensis*: cast of QG1;

19
20 *Dilophosaurus wetherilli*: UCMP 37302). The distal end of the bone is severely damaged, but

21
22 was transversely narrower than those of metatarsals II and III. The general shape of this distal

23
24 end is consistent with that of metatarsal IV in other theropods (e.g. *Dilophosaurus wetherilli*:

25
26 UCMP 37302; *Liliensternus liliensterni*: HMN MB.R. 2175; *Megapnosaurus rhodesiensis*:

27
28 cast of QG1; *Liliensternus liliensterni*: HMN MB.R. 2175; *Dilophosaurus wetherilli*: UCMP

29
30 37302), but its degree of asymmetry cannot be determined. The medial surface of the distal

31
32 end possesses a shallow and oval collateral fossa, with a proximodistal long axis (Fig. 13H:

33
34 clf). On the lateral surface of the bone there is a ~~very~~ shallow depression that would probably

35
36 have continued distally onto the lateral collateral fossa. If this was the case, then it was

37
38 considerably more distally placed than that on the medial surface. This condition resembles

39
40 that of *Dilophosaurus wetherilli* (UCMP 37302). The anterior surface of the distal end of the

41
42 bone is missing.

43
44 The proximal end of a metatarsal is preserved (WARMS G671), but is severely

45
46 damaged and most of its cortical bone is lost (Fig. 13L). The bone was apparently

47
48 transversely expanded at its end and possesses a subrectangular outline in proximal view as

49
50 preserved. The size and outline of the bone rule out its identification as the proximal end of

51
52 metatarsals I, IV₅ and V. By contrast, its size and shape are consistent with those of the

1
2
3 metatarsals II and III of other early neotheropods, which possesses trapezoidal and
4
5 subrectangular outlines in proximal view (e.g. *Dilophosaurus wetherilli*: UCMP 37302;
6
7 *Liliensternus liliensterni*: HMN MB.R. 2175; ~~*Dilophosaurus wetherilli*: UCMP 37302~~). As a
8
9 result, this bone is identified as either the right or left proximal end of a metatarsal II or III.
10
11
12
13
14

15 **Pedal phalanx.** The proximal half of a non-ungual phalanx is preserved (WARMS G687,
16
17 Fig. 13I–K) and belongs to the foot because a manual phalanx would be expected to be
18
19 proportionally narrower. This phalanx is large and its size fits with that expected for the most
20
21 proximal phalanx of digit II or III. In addition, the outline of the bone in proximal view is
22
23 identical to that of phalanx II-1 of *Dilophosaurus wetherilli* (UCMP 37302) and the height
24
25 and width of the proximal end fits perfectly with the distal end of the left metatarsal II. Thus,
26
27 this element is identified as a left phalanx II-1. The proximal surface is heavily covered with
28
29 matrix and it cannot be determined whether the articular facet was undivided as in proximal
30
31 phalanges or not. The proximal end of the bone is more expanded anteriorly than posteriorly
32
33 and, as a result, the former margin of the phalanx is more arched in lateral view. The
34
35 proximolateral margin is slightly more posteriorly developed than the proximomedial one and
36
37 possesses a more squared corner in lateral view than the more acute medial corner. The
38
39 medial margin of the proximal end has a distinct, low apex at mid-height and the lateral
40
41 margin is damaged. The bone is subcircular in cross-section close to its mid-length, where it
42
43 is broken off.
44
45
46
47
48
49
50

51 **Dorsal rib histology.** A thin section of one of the preserved rib shafts (WARMS G676) was
52
53 made to examine bone microstructure (Fig. 14). This portion of the shaft is comma-shaped in
54
55 cross-section, with a concave posterior and a convex anterior surface. The medial surface of
56
57 the bone has broken away post-mortem and the lateral surface is strongly anteroposteriorly
58
59
60

1
2
3 convex. The shaft has a transverse width of 8.0 mm and a maximum preserved
4
5 anteroposterior length of 12.4 mm. The rib thin section lacks one end and the outermost
6
7 region of the bone cortex has been damaged in some areas. The subperiosteal surface
8
9 underwent a prominent diagenetic alteration along nearly the entire circumference of the bone
10
11 (black area on the outermost region of the slice); ~~however,~~ but apart from these superficial
12
13 taphonomic artefacts, the bone microstructure is otherwise ~~very~~-well-preserved. The cross-
14
15 section of the rib is suboval, tapering slightly towards the missing end of the slice. There is
16
17 conspicuous bone remodelling, which is particularly evident in the posterior (upper) region of
18
19 the section as the compact spongy bone (Fig. 14: csb) extends close to the subperiosteal
20
21 surface. Although remodelled, this tissue is not Haversian bone as it lacks cement lines. In the
22
23 non-remodelled region of the slice, the primary bone is composed of fibrolamellar tissue (Fig.
24
25 14: flb), which occupies approximately 14% of the transverse width and 18% of the
26
27 anteroposterior length of the section as preserved. The primary bone has a ~~very~~-high density
28
29 of large, randomly organi~~z~~ed longitudinal primary osteons, which are more densely packed
30
31 in the lateral (left) region of the slice. Only a few vascular canals possess circumferential
32
33 anastomoses that connect to other canals. No Sharpey's fibres are present in the section. The
34
35 outermost region is composed of pseudolamellar bone (= parallel-fibred bone *sensu* de
36
37 Ricqlès, 1975; Fig. 14: plb) and possesses at least seven annuli visible on the upper left of the
38
39 slice (Fig. 14C, D: arrowheads), with older annuli assumed to have been lost due to the
40
41 underlying remodelling. The most external five annuli are closely packed, but there is some
42
43 longitudinal vascularization in the zones that separate these annuli from each other and, as a
44
45 result, it cannot be interpreted as an external fundamental system.
46
47
48
49
50
51
52
53
54
55

56 RESULTS OF THE PHYLOGENETIC ANALYSES

57
58
59
60

1
2
3 **Analysis using *Sarcosaurus woodi*, WARMS G667–690 and ‘*Sarcosaurus andrewsi*’ as**
4 **different terminals.** The analysis of the data matrix using the three neotheropod specimens
5
6 from central England as different terminals found 27 most parsimonious trees (MPTs) of
7
8 1267 steps with a consistency index (CI) of 0.3631 and a retention index (RI) of 0.7052 (best
9
10 score hit 73 times of the 100 replicates). The overall topology of these MPTs is mostly
11
12 congruent with those recovered in the analyses of the most recent iterations of this matrix
13
14 (Ezcurra, 2017; Marsola *et al.*, 2019; Marsh *et al.*, 2019b), but with some differences related
15
16 to unstable terminals within Neotheropoda (see Discussion). Resembling previous analyses,
17
18 we found a major dichotomy at the base of Neotheropoda between Coelophysoidea and a
19
20 lineage leading to Averostra. The strict consensus tree (SCT) generated from the MPTs
21
22 shows a relatively well-constrained position for the three specimens studied here. They are
23
24 nested in the lineage leading to Averostra, in a polytomy together with *Tachiraptor*
25
26 *admirabilis* and Averostra. This polytomy results from the collapse of zero-length branches
27
28 because there are no synapomorphies supporting sister-taxon relationships among WARMS
29
30 G667–690, ‘*Sarcosaurus andrewsi*’ and *Sarcosaurus woodi*, or the placement of any of them
31
32 closer to Averostra. The inclusion of *Tachiraptor admirabilis* in this polytomy is as a result
33
34 of the placement of *Sarcosaurus woodi* as the sister-taxon of Averostra in some MPTs.
35
36
37
38
39
40
41

42 *Sarcosaurus woodi* is recovered as one of the most immediate sister-taxa to Averostra
43
44 because of the presence of the following synapomorphies: ilium with anteroventrally oriented
45
46 ventral margin of the preacetabular process in lateral view, forming a very-narrow gap
47
48 between the process and the pubic peduncle (character 376: 0->1) and femur with poorly
49
50 posteriorly developed fourth trochanter, raised from the shaft as a low ridge (character 377:
51
52 0->1). WARMS G667–690 is placed in one of the successive nodes leading to Averostra
53
54 because of the presence of one synapomorphy of the *Gojirasaurus quayi* + Averostra clade,
55
56 tibia with angle between the main axis of the lateral half of the facet for reception of the
57
58
59
60

1
2
3 ascending process of the astragalus in anterior view and the longitudinal axis of the bone
4
5 $>20^\circ$ (character 378: 1- \rightarrow 2), and the following synapomorphies of the WARMS G667–690 +
6
7 ‘*Sarcosaurus andrewsi*’ + *Sarcosaurus woodi* + *Tachiraptor admirabilis* + Averostra clade,
8
9 astragalus with plate-like/laminar ascending process (character 274: 0- \rightarrow 1) and character state
10
11 377 (0- \rightarrow 1, see above for its explanation). Similarly, ‘*Sarcosaurus andrewsi*’ is recovered in
12
13 the lineage leading to Averostra because of the presence of character state 274 (0- \rightarrow 1). These
14
15 two specimens are excluded from the *Tachiraptor admirabilis* + Averostra clade because of
16
17 the absence of a tibia with a distinct, but shallow posteromedially opened notch on the distal
18
19 end (character 343: 2- \rightarrow 1) and with a subtriangular distal profile and an
20
21 anteroposterior:mediolateral width < 0.6 (character 371: 1- \rightarrow 2).
22
23
24
25

26 The Bremer supports of Neotheropoda and all less inclusive clades nested within it
27
28 (with the exception of Tetanurae) are minimal (=1), whereas that of Tetanurae is 6. The
29
30 absolute and GC bootstrap frequencies for Coelophysoidea, the lineage leading to Averostra
31
32 and all less inclusive clades nested within it (with the exception of Averostra, Ceratosauria
33
34 and Tetanurae) are lower than 50%. The resampling absolute frequency for Neotheropoda is
35
36 50% and its GC frequency is considerably lower, 33%, indicating a relatively high amount of
37
38 contradictory information for this branch. Tetanurae is the best supported branch within
39
40 Neotheropoda with high absolute and GC bootstrap frequencies, both of 98%. The pruning of
41
42 eight topologically unstable terminals among the suboptimal trees (*Camposaurus arizonensis*,
43
44 *Chindesaurus bryansmalli* Long & Murry, 1995, *Gojirasaurus quayi*, *Lepidus praecisio*,
45
46 *Tachiraptor admirabilis*, *Lucinavenator bonoi* Martinez & Apaldetti, 2017, *Gojirasaurus*
47
48 *quayi*, *Nhandumirim waldsangae* Marsola et al., 2019, *Lepidus praecisio*, *Camposaurus*
49
50 *arizonensis*, *Chindesaurus bryansmalli* and *Staurikosaurus pricei* Colbert, 1970 and
51
52 *Tachiraptor admirabilis*; the three specimens from central England were also recovered as
53
54 unstable terminals, but they were not pruned) resulted in increased Bremer supports of 6 for
55
56
57
58
59
60

1
2
3 Neotheropoda, 3 for Coelophysidae and the *Panguraptor lufengensis* [You et al., 2014](#) +
4
5 Coelophysinae branch, and 2 for Averostran.
6
7

8 Under constrained suboptimal topologies, one additional step is necessary to place
9
10 *Sarcosaurus woodi* as the sister taxon of Coelophysidae (a placement supported by character
11
12 state 377: 0->1) and two extra steps to find it as a ceratosaurian averostran (supported by
13
14 character state 377: 0->1 in some trees and no apomorphies in other trees). WARMS G667–
15
16 690 and ‘*Sarcosaurus andrewsi*’ remain as non-averostran, non-coelophysoid neotheropods
17
18 in these two constrained analyses. Regarding ‘*Sarcosaurus andrewsi*’, one additional step is
19
20 necessary to recover it as the sister-taxon of *Gojirasaurus quayi*, two extra steps are required
21
22 to recover it as the earliest branching member of the lineage leading to Averostran, one of the
23
24 earliest branching coelophysoids or the sister-taxon of Neotheropoda, and four extra steps for
25
26 its placement as a ceratosaurian averostran (but no apomorphies support these four positions).
27
28 Under these searches, *Sarcosaurus woodi* and WARMS G667–690 were found in placements
29
30 close to that constrained for ‘*Sarcosaurus andrewsi*’. One additional step is required to find
31
32 WARMS G667–690 as the sister-taxon of Coelophysidae (supported by character state 377:
33
34 0->1) and three extra steps to place it as a ceratosaurian averostran (supported by a fibula
35
36 with a symmetrical or nearly symmetrical proximal portion in lateral view, character state
37
38 262: 1->0; and character state 377: 0->1).
39
40
41
42
43
44
45
46

47 **Analysis merging *Sarcosaurus woodi*, WARMS G667–690 and ‘*Sarcosaurus andrewsi*’**
48
49 **into a single terminal.** The analysis of the matrix with the scoring of *Sarcosaurus woodi*
50
51 (Figs. 15–17), ‘*Sarcosaurus andrewsi*’ (Fig. 18) and WARMS G667–690 as a single terminal
52
53 (‘*Sarcosaurus woodi* combined’) recovered nine MPTs. These trees are of 1266 steps, with a
54
55 CI of 0.3633 and a RI of 0.7055 (best score hit 95 times of the 100 replicates). The MPTs
56
57 show congruent topologies to those described in the previous analysis, including the
58
59
60

1
2
3 placement of ‘*Sarcosaurus woodi* combined’ as the sister-taxon of the *Tachiraptor*
4
5 *admirabilis* + Averostra clade (Fig. 19). The phylogenetic placement of this terminal on the
6
7 branch leading to Averostra is supported by the synapomorphies of the *Gojirasaurus quayi* +
8
9 Averostra clade (character state 378: 1->2), and of the ‘*Sarcosaurus woodi* combined’ +
10
11 Averostra clade (character state 274: 0->1, character state 376: 0->1). ‘*Sarcosaurus woodi*
12
13 combined’ is excluded from the *Tachiraptor admirabilis* + Averostra clade because of the
14
15 absence of character states 343 (2->1) and 371 (1->2).
16
17
18

19
20 The Bremer supports and bootstrap frequencies are similar to those of the previous
21
22 analysis, but generally slightly higher in the branches leading to Averostra. The Bremer
23
24 support of the *Tachiraptor admirabilis* + Averostra branch is 2. The bootstrap absolute
25
26 frequencies are of 50% or higher in the ‘*Sarcosaurus woodi* combined’ + Averostra, and
27
28 *Tachiraptor admirabilis* + Averostra branches. The pruning of topologically unstable
29
30 terminals (excluding the same terminals listed for the first analysis plus *Dracoraptor*
31
32 *hanigani* and *Liliensternus liliensterni*) from the Bremer support calculation resulted in
33
34 increased values of 6 for Neotheropoda, 5 for Coelophysoidea, 4 for Averostra, 2 for the
35
36 *Zupaysaurus rougieri* + Averostra and *Cryolophosaurus ellioti* + Averostra branches, and 3
37
38 for the *Panguraptor lufengensis* + Coelophysinae branch. Tree searches using topological
39
40 constrains show that two additional steps are necessary to force the position of ‘*Sarcosaurus*
41
42 *woodi* combined’ as the earliest branching member of the lineage leading to Averostra (no
43
44 apomorphy supports this position), the sister-taxon of Neotheropoda (no apomorphy supports
45
46 exclusion from Neotheropoda), or the sister-taxon of Coelophysidae (supported by character
47
48 state 377: 0->1), and four extra steps to place it as a ceratosaurian averostran (supported by
49
50 character states 262: 1->0 and 377: 0->1).
51
52
53
54
55
56
57
58
59
60

DISCUSSION

1
2
3
4
5
6 *Ontogenetic stage of the neotheropods from the Early Jurassic of central England*
7

8 The assessment of ontogenetic stage in early dinosaurs and their immediate precursors has
9 important implications for character scorings and, thus, in the inference of the phylogenetic
10 relationships of species (Rowe, 1989; Rowe & Gauthier, 1990; Tykoski & Rowe, 2004;
11 Tykoski, 2005; Griffin, 2018). The bone microstructure of the rib slice of WARMS G667–
12 690 was used to assess the ontogenetic stage of the individual at the time of its death,
13 resembling previous studies that have used ribs to determine the degree of skeletal maturity
14 (e.g. Erickson *et al.*, 2004). The rib thin slice of WARMS G667–690 indicates that the animal
15 was not a juvenile because of the presence of substantial bone remodelling and several
16 annuli, suggesting a minimum age of eight years at the time of its death. These annuli
17 represent periods of diminution of the rate of osseous growth and there is a substantial
18 amount of evidence that these and other growth marks (e.g. lines of arrested growth) have an
19 annual genesis (Erickson, 2005). The number of annuli in the sampled rib should be
20 considered as a minimum count because of bone remodelling and also because histological
21 variation, including in the number of growth marks, is common among the bones of a single
22 individual (Horner *et al.*, 1999, 2000). The absence of an external fundamental system
23 indicates that the specimen had not reached somatic maturity, although its growth had
24 probably already decelerated because of the concentration of annuli close to the periphery of
25 the bone slice. In congruence with the histological evidence, the presence of open
26 neurocentral sutures in the preserved dorsal and caudal vertebrae indicates skeletal
27 immaturity because the centrum and neural arch fuses during ontogeny in both
28 pseudosuchians and extinct dinosaurs, and in extant birds this fusion can occur before
29 (precocial birds) or after hatching (altricial birds) (Starck, 1993; Brochu, 1996; Irmis, 2007).
30 As a result, the absence of fusion between the tibia, fibula and proximal tarsals that is
31
32
33
34
35
36
37
38
39
40
41
42
43
44
45
46
47
48
49
50
51
52
53
54
55
56
57
58
59
60

1
2
3 observed in adult non-tetanuran neotheropod specimens may be a consequence of such
4 skeletal immaturity in WARMS G667–690. In the case of the holotype of ‘*Sarcosaurus*
5 *andrewsi*’, we lack direct evidence of its ontogenetic stage. As a result, the absence of fusion
6 between tibia, fibula and proximal tarsals cannot be unambiguously explained as a
7 consequence of skeletal immaturity in this specimen. Beyond the ontogenetic stage, the tibia
8 of the holotype of ‘*Sarcosaurus andrewsi*’ is considerably longer (c. 45 cm) than that of
9 WARMS G667–690 (c. 30 cm) (Tables 2, 3).

19 The holotype of *Sarcosaurus woodi* has a femoral length ~~very~~-similar to that of
20 WARMS G667–690 (c. 32 cm; Table 4), but it shows some evidence of skeletal maturity.
21 The ilium and pubis are fused to each other, and the femur possesses a trochanteric shelf and
22 a distinct anterior intermuscular line, which are conditions that occur along the ontogeny of
23 several non-tetanuran neotheropods (Rowe, 1989; Rowe & Gauthier, 1990; Tykoski & Rowe,
24 2004; Tykoski, 2005; Griffin & Nesbitt, 2016; Griffin, 2018). It cannot be determined if the
25 fusion between ilium and pubis occurred in WARMS G667–690 because the articular
26 surfaces between these bones are lost in this specimen. However, the absence of a
27 trochanteric shelf and anterior intermuscular line suggests that WARMS G667–690 was less
28 skeletally mature than the holotype of *Sarcosaurus woodi*, despite their similar size. The
29 neurocentral sutures of the preserved dorsal vertebra of *Sarcosaurus woodi* appear to be
30 closed, but poor preservation of the bone precludes a confident assessment. As a result, it can
31 be interpreted that the holotype of *Sarcosaurus woodi* does not belong to a juvenile and was
32 probably somewhat more skeletally mature than WARMS G667–690, but we cannot
33 determine if it had already reached complete somatic maturity and was an adult individual at
34 the time of its death.

1
2
3 *Taxonomy and phylogenetic relationships of the Early Jurassic neotheropods from central*
4 *England*
5
6

7 Carrano & Sampson (2004) concluded that both *Sarcosaurus woodi* and ‘*Sarcosaurus*
8 *andrewsi*’ were *nomina dubia* because of the absence of discernable diagnostic features, and
9 that WARMS G667–690 was referable to cf. *Sarcosaurus woodi*. The results of our
10 phylogenetic analyses indicate that the holotypes of *Sarcosaurus woodi* and ‘*Sarcosaurus*
11 *andrewsi*’ and WARMS G667–690 possess a congruent phylogenetic signal, all three being
12 recovered among the most immediate sister-taxa to *Averostra*. As a result, previous claims of
13 a probable close relationship between these specimens (Andrews, 1921; Huene, 1932;
14 Carrano & Sampson, 2004) are not contradicted by the evidence provided here. Another
15 interesting result of the phylogenetic analyses is the placement of these three specimens in a
16 part of the trees shared only with *Tachiraptor admirabilis*; in other words, there is a unique
17 combination of apomorphies that distinguishes the English specimens from the vast majority
18 of terminals scored in the matrix. As a consequence, these results raise the questions of
19 whether these specimens can be actually distinguished from each other at a species level and
20 from other neotheropod species.
21
22
23
24
25
26
27
28
29
30
31
32
33
34
35
36
37
38
39

40 The ilium of *Sarcosaurus woodi* possesses a morphology that clearly departs from
41 those of *Liliensternus liliensterni*, coelophysids (e.g. ‘*Coelophysis bauri*, *Lucianovenator*
42 *bonoi*, *Syntarsus*’ *kayentakatae*, *Megapnosaurus rhodesiensis*, ‘*Syntarsus*’ *kayentakatae*,
43 *Coelophysis bauri*, *Lucianovenator bonoi*) and *Cryolophosaurus ellioti* in the presence of a
44 strongly anteroventrally oriented main axis of the preacetabular process in lateral view
45 (unknown in *Cryolophosaurus ellioti*), an ischiadic peduncle only incipiently posteriorly
46 projected, and a postacetabular process with a more distinctly posteroventrally slanted dorsal
47 margin in lateral view. Previous claims that the ilium of *Sarcosaurus woodi* closely resembles
48 that of *Dilophosaurus wetherilli* (Carrano & Sampson, 2004) were apparently partially based
49
50
51
52
53
54
55
56
57
58
59
60

1
2
3 on plaster reconstructions of the ilia of the holotype of the latter species (UCMP 37302),
4 which were figured as complete bone by Welles (1984: fig. 30a, c). Indeed, the supposed
5 ‘rounded, lobate preacetabular blade’ of *Dilophosaurus wetherilli* that closely resembles the
6 preacetabular process of *Sarcosaurus woodi* (Carrano & Sampson, 2004: 542) is fully
7 reconstructed with plaster (Fig. 20A, B), and new specimens show that the former species has
8 instead a more squared and horizontal preacetabular process (Tykoski, 2005: fig. 76c) that
9 resembles the condition widespread among early neotheropods. By contrast, the ilium of
10 *Sarcosaurus woodi* differs from that of *Dilophosaurus wetherilli* (UCMP 37302; Tykoski,
11 2005: fig. 76c) in the strong anteroventral orientation of the preacetabular process and the
12 lack of a conspicuous posterior projection of the ischiadic peduncle. Instead, the partial pelvic
13 girdle of *Sarcosaurus woodi* more closely resembles those of the ceratosaurian averostran
14 *Ceratosaurus nasicornis*, an observation already made by Andrews (1921), and the more
15 recently published ceratosaurian *Eoabelisaurus mefi*. Nevertheless, the species from central
16 England differs from *Ceratosaurus nasicornis* (USNM 4735) in the absence of a
17 ventromedial wall of the brevis fossa broadly visible in lateral view and a more pronounced
18 inflexion between the main axes of the pre- and postacetabular processes in lateral view, and
19 from *Eoabelisaurus mefi* (MPEF PV 3990) in the presence of a subcircular anterior articular
20 facet in the preserved posterior dorsal vertebra (distinctly taller than broad in *Eoabelisaurus*
21 *mefi*) and the absence of a well-defined iliac antitrochanter on the ischiadic peduncle (well-
22 developed as a semilunate raised structure in *Eoabelisaurus mefi*). In addition, *Sarcosaurus*
23 *woodi* also differs from these ceratosaurians, as well as other averostrans, in the presence of a
24 dorsolateral trochanter on the proximal end of the femur and the absence of a conspicuous
25 posterior projection of the ischiadic peduncle, which seems to be an autapomorphy of the
26 species among early neotheropods. As a result, we consider the holotype of *Sarcosaurus*
27
28
29
30
31
32
33
34
35
36
37
38
39
40
41
42
43
44
45
46
47
48
49
50
51
52
53
54
55
56
57
58
59
60

1
2
3 *woodi* to be diagnosable using a unique combination of character states, and this genus and
4 species are therefore taxonomically valid (contra Carrano & Sampson, 2004).
5
6

7
8 The anatomical regions that overlap between WARMS G667–690 and the holotype of
9 *Sarcosaurus woodi* possess a congruent morphology (e.g. there are no scoring differences
10 between both specimens in our data matrix); and, as a result, we could not find evidence
11 suggesting that these specimens belong to different species. Conversely, these two specimens
12 can be distinguished from other early neotheropods because of the unique combination of a
13 proportionally short middle–posterior dorsal centrum (length–anterior height ratio <2, also
14 present in non-coelophysid theropods); and femur with a **very**-low fourth trochanter (also
15 present in coelophysids and early ceratosaurian averostrans) and with a dorsolateral
16 trochanter on the proximal end (also present in non-averostran theropods). As a consequence,
17 we consider WARMS G667–690 referable to *Sarcosaurus woodi*.
18
19
20
21
22
23
24
25
26
27
28
29

30
31 As mentioned earlier, the holotypes of *Sarcosaurus woodi* and ‘*Sarcosaurus*
32 *andrewsi*’ lack overlapping bones. However, WARMS G667–690 as a referred specimen of
33 *Sarcosaurus woodi* provides an anatomical bridge between the holotypes. The morphology of
34 the holotype tibia of ‘*Sarcosaurus andrewsi*’ is mostly congruent with those of WARMS
35 G667–690 and the main difference is the presence of a diagonal tuberosity on the anterior
36 surface of the distal end of the bone in the former specimen. However, we consider that this
37 difference is not enough to justify the assignment of these specimens to different species
38 because of their **very**-similar overall morphology and congruent phylogenetic signal. The
39 tibiae of WARMS G667–690 and ‘*Sarcosaurus andrewsi*’ differ from those of coelophysoids
40 (here including *Liliensternus liliensterni*), *Dilophosaurus wetherilli*, *Gojirasaurus quayi*,
41 *Zupaysaurus rougieri*, ~~*Gojirasaurus quayi*~~ and ~~*Dilophosaurus wetherilli*~~ in the presence of an
42 anteroposteriorly less developed facet for reception of the ascending process of the astragalus
43 (Fig. 20C–H). On the other hand, WARMS G667–690 and ‘*Sarcosaurus andrewsi*’ differ
44
45
46
47
48
49
50
51
52
53
54
55
56
57
58
59
60

1
2
3 from *Tachiraptor admirabilis* and *Averostra* in the higher ratio between the anteroposterior
4 depth and transverse width of the distal end (>0.6) and the presence of a distinct and deep
5 posteromedial notch that forms an indented posteromedial margin in distal view (Fig.
6 20G–J), and from *averostrans* in the absence of a well-developed medial malleolus.

12 In order to determine if ‘*Sarcosaurus andrewsi*’ represents a junior synonym of
13 *Sarcosaurus woodi*, we compared the former with other Early Jurassic non-coelophysoid,
14 non-*averostran* theropod species. Only the partial proximal portion of a left tibia of
15 *Dracoraptor hanigani* (early Hettangian of Wales; Martill *et al.*, 2016) can be compared with
16 ‘*Sarcosaurus andrewsi*’. The comparable portion of bone has a congruent morphology in
17 both species, but it also matches the morphology in other non-tetanuran neotheropods. As a
18 result, we do not have enough information to distinguish the two species from each other.
19 Nevertheless, WARMS G667–690 differs from *Dracoraptor hanigani* in the presence of a
20 fibula with a poorly projected and tab-like posterior margin of the proximal end in lateral
21 view. No tibia is known from the Triassic *averostran-like* neotheropod *Notatesseraeraptor*
22 *frickensis* (latest Late Triassic of Switzerland; Zahner & Brinkmann, 2019) and only a few
23 elements overlap with WARMS G667–690 (dorsal centrum and ribs, and partial ilium and
24 pubis), which possess a congruent morphology. However, the phylogenetic placement of
25 *Notatesseraeraptor frickensis* as one of the earliest branching *averostran-like* theropods
26 (Zahner & Brinkmann, 2019) suggests that it is a different species ~~to~~ from WARMS G667–
27 690 and ‘*Sarcosaurus andrewsi*’. The holotype of *Dracovenator regenti* Yates, 2005
28 (Hettangian–Sinemurian of South Africa; Yates, 2005) lacks overlapping bones with
29 ‘*Sarcosaurus andrewsi*’ and WARMS G667–690, whereas only part of the pubic peduncle of
30 the ilium can be compared with the only known specimen of *Lophostropheus airelensis*
31 (Rhaetian–Hettangian of France; Cuny & Galton, 1993; Ezcurra & Cuny, 2007). However,
32 phylogenetic analyses suggest that these two species are not closely related to ‘*Sarcosaurus*
33
34
35
36
37
38
39
40
41
42
43
44
45
46
47
48
49
50
51
52
53
54
55
56
57
58
59
60

1
2
3 *andrewsi*' and WARMS G667–690 (*Dracovenator regenti* has been recovered as one of the
4
5 sister-taxa to the *Dilophosaurus wetherilli* + *Averostra* clade, and *Lophostropheus airelensis*
6
7 has been found as a coleophysoid or one of the sister-taxa to the *Dilophosaurus wetherilli* +
8
9 *Averostra* clade; e.g. Yates, 2005; Ezcurra & Cuny, 2007; Smith *et al.*, 2007; Ezcurra, 2012;
10
11 Langer *et al.*, 2014; Wang *et al.*, 2017b). The few preserved bones of the theropod
12
13 *Dandakosaurus indicus* [Yadagiri, 1982](#) (Sinemurian–Pliensbachian of India; Yadagiri, 1982;
14
15 but considered a *nomen dubium* by Holtz, Molnar & Currie, 2004) do not overlap with those
16
17 of '*Sarcosaurus andrewsi*' and WARMS G667–690, but the presence of opisthocoelous
18
19 dorsal vertebrae (this condition suggests that they are anterior dorsal elements although
20
21 Yadagiri [1982] did not specify their position in the dorsal series) suggests that it is a more
22
23 derived, averostran theropod. Finally, we do not have enough information to compare the
24
25 averostran-like or early averostran *Sinosaurus triassicus* [Young, 1940](#) (Sinemurian–
26
27 Pliensbachian of China; Xing *et al.*, 2014; Currie *et al.* [2019] reported in a preliminary
28
29 communication that the holotype of *Shuangbaisaurus anlongbaoensis* [Wang *et al.*, 2017](#),
30
31 from the same geological unit in China, falls within the range of morphological variability of
32
33 *Sinosaurus triassicus*) with the preserved bones of '*Sarcosaurus andrewsi*' and WARMS
34
35 G667–690.
36
37

38
39
40
41
42 These comparisons show that the holotype of '*Sarcosaurus andrewsi*' and WARMS
43
44 G667–690 can be distinguished from all other early neotheropod species with overlapping
45
46 bones and the unique combination of character states present on the distal end of the tibia
47
48 indicates that they are co-specific. As a result, we propose that the holotype of '*Sarcosaurus*
49
50 *andrewsi*' can be referred to *Sarcosaurus woodi* and that the former species is a subjective
51
52 junior synonym of the latter.
53
54
55
56
57

58 *The fossil record and evolution of Early Jurassic neotheropods*
59
60

1
2
3 The discussion of the early evolution of Neotheropoda in an explicit phylogenetic context is
4 complicated because of the relatively unstable placement of several Late Triassic and Early
5 Jurassic species (e.g. *Liliensternus liliensterni*, *Dracoraptor hanigani*, *Lepidus praecisio*,
6 *Liliensternus liliensterni*, and *Zupaysaurus rougieri*, *Sarcosaurus woodi*, *Sinosaurus*
7 *triassicus* and *Zupaysaurus rougieri*; Carrano, Benson & Sampson, 2012; Wang *et al.*,
8 2017b; Martill *et al.*, 2016; Ezcurra, 2017), even in different iterative analyses of the same
9 phylogenetic matrix (Martill *et al.*, 2016; Ezcurra, 2017; Marsola *et al.*, 2019; Marsh *et al.*,
10 2019b). Here, *Lepidus praecisio* is recovered deeply nested within Coelophysidae as the
11 sister taxon of *Coelophysis bauri*, as in Ezcurra (2017) and similar to Marsola *et al.* (2019),
12 but contrasting with its position as the earliest member of the branch leading to Averostra in
13 Marsh *et al.* (2019b). *Liliensternus liliensterni* is found at the base of Coelophysoidea, as
14 occurs in Ezcurra (2017) and Marsola *et al.* (2019), but it was recovered as one of the
15 successive sister taxa leading to Averostra in Martill *et al.* (2016) and Marsh *et al.* (2019b).
16 *Zupaysaurus rougieri* is recovered as the earliest member of the branch leading to Averostra,
17 resembling the results of Martill *et al.* (2016), Ezcurra (2017) and Marsh *et al.* (2019b), but
18 Marsola *et al.* (2019) found it as a non-coelophysid coelophysoid. Finally, *Dracoraptor*
19 *hanigani* is recovered here as the earliest branching coelophysoid, together with *Liliensternus*
20 *liliensterni*, as occurs in the results of Martill *et al.* (2016), but this species was alternatively
21 recovered in this position or within the branch leading to Averostra by Ezcurra (2017). The
22 instability in the placement of these taxa shows that the phylogenetic relationships around the
23 base of Neotheropoda are still in state of flux and more work is needed on this topic.

24
25
26
27
28
29
30
31
32
33
34
35
36
37
38
39
40
41
42
43
44
45
46
47
48
49
50
51 The phylogenetic position of *Sarcosaurus woodi* has been tested before in several
52 quantitative analyses, yielding contradicting results. The first analysis was that of Rowe
53 (1989; see also Rowe & Gauthier, 1990), which found this species as one of the earliest
54 branching members of Ceratosauria *sensu lato* (Abelisauroidea + Coelophysoidea).
55
56
57
58
59
60

1
2
3 Subsequently, Ezcurra (2012) recovered *Sarcosaurus woodi* within Ceratosauria *sensu stricto*
4
5 in a preliminary analysis, Wang *et al.* (2017b) found this species as one of the earliest
6
7 branching averostran-like neotheropods, and Dal Sasso, Maganuco & Cau (2018) reported it
8
9 as a non-averostran neotheropod in a clade composed of *Dilophosaurus wetherilli* and
10
11 *Cryolophosaurus ellioti*. Here we found *Sarcosaurus woodi* in a placement that was not
12
13 previously recovered, as one of the most immediate sister-taxa to Averostra. Thus,
14
15 *Sarcosaurus woodi* increases the diversity of non-coelophysoid, non-averostran neotheropods
16
17 and their cosmopolitanism during the Early Jurassic, having been identified from Europe,
18
19 Antarctica, North America, Africa, and probably Asia (e.g. Yates, 2005; Smith *et al.*, 2007;
20
21 Dal Sasso, Maganuco & Cau, 2018). In addition, *Sarcosaurus woodi* partially fills a
22
23 morphological gap between ‘coelophysoid-grade’ (e.g. *Zupaysaurus rougieri*,
24
25 *Cryolophosaurus ellioti*, *Dilophosaurus wetherilli*, *Zupaysaurus rougieri*) and averostran
26
27 theropods. For example, the femur of *Sarcosaurus woodi* possesses a dorsolateral trochanter
28
29 and lacks a deep extensor fossa as in non-averostran, non-coelophysoid theropods, but it has a
30
31 ~~very~~ low fourth trochanter as in ceratosaurian averostrans. The distal end of the tibia has a
32
33 deep posteromedial notch and a relatively high distal width-depth ratio as in non-averostran
34
35 neotheropods (with exception of *Tachiraptor admirabilis*), but the presence of an
36
37 anteroposteriorly narrow facet for reception of the ascending process of the astragalus
38
39 resembles more the condition of averostrans (Fig. 20C–J).

40
41
42 The oldest currently known averostran is *Saltriovenator zanellai* Dal Sasso *et al.*,
43
44 2018 from the Sinemurian of Italy (Dal Sasso, Maganuco & Cau, 2018). Nevertheless, the
45
46 phylogenetic position of *Tachiraptor admirabilis* as the sister-taxon of Averostra indicates
47
48 that the split between Ceratosauria and Tetanurae occurred before the Hattengian–Sinemurian
49
50 boundary (ca. 199.3 Mya) (Langer *et al.*, 2014). The placement of the late Hettangian
51
52
53
54
55
56
57
58
59
60

theropod *Sarcosaurus woodi* (Fig. 21) as one of the most immediate sister-taxa to Averostrasaurus. This phylogenetic analysis supports this inference.

ACKNOWLEDGEMENTS

We thank the following curators, researchers and collection managers that provided access to specimens under their care for the purpose of this research: Carl Mehling (AMNH), Max Langer (LPRP/USP), Daniela Schwarz (HMN), Jessica Cundiff (MCZ), Eduardo Ruigomez and Diego Pol (MPEF), Sandra Chapman and Lorna Steel (NHMUK), Caroline Buttler (NMW), Sergio Martin, Emilio Vaccari and Gabriela Cisterna (PULR), Jaime Powell, Pablo Ortiz and Rodrigo Gonzalez (PVL), Ricardo Martínez and Diego Abelín (PVSJ), Rainer Schoch (SMNS), Kevin Padian and Pat Holroyd (UCMP), and Michael Brett-Surman and Hans-Dieter Sues (USNM). Access to the free version of TNT 1.1 was possible due to the Willi Henning Society. Mark Witton is thanked for creating Figures 2 and 21. This project was partially funded by a Sepkoski Grant 2019 of the Paleontological Society International Research Program (to MDE). Amy Scott-Murray (Imaging and Analysis Centre, NHMUK) carried out the scanning and produced the 3D models of NHMUK PV R4840 and R3542.

REFERENCES

Allain R, Tykoski R, Aquesbi N, Jalil NE, Monbaron M, Russell D, Taquet P. 2007. An abelisauroid (Dinosauria: Theropoda) from the Early Jurassic of the High Atlas Mountains, Morocco, and the radiation of ceratosaurs. *Journal of Vertebrate Paleontology* 27: 610–624.

- 1
2
3 **Ambrose K. 2001.** The lithostratigraphy of the Blue Lias Formation (Late Rhaetian – Early
4
5 Sinemurian) in the southern part of the English Midlands. *Proceedings of the*
6
7 *Geologists' Association* **112**: 97–110.
8
9
- 10 **Andrews CW. 1921.** On some remains of a theropodous dinosaur from the Lower Lias of
11
12 Barrow-on-Soar. *Annals and Magazine of Natural History, Series 9* **8**: 570–576.
13
14
- 15 **Arcucci A, Coria RA. 2003.** A new Triassic dinosaur. *Ameghiniana* **40**: 217–228.
16
- 17 **Bakker RT. 1986.** *The dDinosaur hHeresies*. Avon: Bath Press.
18
- 19 **Baumel JJ, Witmer LM. 1993.** Osteologia. In: Baumel JJ, King AS, Breazile JE, Evans HE,
20
21 Vanden Berge JC, eds. *Handbook of aAvian aAnatomy: nNomina aAnatomica*
22
23 *aAvium*. 2nd eEd. Cambridge: Nuttall Ornithology Club, 45–132.
24
25
- 26 **Benson RB. 2010.** The osteology of *Magnosaurus nethercombensis* (Dinosauria, Theropoda)
27
28 from the Bajocian (Middle Jurassic) of the United Kingdom and a re-examination of
29
30 the oldest records of tetanurans. *Journal of Systematic Palaeontology* **8**: 131–146.
31
32
- 33 **Benton MJ, Martill DM, Taylor MA. 1995.** The first Lower Jurassic dinosaur from
34
35 Scotland: limb bone of a ceratosaur theropod from Skye. *Scottish Journal of Geology*
36
37 **31**: 177–182.
38
39
- 40 **Bremer K. 1988.** The limits of amino acid sequence data in angiosperm phylogenetic
41
42 reconstruction. *Evolution* **42**: 795–803.
43
44
- 45 **Bremer K. 1994.** Branch support and tree stability. *Cladistics* **10**: 295–304.
46
- 47 **Brochu CA. 1996.** Closure of neurocentral sutures during crocodylian ontogeny: implications
48
49 for maturity assessment in fossil archosaurs. *Journal of Vertebrate Paleontology* **16**:
50
51 49–62.
52
53
- 54 **Camp CL. 1936.** A new type of small bipedal dinosaur from the Navajo Sandstone of
55
56 Arizona. *University of California Publications, Bulletin of the Department of*
57
58 *Geological Sciences* **24**: 39–56.
59
60

- 1
2
3 **Carpenter K. 1997.** A giant coelophysoid (Ceratosauria) theropod from the Upper Triassic
4 of New Mexico, USA. *Neues Jahrbuch für Geologie und Paläontologie*, -
5
6 *Abhandlungen* **205**: 189–208.
7
8
9
- 10 **Carrano MT, Hutchinson JR. 2002.** Pelvic and hindlimb musculature of *Tyrannosaurus rex*
11 (Dinosauria: Theropoda). *Journal of Morphology* **253**: 207–228.
12
13
- 14 **Carrano MT, Sampson SD. 2004.** A review of coelophysoids (Dinosauria: Theropoda) from
15 the Early Jurassic of Europe, with comments on the late history of the
16 Coelophysoidea. *Neues Jahrbuch für Geologie und Palaontologie* **9**: 537–558.
17
18
- 19 **Carrano MT, Benson RB, Sampson SD. 2012.** The phylogeny of Tetanurae (Dinosauria:
20 Theropoda). *Journal of Systematic Palaeontology* **10**: 211–300.
21
22
- 23 **Coddington J, Scharff N. 1994.** Problems with zero-length branches. *Cladistics* **10**:
24 415–423.
25
26
- 27 **Colbert EH. 1989.** The Triassic dinosaur *Coelophysis*. *Bulletin of the Museum of Northern*
28 *Arizona* **57**: 1–174.
29
30
- 31 **Cope ED. 1869–1870.** Synopsis of the extinct Batrachia, Reptilia and Aves of North
32 America. *Transactions of the American Philosophical Society* **14**: 1–252.
33
34
- 35 **Cope ED. 1889.** On a new genus of Triassic Dinosauria. *American Naturalist* **23**: 626.
36
37
- 38 **Cox BM, Sumbler MG, Ivimey-Cook HC. 1999.** A formational framework for the Lower
39 Jurassic of England and Wales (onshore area). *British Geological Survey Research*
40 *Report*: **RR/99/01**: [1–28](#).
41
42
- 43 **Cuny G, Galton PM. 1993.** Revision of the Airel theropod dinosaur from the Triassic-
44 Jurassic boundary (Normandy, France). *Neues Jahrbuch für Geologie und*
45 *Paläontologie, Abhandlungen* **187**: 261–288.
46
47
48
49
50
51
52
53
54
55
56
57
58
59
60

- 1
2
3 **Currie PJ, Xing L, Wu X, Dong Z. 2019.** Anatomy and relationships of *Sinosaurus*
4 *triassicus* (Theropoda, Coelophysoidea) from the Lufeng Formation (Lower Jurassic)
5 of Yunnan, China. *Canadian Society of Vertebrate Palaeontology 2019 Abstracts*: 17.
6
7
8
9
10 **Dal Sasso C, Maganuco S, Cau A. 2018.** The oldest ceratosaurian (Dinosauria: Theropoda),
11 from the Lower Jurassic of Italy, sheds light on the evolution of the three-fingered
12 hand of birds. *PeerJ* **6**: e5976 .
13
14
15
16
17 **Delsate D, Ezcurra MD. 2014.** The first Early Jurassic (late Hettangian) theropod dinosaur
18 remains from the Grand Duchy of Luxembourg. *Geologica Belgica* **17**: 175–181.
19
20
21 **Donovan DT, Horton A, Ivimey-Cook HC. 1979.** The transgression of the Lower Lias over
22 the northern flank of the London Platform. *Journal of the Geological Society* **136**:
23 165–173.
24
25
26
27
28 **Dzik J, Sulej T, Niedźwiedzki G. 2008.** A dicynodont-theropod association in the latest
29 Triassic of Poland. *Acta Palaeontologica Polonica* **53**: 733–739.
30
31
32
33 **Erickson GM, Makovicky PJ, Currie PJ, Norell MA, Yerby SA, Brochu CA. 2004.**
34 Gigantism and comparative life-history parameters of tyrannosaurid dinosaurs. *Nature*
35 **430**: 772–775.
36
37
38
39
40 **Erickson GM. 2005.** Assessing dinosaur growth patterns: a microscopic revolution. *Trends*
41 *in Ecology & Evolution* **20**: 677–684.
42
43
44
45 **Ezcurra MD. 2012.** Phylogenetic analysis of Late Triassic – Early Jurassic neotheropod
46 dinosaurs: implications for the early theropod radiation. *Society of Vertebrate*
47 *Paleontology, Supplement to the online Journal of Vertebrate Paleontology, 2012*:
48 91A.
49
50
51
52
53
54 **Ezcurra MD. 2017.** A new early coelophysoid neotheropod from the Late Triassic of
55 northwestern Argentina. *Ameghiniana* **54**: 506–539.
56
57
58
59
60

- 1
2
3 **Ezcurra MD, Cuny G. 2007.** The coelophysoid *Lophostropheus airelensis* nov. gen.: a
4
5 review of the systematics of “*Liliensternus*” *airelensis* from the Triassic-Jurassic
6
7 outcrops of Normandy (France). *Journal of Vertebrate Paleontology* **27**: 73–86.
8
9
- 10 **Ezcurra MD, Novas FE. 2007.** Phylogenetic relationships of the Triassic theropod
11
12 *Zupaysaurus rougieri* from NW Argentina. *Historical Biology* **19**: 35–72.
13
14
- 15 **Ezcurra MD, Brusatte SL. 2011.** Taxonomic and phylogenetic reassessment of the early
16
17 neotheropod dinosaur *Camposaurus arizonensis* from the Late Triassic of North
18
19 America. *Palaeontology* **54**: 763–772.
20
21
- 22 **Felsenstein J. 1985.** Confidence limits on phylogenies: an approach using the bootstrap.
23
24 *Evolution* **39**: 783–791.
25
- 26 **Fraas E. 1913.** Die neuesten Dinosaurierfunde der schwäbischen Trias. *Naturwissenschaften*
27
28 **45**: 1097–1100.
29
- 30 **Furin S, Preto N, Rigo M, Roghi G, Gianolla P, Crowley JL, Bowring SA. 2006.** High-
31
32 precision U-Pb zircon age from the Triassic of Italy: implications for the Triassic
33
34 time scale and the Carnian origin of calcareous nannoplankton and dinosaurs.
35
36 *Geology* **34**: 1009–1012.
37
38
- 39 **Gauthier JA. 1986.** Saurischian monophyly and the origin of birds. *Memoirs of the*
40
41 *California Academy of Science* **8**: 1–55.
42
43
- 44 **Gauthier JA, Padian K. 1985.** *Phylogenetic, functional, and aerodynamic analyses of the*
45
46 *origin of birds and their flight*. Eichstatt: The Beginning of Birds; Freunde des Jura
47
48 Museums, 185–197.
49
- 50 **Goloboff PA, Catalano SA. 2016.** TNT version 1.5, including a full implementation of
51
52 phylogenetic morphometrics. *Cladistics* **32**: 221–238.
53
54
- 55 **Goloboff PA, Farris JS, Källersjö M, Oxelman B, Ramírez M, Szumik C. 2003.**
56
57 Improvements to resampling measures of group support. *Cladistics* **19**: 324–332.
58
59
60

- 1
2
3 **Goloboff P, Farris J, Nixon K. 2008.** TNT: a free program for phylogenetic analysis.
4
5 *Cladistics* **24**: 774–786.
6
7
8 **Griffin CT. 2018.** Developmental patterns and variation among early theropods. *Journal of*
9
10 *Anatomy* **232**: 604–640.
11
12 **Griffin CT. 2019.** Large neotheropods from the Upper Triassic of North America and the
13
14 early evolution of large theropod body sizes. *Journal of Paleontology* **93**: 1010–1030.
15
16
17 **Griffin CT, Nesbitt SJ. 2016.** Anomalously high variation in postnatal development is
18
19 ancestral for dinosaurs but lost in birds. *Proceedings of the National Academy of*
20
21 *Sciences* **113**: 14757–14762.
22
23
24 **Hallam A. 1997.** Estimates of the amount and rate of sea-level change across the Rhaetian–
25
26 Hettangian and Pliensbachian–Toarcian boundaries (latest Triassic to Early Jurassic).
27
28 *Journal of the Geological Society* **154**: 773–779.
29
30
31 **Hammer WR, Hickerson WJ. 1994.** A crested theropod dinosaur from Antarctica. *Science*
32
33 **264**: 828–830.
34
35
36 **Hesselbo SP. 2008.** Sequence stratigraphy and inferred relative sea-level change from the
37
38 onshore British Jurassic. *Proceedings of the Geologists' Association* **119**: 19–34.
39
40
41 **Holtz TR, Molnar R, Currie PJ. 2004.** Basal Tetanurae. In: Weishampel DB, Dodson P,
42
43 Osmólska H, eds. *The ~~d~~Dinosauria, ~~s~~Second ~~e~~Edition*. Berkeley: University of
44
45 California Press, 71–110.
46
47
48 **Horner JR, de Ricqlès A, Padian K. 1999.** Variation in skeletochronological indicators:
49
50 implications for age assessment and physiology. *Paleobiology* **25**: 295–304.
51
52
53 **Horner JR, de Ricqlès A, Padian K. 2000.** Long bone histology of the hadrosaurid dinosaur
54
55 *Maiasaura peeblesorum*: growth dynamics and physiology based on an ontogenetic
56
57 series of skeletal elements. *Journal of Vertebrate Paleontology* **20**: 115–129.
58
59
60

- 1
2
3 **Hu S. 1993.** A new Theropoda (*Dilophosaurus sinensis* sp. nov.) from Yunnan, China.
4
5 *Vertebrata Palasiatica* **31**: 65–69.
6
7
8 **von Huene F-von. 1926.** The carnivorous Saurischia in the Jura and Cretaceous formations,
9
10 principally in Europe. *Revista del Museo de la Plata* **29**: 35–167.
11
12 **von Huene F-von. 1932.** Die fossile Reptil-Ordnung Saurischia, ihre Entwicklung und
13
14 Geschichte. *Monographien zur Geologie und Palaeontologie, Serie 1*: 1–361.
15
16
17 **von Huene F-von. 1934.** Ein neuer Coelurosaurier in der Thüringischen Trias.
18
19 *Palaeontologische Zeitschrift* **16**: 145–170.
20
21 **Hunt AP, Lucas SG, Heckert AB, Sullivan RM, Lockley MG. 1998.** Late Triassic
22
23 dinosaurs from the western United States. *Geobios* **31**: 511–531.
24
25
26 **Hutchinson JR. 2001.** The evolution of pelvic osteology and soft tissues on the line to extant
27
28 birds (Neornithes). *Zoological Journal of the Linnean Society* **131**: 123–168.
29
30
31 **Hutchinson JR, Gatesy SM. 2000.** Adductors, abductors, and the evolution of archosaur
32
33 locomotion. *Paleobiology* **26**: 734–751.
34
35
36 **Irmis RB. 2004.** First report of *Megapnosaurus* (Theropoda: Coelophysoidea) from China.
37
38 *PaleoBios* **24**: 11–18.
39
40 **Irmis RB. 2007.** Axial skeleton ontogeny in the Parasuchia (Archosauria: Pseudosuchia) and
41
42 its implications for ontogenetic determination in archosaurs. *Journal of Vertebrate*
43
44 *Paleontology* **27**: 350–361.
45
46
47 **Irmis RB, Nesbitt SJ, Padian K, Smith ND, Turner AH, Woody D, Downs A. 2007.** A
48
49 Late Triassic dinosauromorph assemblage from New Mexico and the rise of
50
51 dinosaurs. *Science* **317**: 358–361.
52
53
54 **Jaekel O. 1913.** Über die Wirbeltierfunde aus der oberen Trias von Halberstadt.
55
56 *Palaeontologische Zeitschrift* **1**: 155–215.
57
58
59
60

- 1
2
3 **Langer MC, Benton MJ. 2006.** Early dinosaurs: [aA](#) phylogenetic study. *Journal of*
4
5 *Systematic Palaeontology* **4**: 309–358.
6
7
8 **Langer MC, Rincón AD, Ramezani J, Solórzano A, Rauhut OW. 2014.** New dinosaur
9
10 (Theropoda, stem-Averostra) from the earliest Jurassic of the La Quinta formation,
11
12 Venezuelan Andes. *Royal Society Open Science* **-1**: 140184.
13
14
15 **Langer MC, Ramezani J, Da Rosa ÁA. 2018.** U-Pb age constraints on dinosaur rise from
16
17 south Brazil. *Gondwana Research* **57**: 133–140.
18
19
20 **Lucas SG, Heckert AB. 2001.** Theropod dinosaurs and the Early Jurassic age of the
21
22 Moenave Formation, Arizona-Utah, USA. *Neues Jahrbuch für Geologie und*
23
24 *Paläontologie-Monatshefte* **2001**: 435–448.
25
26
27 **Marsh AD, Parker WG, Stockli DF, Martz JW. 2019a.** Regional correlation of the Sonsela
28
29 Member (Upper Triassic Chinle Formation) and detrital U-Pb zircon data from the
30
31 Sonsela Sandstone bed near the Sonsela Buttes, northeastern Arizona, USA, support
32
33 the presence of a distributive fluvial system. *Geosphere* **15**: 1128–1139.
34
35
36 **Marsh AD, Parker WG, Langer MC, Nesbitt SJ. 2019b.** Redescription of the holotype
37
38 specimen of *Chindesaurus bryansmalli* Long and Murry, 1995 (Dinosauria,
39
40 Theropoda), from Petrified Forest National Park, Arizona. *Journal of Vertebrate*
41
42 *Paleontology* **39**: e1645682.
43
44
45 **Marsh OC. 1881.** Principal characters of American Jurassic dinosaurs. *American Journal of*
46
47 *Science (3rd series)* **21**: 417–423.
48
49
50 **Marsola JC, Bittencourt JS, Butler RJ, Da Rosa ÁA, Sayão JM, Langer MC. 2019.** A
51
52 new dinosaur with theropod affinities from the Late Triassic Santa Maria Formation,
53
54 South Brazil. *Journal of Vertebrate Paleontology* **38**: e1531878.
55
56
57 **Martill DM, Vidovic SU, Howells C, Nudds JR. 2016.** The oldest Jurassic dinosaur: [aA](#)
58
59 basal neotheropod from the Hettangian of Great Britain. *PLoS One* **11**: e0145713.
60

- 1
2
3 **Martínez RN, Apaldetti C. 2017.** A late Norian-Rhaetian coelophysid neotheropod
4
5 (Dinosauria, Saurischia) from the Quebrada del Barro Formation, northwestern
6
7 Argentina. *Ameghiniana* **54**: 488–506.
8
9
- 10 **Martínez RN, Sereno PC, Alcober OA, Colombi CE, Renne PR, Montañez IP, Currie**
11
12 **BS. 2011.** A basal dinosaur from the dawn of the dinosaur era in southwestern
13
14 Pangaea. *Science* **331**: 206–210.
15
16
- 17 **Munter RC, Clark JM. 2006.** Theropod dinosaurs from the Early Jurassic of Huizachal
18
19 Canyon, Mexico. In: Carrano MT, Gaudin TJ, Blob RW, Wible JR, eds. *Amniote*
20
21 *paleobiology: perspectives on the evolution of mammals, birds, and reptiles*. Chicago:
22
23 University of Chicago Press, 53–75.
24
25
- 26 **Nesbitt SJ. 2011.** The early evolution of Archosauria: relationships and the origin of major
27
28 clades. *Bulletin of the American Museum of Natural History* **352**: 1–292.
29
30
- 31 **Nesbitt SJ, Ezcurra MD. 2015.** The early fossil record of dinosaurs in North America: **aA**
32
33 new neotheropod from the base of the Upper Triassic Dockum Group of Texas. *Acta*
34
35 *Palaeontologica Polonica* **60**: 513–526.
36
37
- 38 **Nesbitt SJ, Smith ND, Irmis RB, Turner AH, Downs A, Norell MA. 2009.** A complete
39
40 skeleton of a Late Triassic saurischian and the early evolution of dinosaurs. *Science*
41
42 **326**: 1530–1533.
43
44
- 45 **Novas FE, Ezcurra MD, Chatterjee S, Kuttly TS. 2010.** New dinosaur species from the
46
47 Upper Triassic Upper Maleri and Lower Dharmaram formations of central India.
48
49 *Earth and Environmental Science Transactions of the Royal Society of Edinburgh*
50
51 **101**: 333–349.
52
53
- 54 **Old RA, Sumblar MG, Ambrose K. 1987.** The geology of the country around Warwick.
55
56 *Memoir of the British Geological Survey of Great Britain*, Sheet 184 (England and
57
58 Wales). **Keyword: British Geological Survey.**
59
60

- 1
2
3 **Old RA, Hamblin RJOH., Ambrose K. 1991.** The geology of the country around Redditch.
4
5 *Memoir of the British Geological Survey of Great Britain*, Sheet 183 (England and
6
7 Wales). [Keyworth: British Geological Survey.](#)
8
9
- 10 **Owen R. 1842.** Report on British fossil reptiles. Part 2. *Report of the British Association for*
11
12 *the Advancement of Science* **11**: 60–204.
13
14
- 15 **Padian K. 1986.** On the type material of *Coelophysis* Cope (Saurischia: Theropoda) and a
16
17 new specimen from the Petrified Forest of Arizona (Late Triassic: Chinle Formation).
18
19 In: Padian K. ed. *The beginning of the age of ~~d~~Dinosaurs, faunal change across the*
20
21 *Triassic-Jurassic boundary*. Cambridge: Cambridge University Press, 45–60.
22
23
- 24 **Padian K, May CL. 1993.** The earliest dinosaurs. The Nonmarine Triassic. *New Mexico*
25
26 *Museum of Natural History and Science Bulletin* **3**: 379–381.
27
28
- 29 **Pol D, Escapa IH. 2009.** Unstable taxa in cladistic analysis: ~~i~~Identification and the
30
31 assessment of relevant characters. *Cladistics* **25**: 515–527.
32
33
- 34 **Pol D, Rauhut OWM. 2012.** A Middle Jurassic abelisaurid from Patagonia and the early
35
36 diversification of theropod dinosaurs. *Proceedings of the Royal Society B* **279**: 3170–
37
38 3175.
39
- 40 **Raath MA. 1969.** A new coelurosaurian dinosaur from the Forest Sandstone of Rhodesia.
41
42 *Arnoldia* **4**: 1–25.
43
44
- 45 **Raath MA. 1977.** *The anatomy of the Triassic theropods Syntarsus rhodesiensis (Saurischia:*
46
47 *Podokesauridae) and a consideration of its biology.* [Salisbury: Ph.D. thesis.](#)
48
49 [Salisbury: Rhodes University, Ph.D. thesis.](#)
50
51
- 52 **Raath MA, Carpenter K, Currie PJ. 1990.** Morphological variation in small theropods and
53
54 its meaning in systematics: evidence from *Syntarsus*. In: Carpenter K, Currie PJ, eds.
55
56 *In ~~d~~Dinosaur systematics: approaches and perspectives*. Cambridge: Cambridge
57
58 University Press, 91–105.
59
60

- 1
2
3 **Radley JD. 2003.** Warwickshire's Jurassic geology, past, present and future. *Mercian*
4
5 *Geologist* **15**: 209–218.
6
7
- 8 **Ramezani J, Fastovsky DE, Bowring SA. 2014.** Revised chronostratigraphy of the lower
9
10 Chinle Formation strata in Arizona and New Mexico (USA): high-precision U-Pb
11
12 geochronological constraints on the Late Triassic evolution of dinosaurs. *American*
13
14 *Journal of Science* **314**: 981–1008.
15
16
- 17 **Rauhut OWM, Hungerbühler A. 2000.** A review of European Triassic theropods. *Gaia* **15**:
18
19 75–88.
20
21
- 22 **Rauhut OWM. 2003.** The interrelationships and evolution of basal theropod dinosaurs.
23
24 *Special Papers in Palaeontology* **69**: 1–214.
25
- 26 **de Ricqlès AJ-de. 1975.** Recherches paleohistologiques sur les os longs des tetrapodes. VII.
27
28 Sur la classification, la signification fonctionnelle et l'histoire des tissues osseux des
29
30 tetrapodes. Première partie: structures. *Annales de Paleontologie (Vertebres)* **61**:
31
32 49–129.
33
34
- 35 **Rogers RR, Swisher CC, Sereno PC, Monetta AM, Forster CA, Martínez RN. 1993.** The
36
37 Ischigualasto tetrapod assemblage (Late Triassic, Argentina) and $^{40}\text{Ar}/^{39}\text{Ar}$ dating of
38
39 dinosaur origins. *Science* **260**: 794–797.
40
41
- 42 **Rowe T. 1989.** A new species of the theropod dinosaur *Syntarsus* from the Early Jurassic
43
44 Kayenta Formation of Arizona. *Journal of Vertebrate Paleontology* **9**: 125–136.
45
46
- 47 **Rowe T, Gauthier J. 1990.** Ceratosauria. In: Weishampel DB, Dodson P, Osmólska H, eds.
48
49 *The dDinosauria*. Berkeley: University of California Press, 505–518.
50
51
- 52 **Sereno PC. 1998.** A rationale for phylogenetic definitions, with application to the higher-
53
54 level taxonomy of Dinosauria. *Neues Jahrbuch für Geologie und Paläontologie,*
55
56 *Abhandlungen* **210**: 41–83.
57
58
59
60

- 1
2
3 **Simms MJ, Chidlaw N, Morton N, Page KN. 2004.** *British Lower Jurassic stratigraphy*.
4
5 Peterborough: Joint Nature Conservation Committee, Geological Conservation
6
7 Review Series.
8
9
- 10 **Smith ND, Makovicky PJ, Hammer WR, Currie PJ. 2007.** Osteology of *Cryolophosaurus*
11
12 *elliotti* (Dinosauria: Theropoda) from the Early Jurassic of Antarctica and implications
13
14 for early theropod evolution. *Zoological Journal of the Linnean Society* **151**:
15
16 377–421.
17
18
- 19 **Starck JM. 1993.** Evolution of avian ontogenies. *Current Ornithology* **10**: 275–366.
20
- 21 **Swofford DL, Begle DP. 1993.** *User's manual for PAUP: phylogenetic analysis using*
22
23 *parsimony, Version 3.1*. Washington D.C.: Smithsonian Institution, ~~available from~~
24
25 ~~authors.~~
26
27
- 28 **Talbot M. 1911.** *Podokesaurus holyokensis*, a new dinosaur from the Triassic of the
29
30 Connecticut Valley. *American Journal of Science* **186**: 469–479.
31
32
- 33 **Tykoski RS. 2005.** *Osteology, ontogeny, and relationships of the coelophysoid theropods.*
34
35 Ph.D. thesis. Austin: University of Texas, ~~Ph.D. thesis.~~
36
37
- 38 **Tykoski RS, Rowe T. 2004.** Ceratosauria. In: Weishampel DB, Dodson P, Osmólska H, eds.
39
40 *The ~~d~~Dinosauria, 2nd ~~e~~Edition*. Berkeley: University of California Press, 47–70.
41
42
- 43 **Waldman M. 1974.** Megalosaurids from the Bajocian (Middle Jurassic) of Dorset.
44
45 *Palaeontology* **17**: 325–339.
46
- 47 **Wang GF, You HL, Pan SG, Wang T. 2017a.** A new crested theropod dinosaur from the
48
49 Early Jurassic of Yunnan Province, China. *Vertebrata Palasiatica* **55**: 177–186.
50
- 51 **Wang S, Stiegler J, Amiot R, Wang X, Du GH, Clark JM, Xu X. 2017b.** Extreme
52
53 ontogenetic changes in a ceratosaurian theropod. *Current Biology* **27**: 144–148.
54
55
- 56 **Weedon GP, Jenkyns HC, Page KN. 2017.** Combined sea-level and climatic control on
57
58 limestone formation, hiatuses and ammonite preservation in the Blue Lias Formation,
59
60

- 1
2
3 South Britain (uppermost Triassic – Lower Jurassic). *Geological Magazine* **155**:
4
5 1117–1149.
6
7
8 **Welles SP. 1954.** New Jurassic dinosaur from the Kayenta Formation of Arizona. *Bulletin of*
9
10 *the Geological Society of America* **65**: 591–598.
11
12 **Welles SP. 1984.** *Dilophosaurus wetherilli* (Dinosauria, Theropoda) osteology and
13
14 comparisons. *Palaeontographica* **185A**: 85–180.
15
16
17 **Woodward AS. 1908.** XLI.—Note on a Megalosaurian tibia from the lower Lias of
18
19 Wilmcote, Warwickshire. *Annals and Magazine of Natural History* **1**: 257–259.
20
21
22 **Xing LD, Paulina-Carabajal A, Currie PJ, Xu X, Zhang J, Wang T, Burns ME, Dong Z.**
23
24 **2014.** Braincase anatomy of the basal theropod *Sinosaurus* from the Early Jurassic of
25
26 China. *Acta Geologica Sinica* **88**: 1653–1664.
27
28
29 **Yadagiri P. 1982.** *Osteological studies of a carnosaurian dinosaur from Lower Jurassic*
30
31 *Kota Formation: Andhra Pradesh. Geological Survey of India. Progress Report for*
32
33 *Field Season Programme 1981–1982, 2–7.*
34
35
36 **Yates AM. 2005.** A new theropod dinosaur from the Early Jurassic of South Africa and its
37
38 implication for the early evolution of theropods. *Palaeontologia Africana* **41**:
39
40 105–122.
41
42
43 **You H-L, Azuma Y, Wang T, Wang Y-M, Dong Z-M. 2014.** The first well-preserved
44
45 coelophysoid theropod dinosaur from Asia. *Zootaxa* **3873**: 233–249.
46
47
48 **Young CC. 1948.** On two new Saurischia from Lufeng, Yunnan. *Bulletin of the Geological*
49
50 *Society of China* **28(1–2)**: 75–90.
51
52
53 **Zahner M, Brinkmann W. 2019.** A Triassic averostran-line theropod from Switzerland and
54
55 the early evolution of dinosaurs. *Nature Ecology & Evolution* **3**: 1146–1152.
56
57
58
59
60

FIGURE LEGENDS

1
2
3
4
5
6 **Figure 1.** Map showing the geographic occurrences of the holotype of *Sarcosaurus woodi*
7
8 (Barrow-on-Soar) and referred specimens (Wilmcote) indicated with stars. The outcrop of the
9
10 Lias Group is shown in grey.
11
12

13
14
15 **Figure 2.** Silhouette showing the preserved bones of referred specimen of *Sarcosaurus*
16
17 *woodi*, WARMS G667–690. Skeletal reconstruction from Mark Witton.
18
19

20
21
22 **Figure 3.** Close-up of bioencrusters on the anterior surface of the left femur of referred
23
24 specimen of *Sarcosaurus woodi* (WARMS G681).
25
26

27
28
29 **Figure 4.** Middle or posterior dorsal vertebra of referred specimen of *Sarcosaurus woodi*,
30
31 WARMS G678, in left lateral (A), right lateral (B), ventral (C) and anterior (D) views.
32
33 Arrows point towards anterior direction. Abbreviations: acdl, anterior centrodiapophyseal
34
35 lamina; fos, fossa on lateral surface of centrum; ncs, neurocentral suture; pcld, posterior
36
37 centrodiapophyseal lamina.
38
39

40
41
42 **Figure 5.** Anterior or middle caudal vertebra of referred specimen of *Sarcosaurus woodi*,
43
44 WARMS G679, in ventral (A), dorsal (B) and lateral (C, D) views. Abbreviations: f.na,
45
46 interdigitated articular facet for neural arch; fos, fossa on lateral surface of centrum.
47
48

49
50
51 **Figure 6.** Fragmentary dorsal rib shafts of referred specimen of *Sarcosaurus woodi*,
52
53 WARMS G670 (A, B), G675 (C, D) and G676 (E) in probable posterior (A, E) and anterior
54
55 (B, C, D) views. Abbreviation: gr, groove.
56
57
58
59
60

1
2
3 **Figure 7.** Pelvic fragments of referred specimen of *Sarcosaurus woodi*, WARMS G690 (A–
4 C), G688 (D–F) and G683/G684 (G–I). Partial pubic peduncle of left ilium in posterior (A)
5 and lateral (B) views, and cross section of peduncle (C). Partial left pubis in lateral (D),
6 and medial (E) and anterodorsal (F) views. Partial right pubis in lateral (G), medial (H) and
7 anterodorsal (I) views. Arrows point towards anterior direction. Abbreviations: dp,
8 longitudinal depression; pub.ap, pubic apron; sac, supraacetabular crest.
9
10
11
12
13
14
15
16
17
18

19 **Figure 8.** Left femur of referred specimen of *Sarcosaurus woodi*, WARMS G681, in
20 posterior (A), medial (B), anterior (C) and lateral (D) views. Arrows point towards anterior
21 direction. Abbreviations: atr, anterior trochanter; cfl, depression associated with the insertion
22 of the *M. caudofemoralis longus*; dltr, dorsolateral trochanter; ft, fourth trochanter; ife,
23 insertion scar of the *M. iliofemoralis externus*; ri, ridge.
24
25
26
27
28
29
30
31
32

33 **Figure 9.** Right femur of referred specimen of *Sarcosaurus woodi*, WARMS G682, in
34 posterior (A), medial (B), anterior (C), lateral (D) and distal (E) views. Arrows point towards
35 anterior direction. Abbreviations: afl, insertion of the *M. adductor femoris 1*; atr, anterior
36 trochanter; cfl, depression associated with the insertion of the *M. caudofemoralis longus*; dltr,
37 dorsolateral trochanter; fc, fibular condyle; ft, fourth trochanter; fte, attachment of the distal
38 portion of the *M. femorotibialis externus*; gpl, insertion scar of the *M. gastrocnemius pars*
39 *lateralis/M. flexor hallucis longus*; gr, groove; icc, intercondylar cleft; ife, insertion scar of
40 the *M. iliofemoralis externus*; mdc, medioidistal crest; pf, popliteal fossa; tc, tibial condyle;
41 tfc, tibiofibular crest.
42
43
44
45
46
47
48
49
50
51
52
53
54
55

56 **Figure 10.** Left tibia of referred specimen of *Sarcosaurus woodi*, WARMS G668, in anterior
57 (A), lateral (B), medial (C), posterior (D), proximal (E) and distal (F) views. Arrows point
58
59
60

1
2
3 towards anterior direction. Abbreviations: cn, cnemial crest; fap, facet for reception of
4
5 ascending process of astragalus; fc, fibular crest; pc, posterior hemicondyles; plc,
6
7 posterolateral concavity; plp, posterolateral process; pmn, posteromedial notch; pmr,
8
9 posteromedial ridge; str, striations.
10
11
12
13

14
15 **Figure 11.** Right tibia of referred specimen of *Sarcosaurus woodi*, WARMS G680, in
16
17 anterior (A), lateral (B), medial (C), posterior (D), proximal (E) and distal (F) views. Arrows
18
19 point towards anterior direction. Abbreviations: cn, cnemial crest; fap, facet for reception of
20
21 ascending process of astragalus; fc, fibular crest; gms, origin scar of the *M. gastocnemius*
22
23 *pars medialis*; pc, posterior hemicondyles; plp, posterolateral process; pmn, posteromedial
24
25 notch; pmr, posteromedial ridge; str, striations.
26
27
28
29

30
31 **Figure 12.** Fibula of referred specimen of *Sarcosaurus woodi*, WARMS G669 (A–C) and
32
33 G674 (D, E). Proximal end of left fibula in lateral (A), medial (B) and proximal (C) views.
34
35 Distal portion of fibula from indeterminate side in lateral/medial views (D, E). Arrows point
36
37 towards anterior direction. Abbreviations: gr, groove; rug, rugosity.
38
39
40
41

42
43 **Figure 13.** Partial left pedal autopodium (A–K) and metatarsal of indeterminate side (L) of
44
45 referred specimen of *Sarcosaurus woodi*, WARMS G672 (A–C), G673 (D–F), G677 (G, H),
46
47 G687 (I–K) and G671 (L). Metatarsal II in anterior (A), lateral (B) and distal (C) views.
48
49 Metatarsal III in proximal (D), anterior (E) and lateral (F) views. Metatarsal IV in anterior
50
51 (G) and lateral (H) views. Phalanx II-1 in anterior (I), proximal (J) and lateral (K) views.
52
53 Proximal end of metatarsal II or III in lateral/medial view (L). Arrows point towards anterior
54
55 direction. Abbreviations: clf, collateral fossa.
56
57
58
59
60

1
2
3 **Figure 14.** Photomicrographs of a thin section of dorsal rib shaft of referred specimen of
4 *Sarcosaurus woodi*, WARMS G676, under plain-polarized light (A, C) and polarized light
5 with a gypsum plate (B, D). White rectangles in (A, B) indicate the magnified areas shown in
6 (C, D). Arrowheads in (C, D) indicate annuli. Abbreviations: csb, compact spongy bone; flb,
7 fibrolamellar bone; plb, pseudolamellar bone; trb, trabeculae.
8
9
10
11
12
13
14
15
16

17 **Figure 15.** Posterior dorsal vertebra of holotype of *Sarcosaurus woodi*, NHMUK PV R4840,
18 in left lateral (A), right lateral (B), ventral (C), dorsal (D), anterior (E) and posterior (F)
19 views. Arrows point towards anterior direction. Abbreviations: aaf, anterior articular facet;
20 hyp, hypantrum; lfo, lateral fossa; prz, prezygapophysis; tp, transverse process.
21
22
23
24
25
26
27

28 **Figure 16.** Partial pelvic girdle of holotype of *Sarcosaurus woodi*, NHMUK PV R4840.
29 Photographs (A–D) and surface scans (E, F) of left ilium and pubis (A, B) and right ilium and
30 pubis (C–F) in lateral (A, C), medial (B, D), lateral and slightly posterior (E), and dorsal and
31 slightly lateral (F) views. Arrows point towards anterior direction. Grey shaded regions are
32 reconstructed. Abbreviations: brs, brevis shelf; brs-sac connection between brevis shelf and
33 supraacetabular crest; isp, ischiadic peduncle; obt, obturator foramen; pipl, puboischadic
34 plate; pla, plaster; poap, postacetabular process; prap, preacetabular process; pub, pubis; pup,
35 pubic peduncle; sac, supraacetabular crest.
36
37
38
39
40
41
42
43
44
45
46
47
48

49 **Figure 17.** Left femur of holotype of *Sarcosaurus woodi*, NHMUK PV R4840. Photographs
50 (A–D) and surface scan (E) in posterior (A), medial (B), anterior (C), lateral (D), and lateral
51 and slightly anterior (E) views. Arrows point towards anterior direction. Abbreviations: aiml,
52 anterior intermuscular line; atr, anterior trochanter; cfl, depression associated with the
53
54
55
56
57
58
59
60

1
2
3 insertion of the *M. caudofemoralis longus*; dltr, dorsolateral trochanter; ft, fourth trochanter;
4
5 trsh, trochanteric shelf.
6
7
8
9

10 **Figure 18.** Right tibia of referred specimen of *Sarcosaurus woodi*, NHMUK PV R3542
11
12 (holotype of ‘*Sarcosaurus andrewsi*’). Photographs (A–F) and surface scan (G) in lateral (A),
13
14 medial (B), anterior (C), posterior (D), proximal (E), distal (F), and medial and slightly
15
16 anterior (G) views. Arrows point towards anterior direction. Abbreviations: adt, anterior
17
18 diagonal tuberosity; cn, cnemial crest; fap, facet for reception of ascending process of
19
20 astragalus; fc, fibular crest; mma, medial malleolus; pamr, paramarginal ridge; pc, posterior
21
22 hemicondyles; plp, posterolateral process; pmn, posteromedial notch; pmr, posteromedial
23
24 ridge.
25
26
27
28
29
30

31 **Figure 19.** Time-calibrated strict consensus tree showing the phylogenetic relationships of
32
33 selected non-neotheropod and all neotheropod species sampled in the phylogenetic analysis.
34
35 Values next to each branch represent Bremer support, absolute bootstrap frequency, and GC
36
37 bootstrap frequency, respectively. Thick black bars with a vertical line represent the
38
39 chronostratigraphic uncertainty of taxa and thick black bars without a vertical line represent
40
41 biochrons.
42
43
44
45
46

47 **Figure 20.** Comparison among partial ilia in lateral view (A, B) and tibiae in distal view
48
49 (C–J) of selected neotheropod species. *Dilophosaurus wetherilli* (A, F), *Sarcosaurus woodi*
50
51 (B, G, H), *Coelophysis bauri* (C), *Liliensternus liliensterni* (D), *Zupaysaurus rougieri* (E),
52
53 *Tachiraptor admirabilis* (I) and *Piatnitzkysaurus floresi* (J). UCMP 37302 (A), NHMUK PV
54
55 R4840 (B), AMNH unnumbered, reversed (C), HMN MB.R. 2175 (D), PULR 076 (E),
56
57 UCMP 77270 (F), composite reconstruction using WARMS G668, 680 (G), NHMUK PV
58
59
60

R3542 (H), LPRP/USP 0747, cast of IVIC-P-2867 (I) and MACN-Pv CH 895, reversed (J). Arrows point towards anterior direction. Abbreviations: fap, facet for reception of ascending process of astragalus; isp, ischiadic peduncle; pla, plaster; plp, posterolateral process; pmr, posteromedial ridge; pmn, posteromedial notch; poap, postacetabular process; prap, preacetabular process; pub, pubis; vmbf, ventromedial margin of brevis fossa. (C–J) Not to scale.

Figure 21. Life reconstruction of the non-averostran neotheropod *Sarcosaurus woodi* from the late Hettangian–early Sinemurian of central England. Artwork by Mark Witton, who retains the copyright.

TABLES

Table 1. Measurements (in millimetres) of the preserved vertebrae of WARMS G667–690, referred specimen of *Sarcosaurus woodi*. Values in parentheses indicate incomplete measurements (owing to post-mortem damage), values in square brackets indicate estimated measurements (owing to post-mortem deformation) and the value given is the maximum measurable. The maximal deviation of the calliper is 0.02 mm, but measurements were rounded to the nearest 0.1 mm. Abbreviations: a-m C, anterior-middle caudal vertebra; m-p D, middle-posterior dorsal vertebra.

	<i>m-p D</i>	<i>a-m C</i>
Centrum length	44.3	50.3
Centrum anterior height	[26.5]	-
Centrum anterior width	[21.0]	-
Centrum posterior height	[27.0]	-
Centrum posterior width	[22.4]	-
Centrum height	-	21.3
Centrum width	-	19.3
Vertebra height	(44.7)	(26.3)

Table 2. Measurements (in millimetres) of pelvic and hindlimb bones of WARMS G667–

690, referred specimen of *Sarcosaurus woodi*. Values in parentheses indicate incomplete measurements (owing to post-mortem damage), values in square brackets indicate estimated measurements (owing to post-mortem deformation) and the value given is the maximum measurable. The maximal deviation of the calliper is 0.02 mm, but measurements were rounded to the nearest 0.1 mm. Abbreviations: Dist, distal; Pr, proximal.

	<i>Length</i>	<i>Pr depth</i>	<i>Pr width</i>	<i>Dist depth</i>	<i>Dist width</i>
Iliac pubic peduncle	(45.3)	-	-	(28.3)	(16.9)
Pubis (right)	(107.2)	(34.3)	(11.7)	-	-
Pubis (left)	(84.4)	(16.9)	-	-	-
Femur (right)	(286)	-	-	(35.0)	(50.9)
Femur (left)	[317]	(40.8)	(19.9)	(26.9)	-
Tibia (right)	(296)	(55.6)	(21.8)	26.1	(32.9)
Tibia (left)	[297]	(53.8)	[24.8]	(25.0)	(33.4)
Fibula proximal end (left)	(45.9)	37.8	13.6	-	-
Fibula distal portion	(114.7)	-	-	20.3	11.8
Metatarsal II (left)	(94.8)	-	-	(18.3)	(17.2)
Metatarsal III (left)	(42.1)	-	-	(18.7)	17.8
Metatarsal IV (left)	(80.1)	-	-	(16.7)	(14.0)

Table 3. Measurements (in millimetres) of referred specimen of *Sarcosaurus woodi* (right

tibia, NHMUK PV R4840, holotype of '*Sarcosaurus andrewsi*'). Values in parentheses indicate incomplete measurements (owing to post-mortem damage), values in square brackets indicate estimated measurements (owing to post-mortem deformation) and the value given is the maximum measurable. The maximal deviation of the calliper is 0.02 mm, but measurements were rounded to the nearest 0.1 mm.

Length	450
Proximal depth	104.6
Proximal width	[43.0]
Distal depth	41.7
Distal width	64.4

Table 4. Selected measurements (in millimetres) of preserved bones of the holotype of *Sarcosaurus woodi* (NHMUK PV R4840). Values in parentheses indicate incomplete measurements (owing to post-mortem damage), values in square brackets indicate estimated measurements (owing to post-mortem deformation) and the value given is the maximum measurable. The maximal deviation of the calliper is 0.02 mm, but measurements were rounded to the nearest 0.1 mm.

Centrum length	(39.8)
Centrum anterior height	39.6
Centrum anterior width	(36.5)
Femoral length (left)	(316)

SUPPORTING INFORMATION

Additional Supporting Information may be found in the online version of this article at the publisher's website:

Supporting Information I. Modifications to the phylogenetic character matrix of Nesbitt *et al.* (2009) and its subsequent iterations.

Supporting Information II. Phylogenetic data matrix in NEXUS format.

Supporting Information III. Phylogenetic data matrix in TNT format.

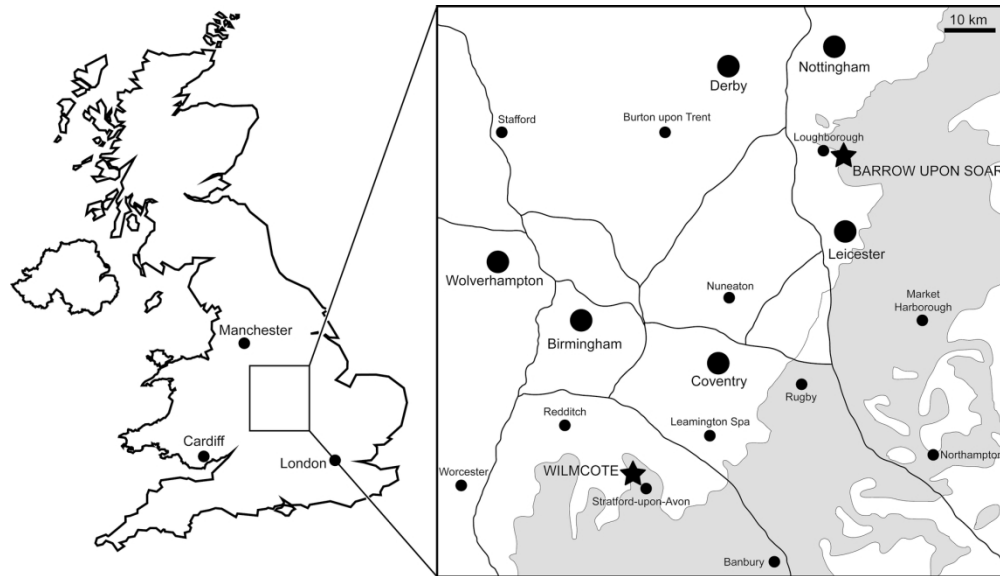


Figure 1. Map showing the geographic occurrences of the holotype of *Sarcosaurus woodi* (Barrow-on-Soar) and referred specimens (Wilmcote) indicated with stars. The outcrop of the Lias Group is shown in grey.

167x96mm (300 x 300 DPI)

1
2
3
4
5
6
7
8
9
10
11
12
13
14
15
16
17
18
19
20
21
22
23
24
25
26
27
28
29
30
31
32
33
34
35
36
37
38
39
40
41
42
43
44
45
46
47
48
49
50
51
52
53
54
55
56
57
58
59
60

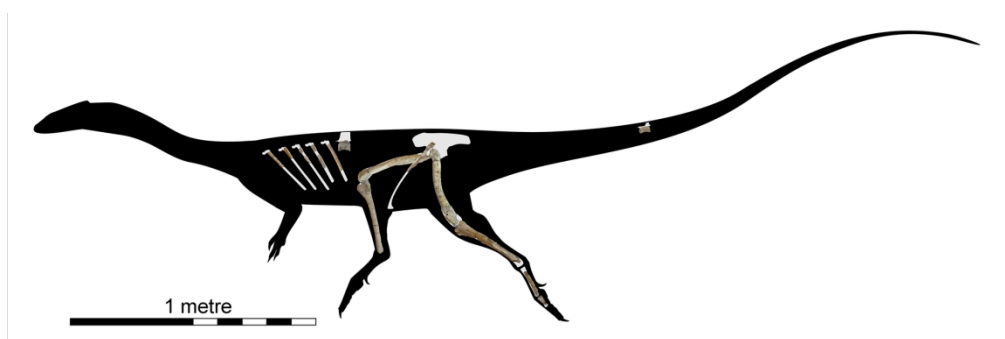


Figure 2. Silhouette showing the preserved bones of referred specimen of *Sarcosaurus woodi*, WARMs G667–690. Skeletal reconstruction from Mark Witton.

167x55mm (300 x 300 DPI)

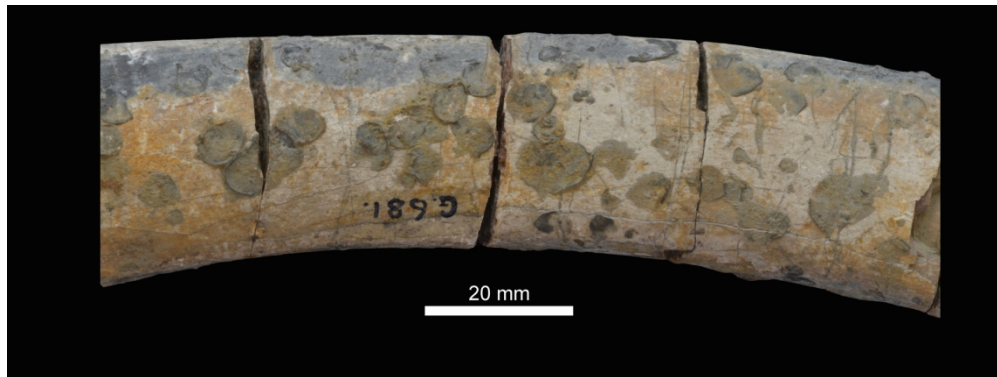


Figure 3. Close-up of bioencrusters on the anterior surface of the left femur of referred specimen of *Sarcosaurus woodi* (WARMS G681).

167x62mm (300 x 300 DPI)

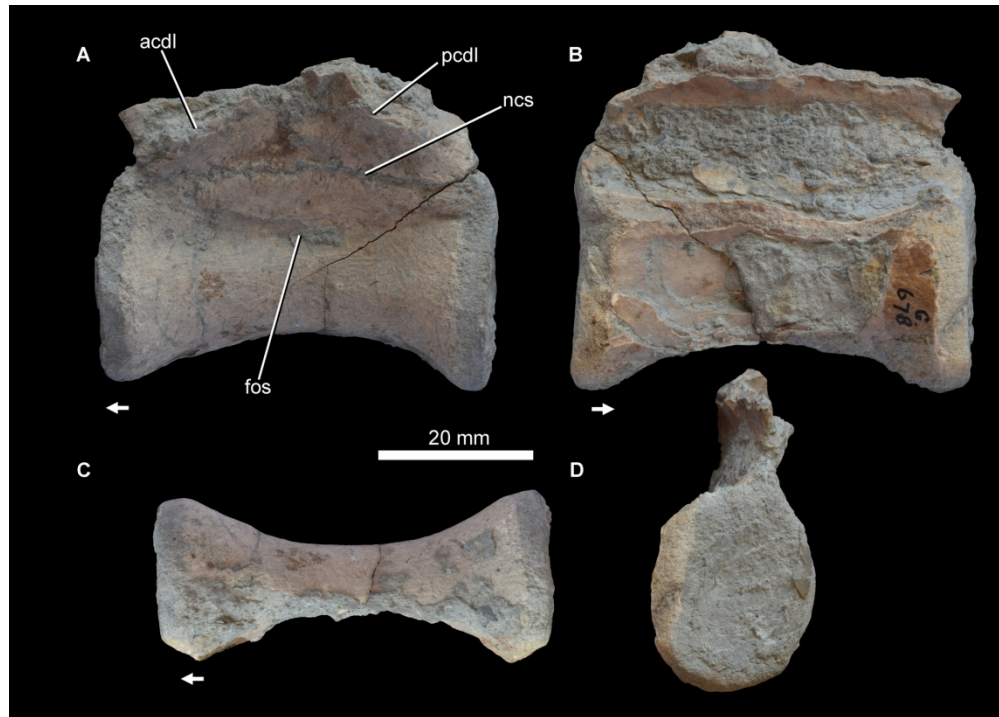


Figure 4. Middle or posterior dorsal vertebra of referred specimen of *Sarcosaurus woodi*, WARMS G678, in left lateral (A), right lateral (B), ventral (C) and anterior (D) views. Arrows point towards anterior direction. Abbreviations: acdl, anterior centrodiaepophyseal lamina; fos, fossa on lateral surface of centrum; ncs, neurocentral suture; pcdl, posterior centrodiaepophyseal lamina.

167x119mm (300 x 300 DPI)

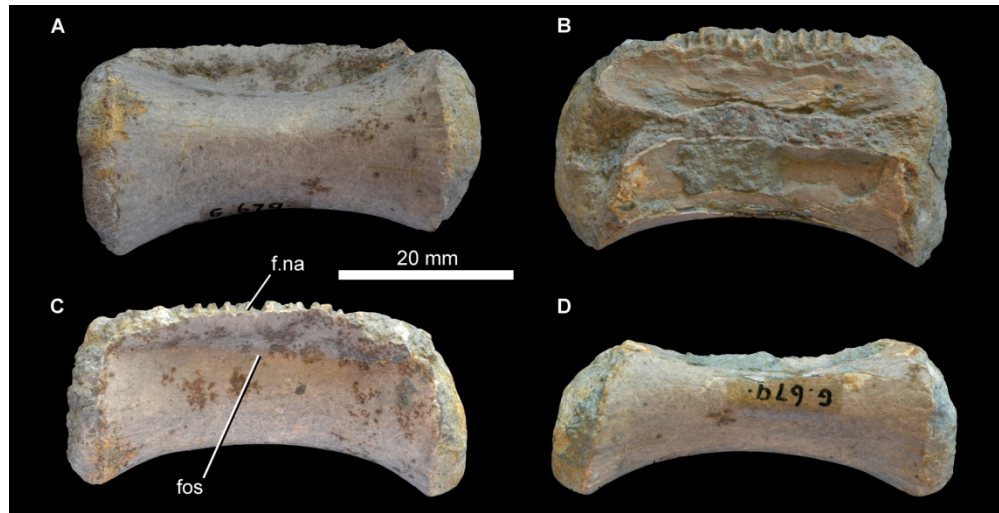


Figure 5. Anterior or middle caudal vertebra of referred specimen of *Sarcosaurus woodi*, WARMS G679, in ventral (A), dorsal (B) and lateral (C, D) views. Abbreviations: f.na, interdigitated articular facet for neural arch; fos, fossa on lateral surface of centrum.

167x85mm (300 x 300 DPI)

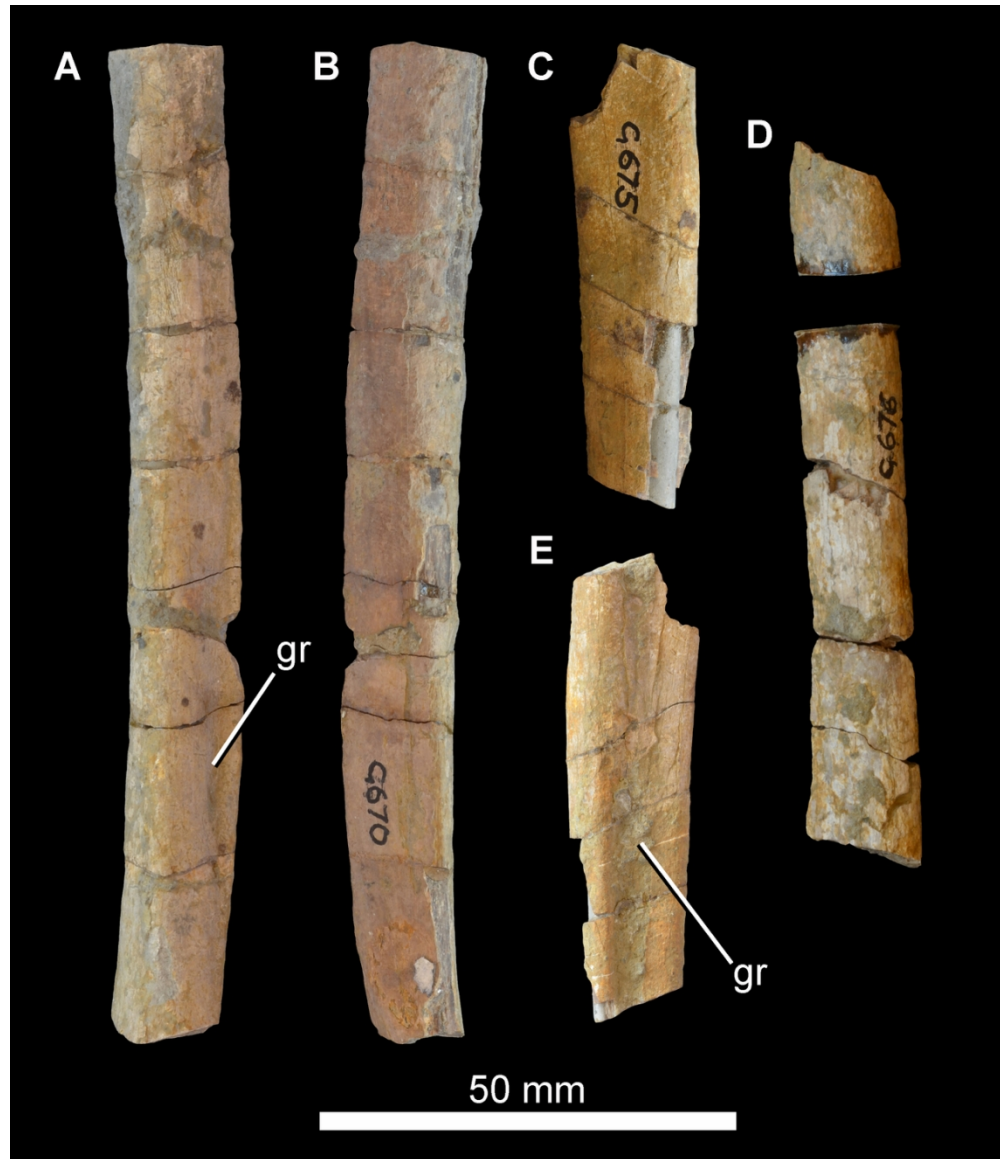


Figure 6. Fragmentary dorsal rib shafts of referred specimen of *Sarcosaurus woodi*, WARMS G670 (A, B), G675 (C, D) and G676 (E) in probable posterior (A, E) and anterior (B, C, D) views. Abbreviation: gr, groove.

109x126mm (300 x 300 DPI)

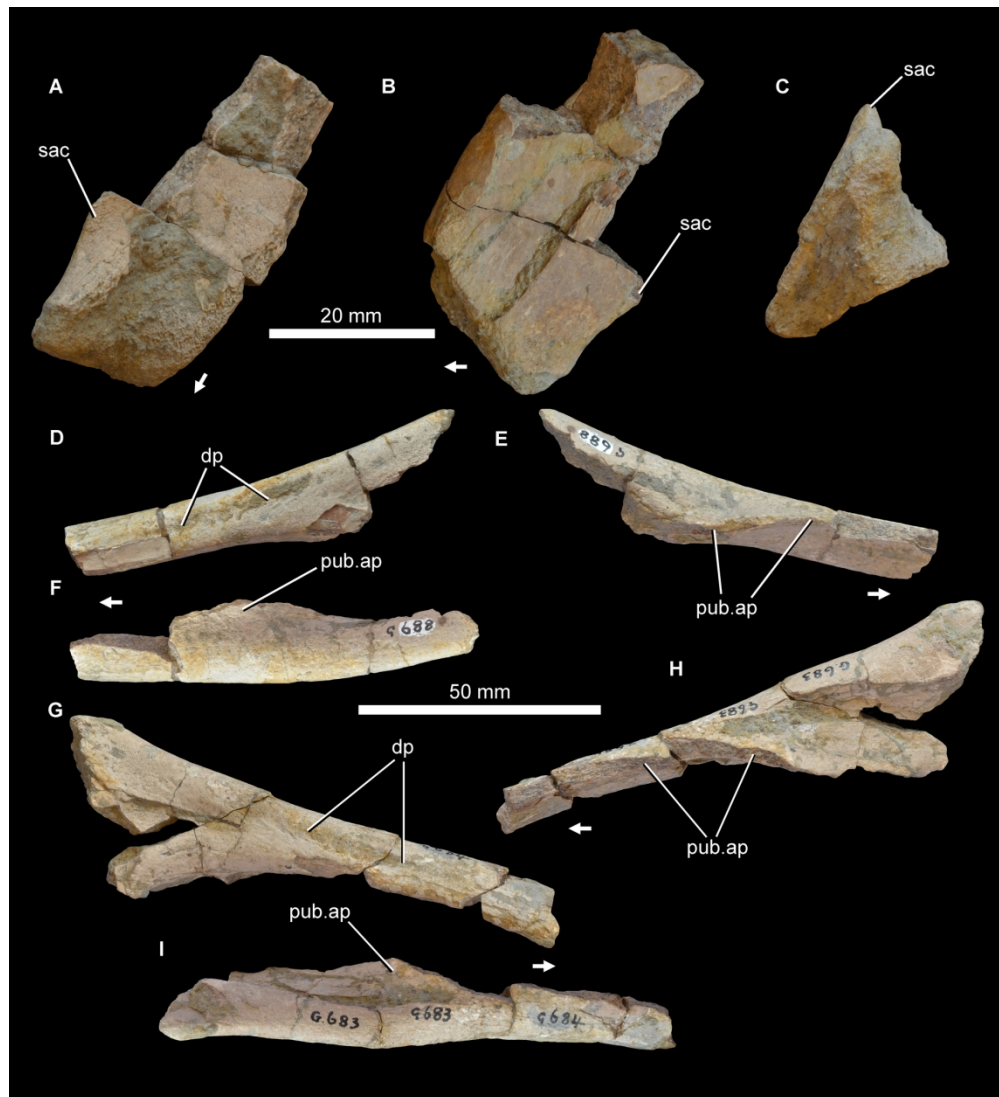
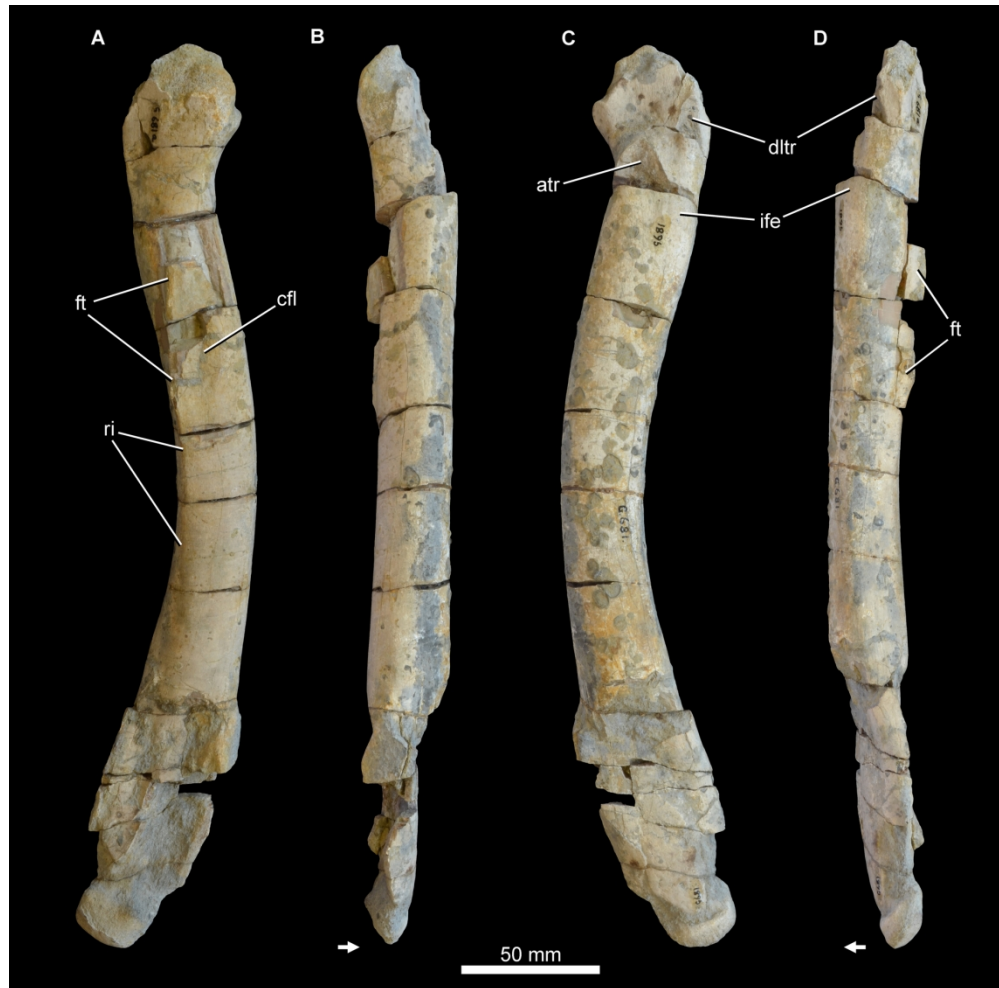


Figure 7. Pelvic fragments of referred specimen of *Sarcosaurus woodi*, WARMS G690 (A–C), G688 (D–F) and G683/G684 (G–I). Partial pubic peduncle of left ilium in posterior (A) and lateral (B) views, and cross section of peduncle (C). Partial left pubis in lateral (D), medial (E) and anterodorsal (F) views. Partial right pubis in lateral (G), medial (H) and anterodorsal (I) views. Arrows point towards anterior direction. Abbreviations: dp, longitudinal depression; pub.ap, pubic apron; sac, supraacetabular crest.

167x183mm (300 x 300 DPI)



38
39
40
41
42

Figure 8. Left femur of referred specimen of *Sarcosaurus woodi*, WARMS G681, in posterior (A), medial (B), anterior (C) and lateral (D) views. Arrows point towards anterior direction. Abbreviations: atr, anterior trochanter; cfl, depression associated with the insertion of the *M. caudofemoralis longus*; dltr, dorsolateral trochanter; ft, fourth trochanter; ife, insertion scar of the *M. iliofemoralis externus*; ri, ridge.

43
44
45
46
47
48
49
50
51
52
53
54
55
56
57
58
59
60

167x165mm (300 x 300 DPI)

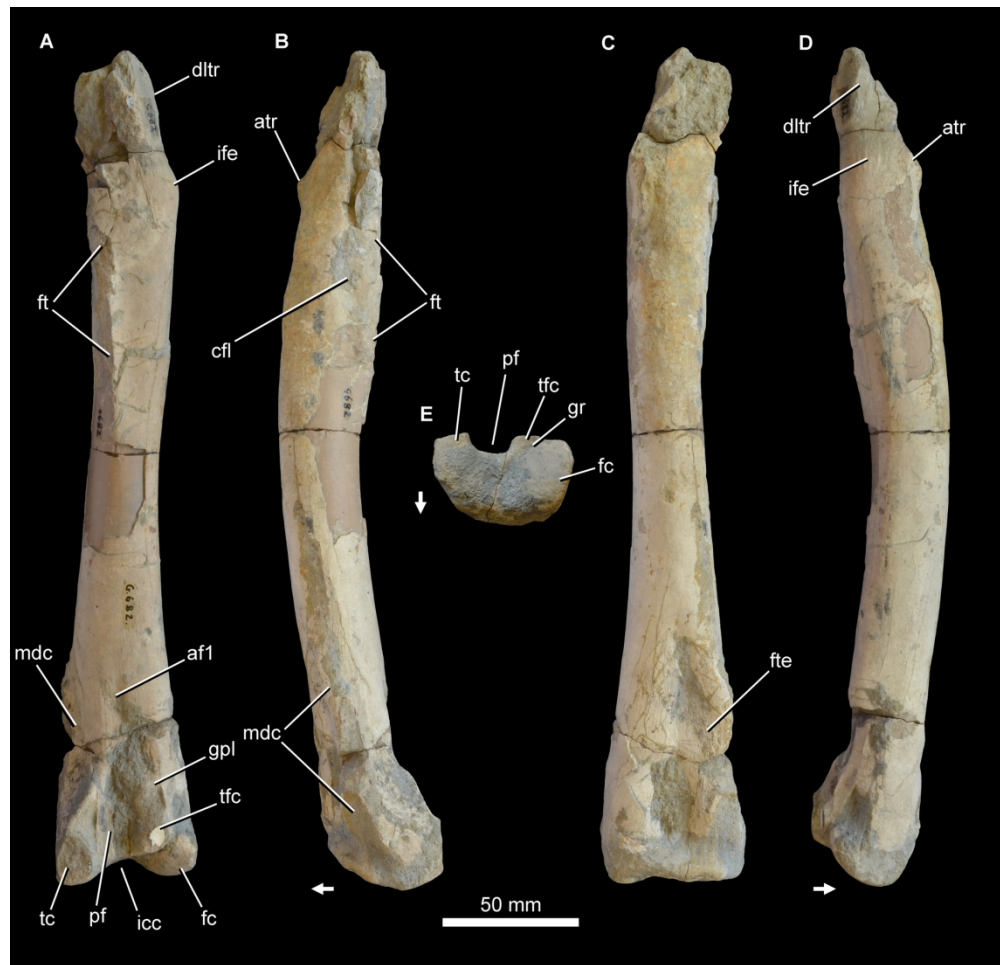


Figure 9. Right femur of referred specimen of *Sarcosaurus woodi*, WARMS G682, in posterior (A), medial (B), anterior (C), lateral (D) and distal (E) views. Arrows point towards anterior direction. Abbreviations: af1, insertion of the *M. adductor femoris 1*; atr, anterior trochanter; cfl, depression associated with the insertion of the *M. caudofemoralis longus*; dltr, dorsolateral trochanter; fc, fibular condyle; ft, fourth trochanter; fte, attachment of the distal portion of the *M. femorotibialis externus*; gpl, insertion scar of the *M. gastrocnemius pars lateralis/M. flexor hallucis longus*; gr, groove; icc, intercondylar cleft; ife, insertion scar of the *M. iliofemoralis externus*; mdc, mediolateral crest; pf, popliteal fossa; tc, tibial condyle; tfc, tibiofibular crest.

167x161mm (300 x 300 DPI)

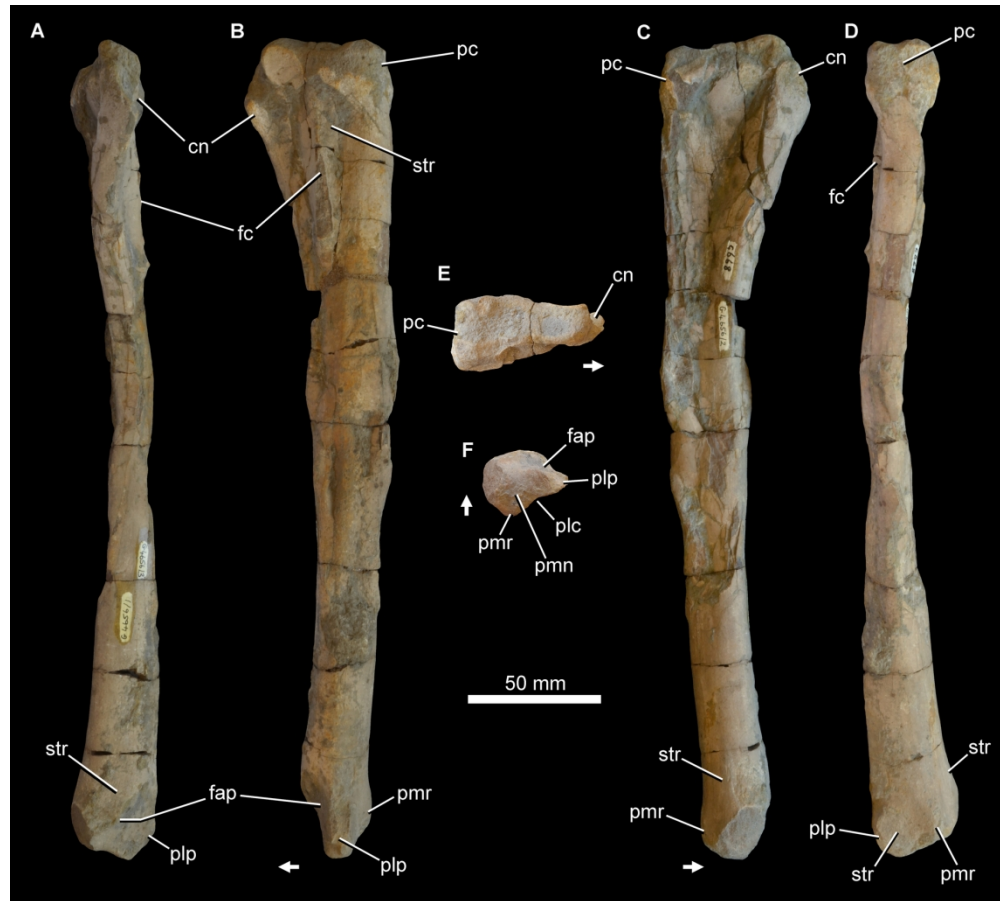


Figure 10. Left tibia of referred specimen of *Sarcosaurus woodi*, WARMS G668, in anterior (A), lateral (B), medial (C), posterior (D), proximal (E) and distal (F) views. Arrows point towards anterior direction. Abbreviations: cn, cnemial crest; fap, facet for reception of ascending process of astragalus; fc, fibular crest; pc, posterior hemicondyles; plc, posterolateral concavity; plp, posterolateral process; pmn, posteromedial notch; pmr, posteromedial ridge; str, striations.

167x151mm (300 x 300 DPI)



Figure 11. Right tibia of referred specimen of *Sarcosaurus woodi*, WARMS G680, in anterior (A), lateral (B), medial (C), posterior (D), proximal (E) and distal (F) views. Arrows point towards anterior direction. Abbreviations: cn, cnemial crest; fap, facet for reception of ascending process of astragalus; fc, fibular crest; gms, origin scar of the *M. gastrocnemius pars medialis*; pc, posterior hemicondyles; plp, posterolateral process; pmn, posteromedial notch; pmr, posteromedial ridge; str, striations.

167x155mm (300 x 300 DPI)

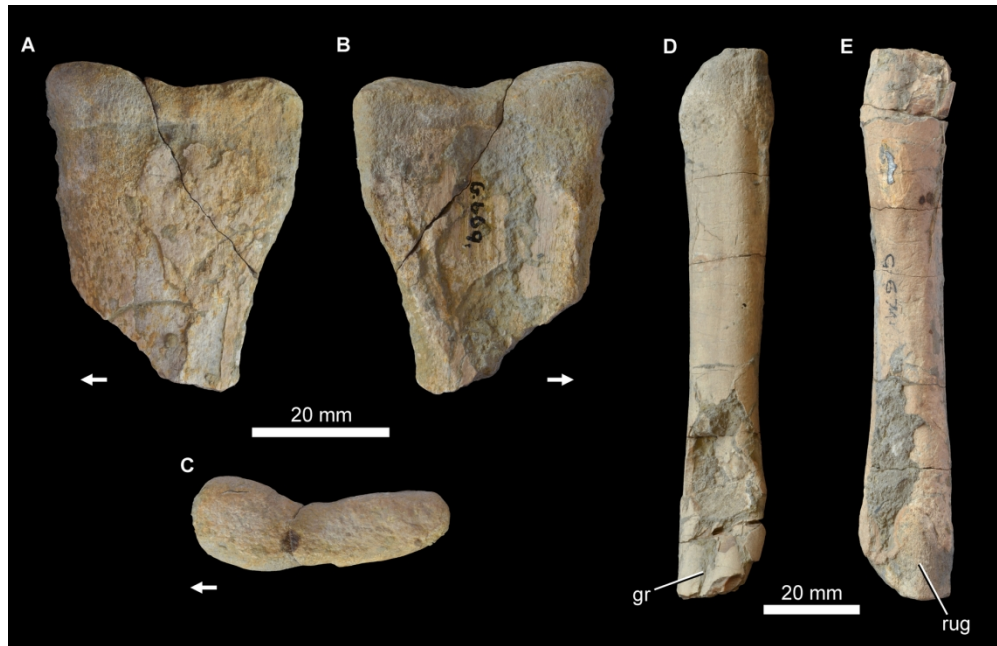


Figure 12. Fibula of referred specimen of *Sarcosaurus woodi*, WARMS G669 (A–C) and G674 (D, E). Proximal end of left fibula in lateral (A), medial (B) and proximal (C) views. Distal portion of fibula from indeterminate side in lateral/medial views (D, E). Arrows point towards anterior direction. Abbreviations: gr, groove; rug, rugosity.

167x108mm (300 x 300 DPI)



Figure 13. Partial left pedal autopodium (A–K) and metatarsal of indeterminate side (L) of referred specimen of *Sarcosaurus woodi*, WARMS G672 (A–C), G673 (D–F), G677 (G, H), G687 (I–K) and G671 (L). Metatarsal II in anterior (A), lateral (B) and distal (C) views. Metatarsal III in proximal (D), anterior (E) and lateral (F) views. Metatarsal IV in anterior (G) and lateral (H) views. Phalanx II-1 in anterior (I), proximal (J) and lateral (K) views. Proximal end of metatarsal II or III in lateral/medial view (L). Arrows point towards anterior direction. Abbreviations: clf, collateral fossa.

167x181mm (300 x 300 DPI)

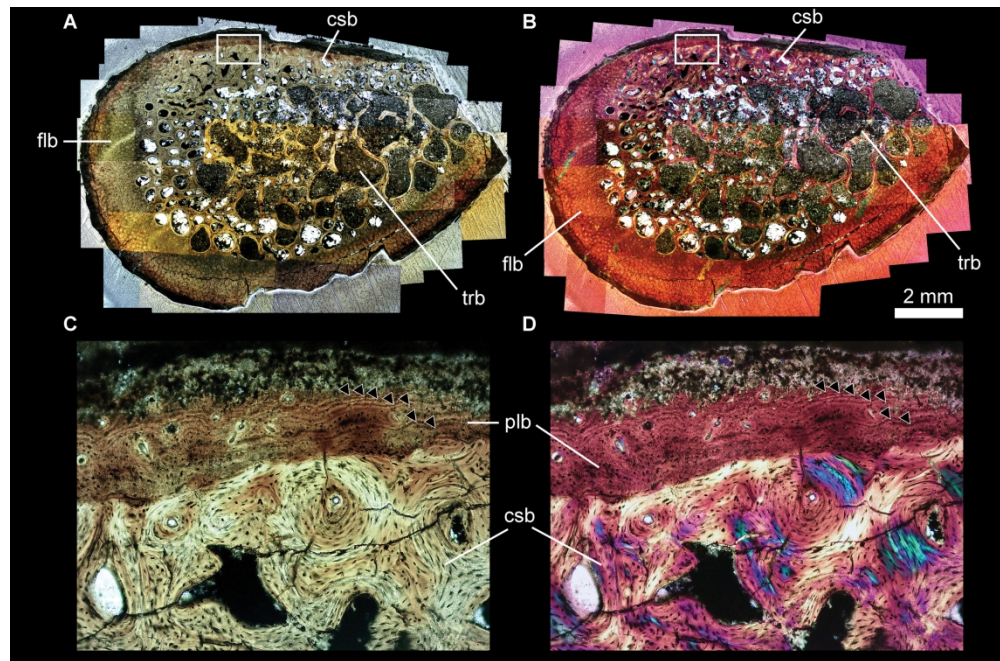


Figure 14. Photomicrographs of a thin section of dorsal rib shaft of referred specimen of *Sarcosaurus woodi*, WARMS G676, under plain-polarized light (A, C) and polarized light with a gypsum plate (B, D). White rectangles in (A, B) indicate the magnified areas shown in (C, D). Arrowheads in (C, D) indicate annuli. Abbreviations: csb, compact spongy bone; flb, fibrolamellar bone; plb, pseudolamellar bone; trb, trabeculae.

209x138mm (300 x 300 DPI)

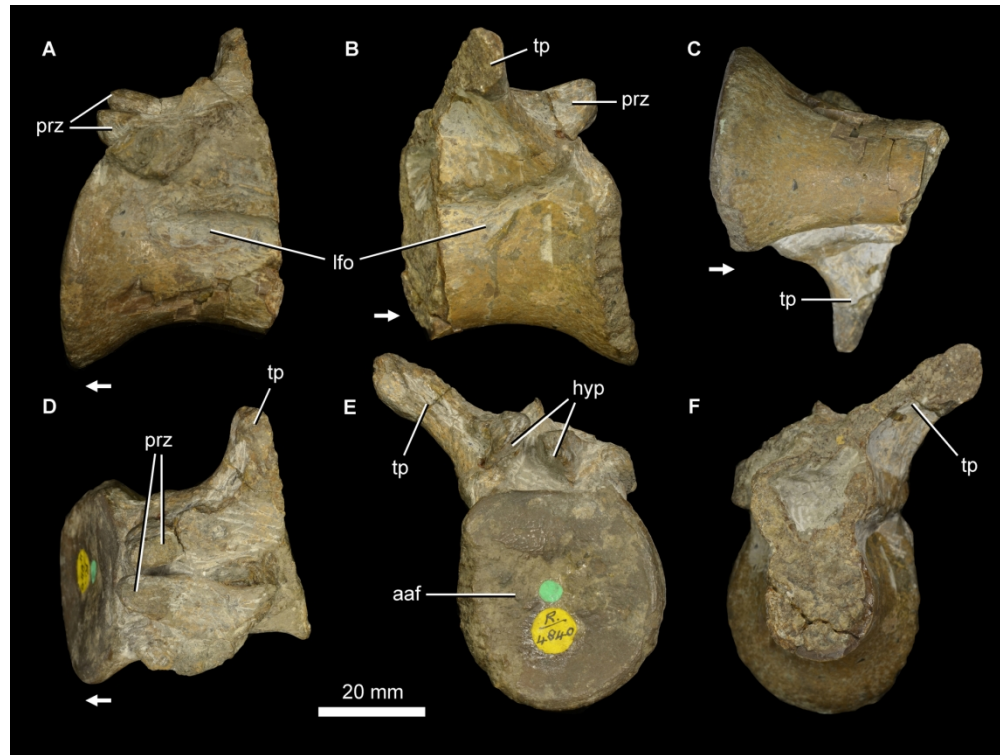


Figure 15. Posterior dorsal vertebra of holotype specimen of *Sarcosaurus woodi*, NHMUK PV R4840, in left lateral (A), right lateral (B), ventral (C), dorsal (D), anterior (E) and posterior (F) views. Arrows point towards anterior direction. Abbreviations: aaf, anterior articular facet; hyp, hypantrum; lfo, lateral fossa; prz, prezygapophysis; tp, transverse process.

167x126mm (300 x 300 DPI)

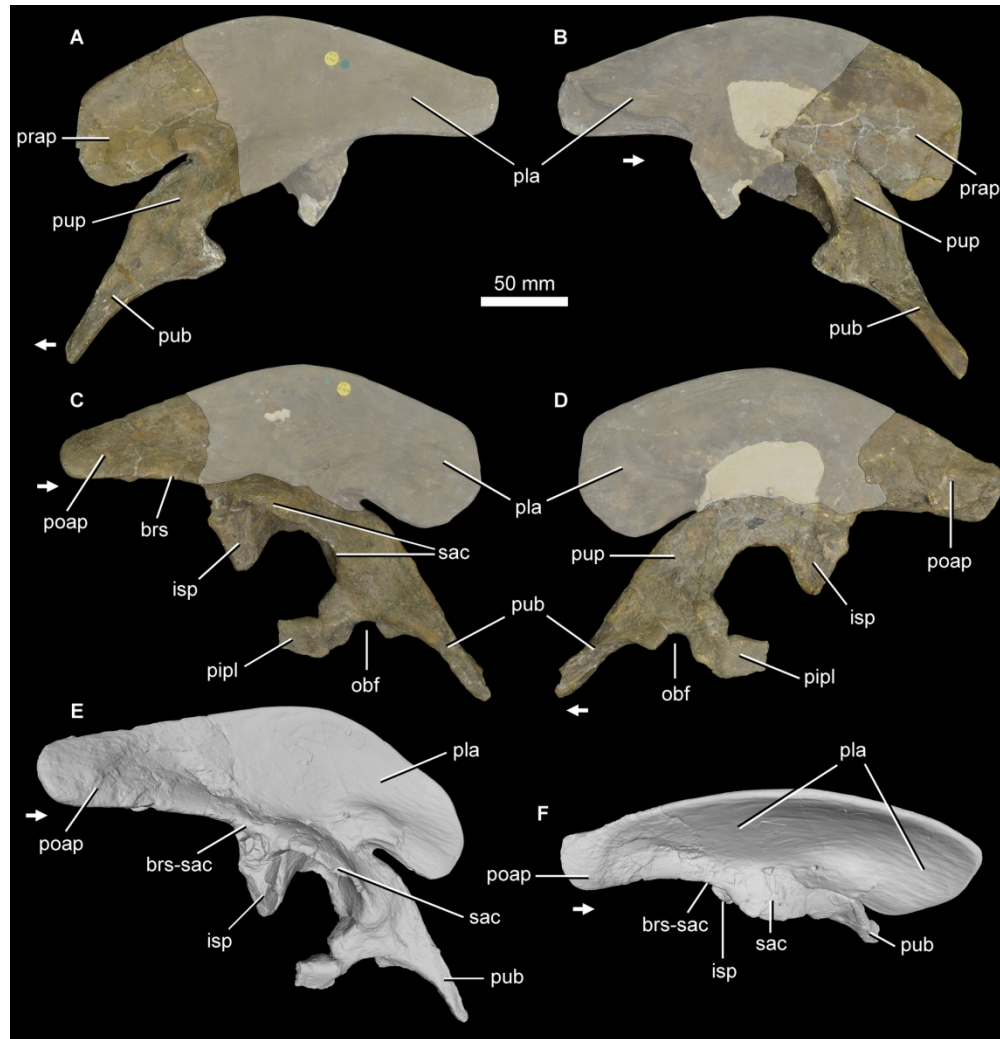


Figure 16. Partial pelvic girdle of holotype specimen of *Sarcosaurus woodi*, NHMUK PV R4840. Photographs (A–D) and surface scans (E, F) of left ilium and pubis (A, B) and right ilium and pubis (C–F) in lateral (A, C), medial (B, D), lateral and slightly posterior (E), and dorsal and slightly lateral (F) views. Arrows point towards anterior direction. Grey shaded regions are reconstructed. Abbreviations: brs, brevis shelf; brs-sac, connection between brevis shelf and supraacetabular crest; isp, ischiadic peduncle; obt, obturator foramen; pipl, pubo-ischiadic plate; pla, plaster; poap, postacetabular process; prap, preacetabular process; pub, pubis; pup, pubic peduncle; sac, supraacetabular crest.

167x173mm (300 x 300 DPI)

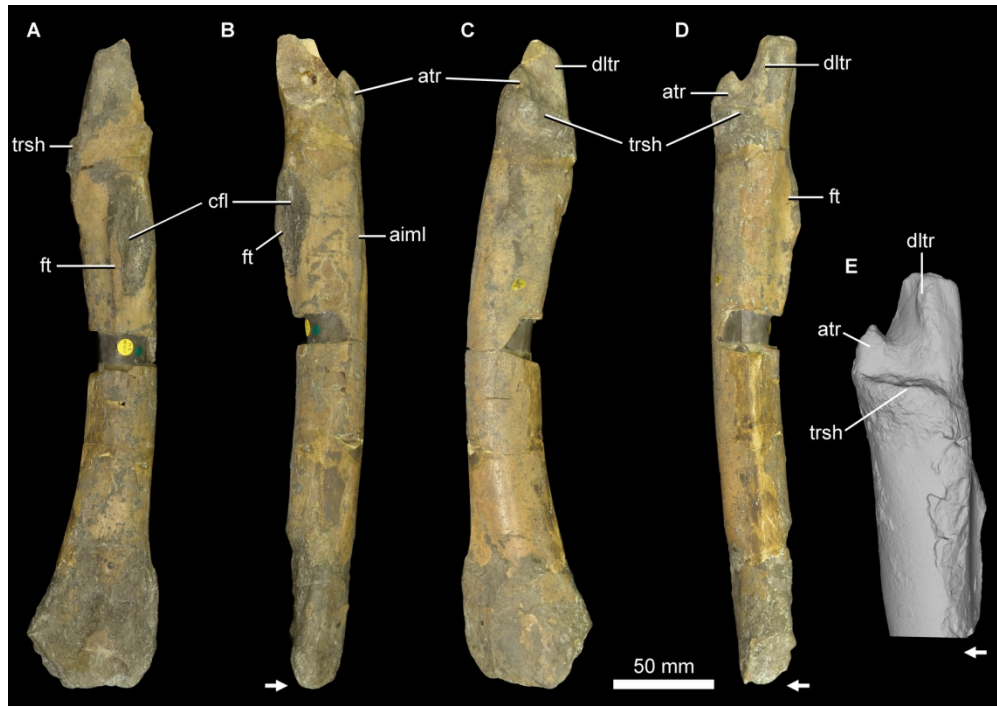


Figure 17. Left femur of holotype specimen of *Sarcosaurus woodi*, NHMUK PV R4840. Photographs (A–D) and surface scan (E) in posterior (A), medial (B), anterior (C), lateral (D), and lateral and slightly anterior (E) views. Arrows point towards anterior direction. Abbreviations: aiml, anterior intermuscular line; atr, anterior trochanter; cfl, depression associated with the insertion of the *M. caudofemoralis longus*; dltr, dorsolateral trochanter; ft, fourth trochanter; trsh, trochanteric shelf.

167x117mm (300 x 300 DPI)



Figure 18. Right tibia of referred specimen of *Sarcosaurus woodi*, NHMUK PV R3542 (holotype of '*Sarcosaurus andrewsi*'). Photographs (A–F) and surface scan (G) in lateral (A), medial (B), anterior (C), posterior (D), proximal (E), distal (F), and medial and slightly anterior (G) views. Arrows point towards anterior direction. Abbreviations: adt, anterior diagonal tuberosity; cn, cnemial crest; fap, facet for reception of ascending process of astragalus; fc, fibular crest; mma, medial malleolus; pamr, paramarginal ridge; pc, posterior hemicondyles; plp, posterolateral process; pmn, posteromedial notch; pmr, posteromedial ridge.

167x149mm (300 x 300 DPI)

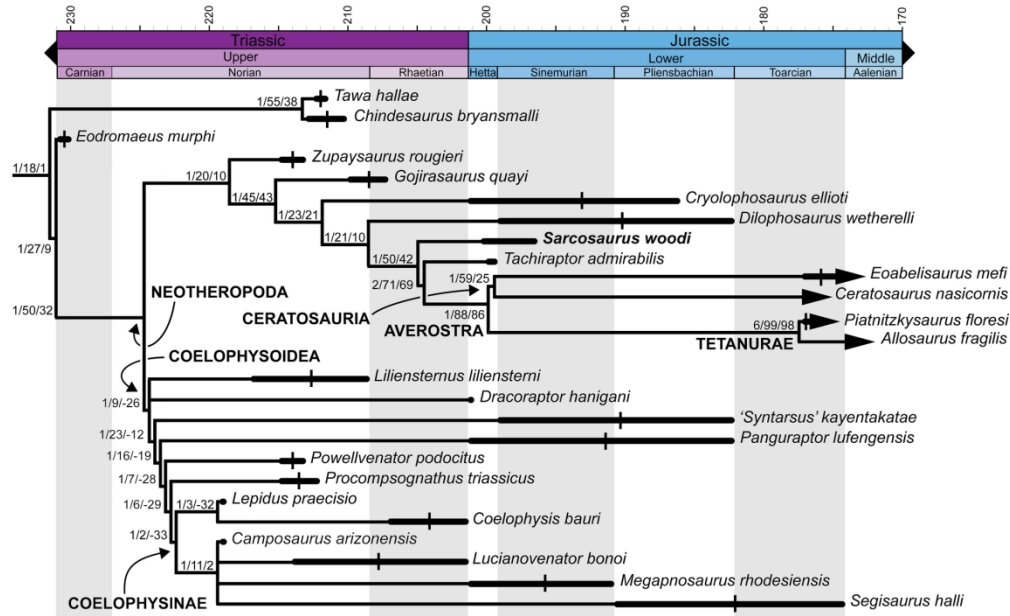


Figure 19. Time-calibrated strict consensus tree showing the phylogenetic relationships of selected non-neotheropod and all neotheropod species sampled in the phylogenetic analysis. Values next to each branch represent Bremer support, absolute bootstrap frequency, and GC bootstrap frequency, respectively. Thick black bars with a vertical line represent the chronostratigraphic uncertainty of taxa and thick black bars without a vertical line represent biochrons.

167x104mm (300 x 300 DPI)

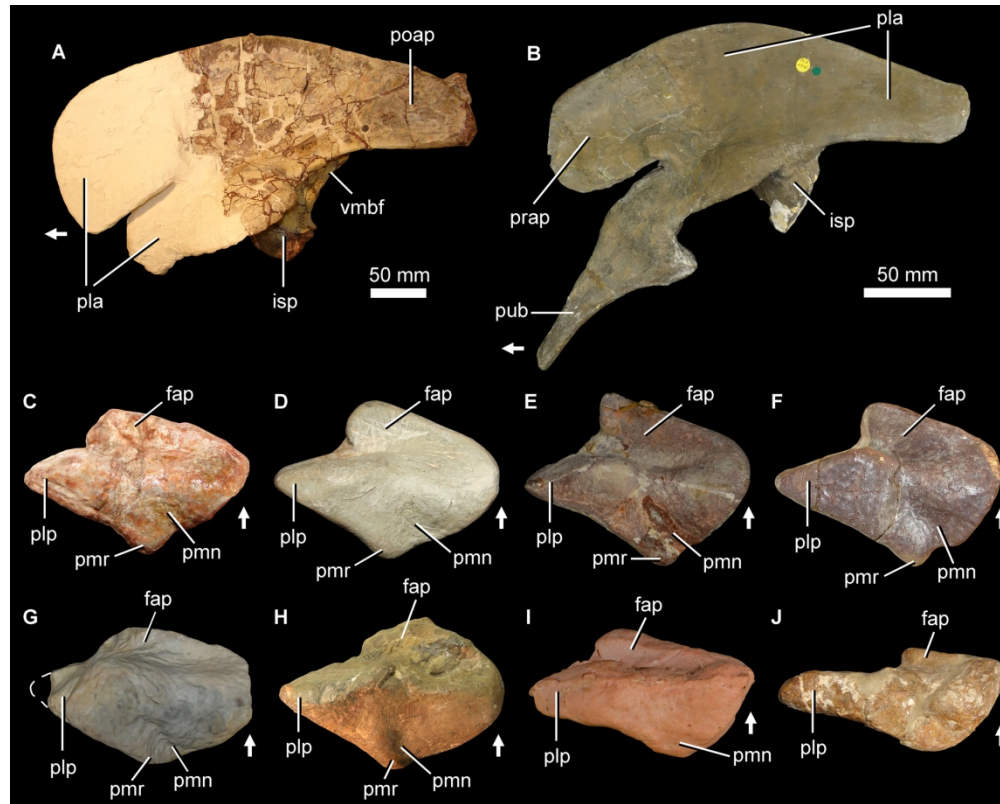


Figure 20. Comparison among partial ilia in lateral view (A, B) and tibiae in distal view (C–J) of selected neotheropod species. *Dilophosaurus wetherilli* (A, F), *Sarcosaurus woodi* (B, G, H), *Coelophysis bauri* (C), *Liliensternus liliensterni* (D), *Zupaysaurus rougieri* (E), *Tachiraptor admirabilis* (I) and *Piatnitzkysaurus floresii* (J). UCMP 37302 (A), NHMUK PV R4840 (B), AMNH unnumbered, reversed (C), HMN MB.R. 2175 (D), PULR 076 (E), UCMP 77270 (F), composite reconstruction using WARMS G668, 680 (G), NHMUK PV R3542 (H), LPRP/USP 0747, cast of IVIC-P-2867 (I) and MACN-Pv CH 895, reversed (J). Arrows point towards anterior direction. Abbreviations: fap, facet for reception of ascending process of astragalus; isp, ischiadic peduncle; pla, plaster; plp, posterolateral process; pmr, posteromedial ridge; pmn, posteromedial notch; poap, postacetabular process; prap, preacetabular process; pub, pubis; vmbf, ventromedial margin of brevis fossa. (C–J) Not to scale.

167x134mm (300 x 300 DPI)



Figure 21. Life reconstruction of the non-averostran neotheropod *Sarcosaurus woodi* from the late Hettangian–early Sinemurian of central England. Artwork by Mark Witton, who retains the copyright.

167x83mm (600 x 600 DPI)